10-20-2017 10:30 AM

The Human First Metatarsal in Bioarchaeological Research: New Insights into Human Variation and Bone Health Research from Kellis 2, Dakhleh Oasis, Egypt (50-450CE)

Mathew A. Teeter, *The University of Western Ontario*

Supervisor: Dr. J.E. Molto, *The University of Western Ontario*
A thesis submitted in partial fulfillment of the requirements for the Doctor of Philosophy degree in Anthropology
© Mathew A. Teeter 2017

Abstract

Objectives: This research tests the efficacy of using the human first metatarsal (MT1) in bioarchaeological research, specifically to investigate human variation (nonmetric traits and sexual dimorphism) and skeletal health (Osteo-Volumetric Density and μCT analysis) in antiquity. To date, this bone has had limited applications in bioarchaeology.

Materials and Methods: This study used human remains from the Kellis 2 (K2) cemetery, located in the Dakhleh Oasis, Egypt (50-450CE). Specifically, 377 MT1s, representing 212 individuals were used to investigate human variation and osteo-volumetric density (OVD) in the K2 skeletal population. Additionally, skeletal health was further assessed in a female sub-sample (n=44) of the population using μCT analysis. μCT imaging of the MT1s was conducted using *eXplore speCZT scanner*, and analyses were done in *MicroView* with the *Advanced Bone Analysis Application* software add-in (Version 2.1.2, GE Healthcare Biosciences, London, ON)

Results: The intermetatarsal facet had a prevalence of 28% in the K2 skeletal population. Moreover, significant sexual dimorphism was observed for MT1 metrics, and logistic regression models could predict the sex of an individual from K2 between ~80-90% of the time. The novel OVD method was found reliable/reproducible through intra-/inter-observer statistical analyses. The OVD patterns differed significantly between males and females, as well as between age-cohorts. The inverse relationship between age and the estimated OVD in K2 females was much more pronounced than was seen in K2 males. Additionally, an inverse relationship between biological age and the standard measures associated with bone strength/architecture using μCT analyses was observed for the female sub-population. The T-scores of individuals previously diagnosed with

i

osteoporosis (based on age and fractures) were significantly below the mean of the "*healthy*" population using both OVD and µCT analyses of the MT1.

Conclusions: The first metatarsal is a suitable element for the study of human variation and skeletal health in antiquity. Although not an area normally associated with osteoporosis-related fractures, this research shows that the MT1 is not spared from age-related bone loss, and may prove useful for investigating skeletal health when the more traditionally-used elements are not available.

Keywords

First Metatarsal, Dakhleh Oasis Egypt, Kellis, Bioarchaeology, Human Skeletal Variation, Human Skeletal Health, Nonmetric Trait, Intermetatarsal Facet, Sexing, Osteo-Volumetric Density, Age-Related Bone Loss, Primary Osteoporosis, Hip Fractures, Micro-Computed Tomography, µCT, Bone Mineral Density, Cortical Index, Trabecular Architecture.

Acknowledgments

I wish to thank the Egyptian Ministry of State for Antiquities for their continued support and to the members of the Dakhleh Oasis Project and their field support staff. Particular thanks to Dr. Peter Sheldrick, the director of the Bioarchaeology Program. Thanks to Dr. Ian Colquhoun for his constructive comments on earlier versions of this dissertation. Also, thanks to Jim Keron (UWO) for creating the K2 maps, and Edward Eastaugh for his photography. I would also like to thank my cohort, the administration staff (Christine Wall and Laura Cousins), and the many great friends that I have met in the Department of Anthropology at the University of Western Ontario. Your support over the many years has made this a wonderful experience.

I would like to specifically thank Isabella Graham for her many hours measuring and recording metatarsals for my project. Your humour and attitude always brightened my day. I would also like to thank Dr. David Holdsworth at Robarts for allowing me to use the equipment. I would especially like to thank Dr. Joseph Umoh for guiding me in μCT analysis and for his endless patience. I would also like to thank Paul Szpak, Flannery Surette, Amy Scott, Jenn Morgan, Karyn Olsen, Ramsay Macfie, Tom Porawski, Zoe Morris, John Moody, Leanne Bekeris and many others who made my time in graduate school amazing.

I would like to give special thanks to Dr. Alexis Dolphin for her past and continued support and motivation. I could not have completed graduate school without her kindness and guidance. I would also like to thank Dr. JE Molto (El to those who know him) for being the truest definition of the words mentor and friend. You have

always supported me and have fought hard for my best interests, as well as for those who follow me. You are an unbelievable scientist and person, and I hope I can live up to your expectations.

I would also like to thank my family – Scott Teeter, Ryan Teeter, Kelly Teeter, Jason Teeter, Emilie Teeter, Paige Teeter, Owen Teeter, Joan Moyer, Barb Kohl, and Dave Lima – for all your love and support over these many years. I would also like to thank my dad, Robert Teeter, for the years of guidance, support, and especially the laughs from your views on politics. Finally, a special acknowledgement to my mother, Lorraine Teeter. You have always done everything in your power to help me, even when it was at a cost to yourself, and I truly appreciate it. I could not have continued with this pursuit without your love, support, generosity, and humour.

Table of Contents

List of Tables

List of Figures

List of Appendices

Chapter 1

1   INTRODUCTION

1.1   Statement of the Problem

Biological anthropology has had a long history of using individual skeletal elements for developing methods for osteobiographical research (i.e., determination of age, sex, stature, genetic affinities, life history, etc.) (Saul and Saul 1989). These methods have primarily focused on osteometric and nonmetric variants of the skull, hips and the larger long bones. In building on this trend of using individual bones as a proxy for individual characteristics, this thesis explores new applications for the human first metatarsal (MT1) in bioarchaeology. Specifically, it focuses on human variation (e.g., nonmetric traits, and sexual dimorphism), and methods of investigating bone health (e.g., osteoporosis) in antiquity using analysis of the MT1. To date, this bone has had limited applications in bioarchaeology – its main contributions have been in palaeoanthropology.

With respect to human evolution, one of the initial defining characteristics of our hominin lineage was the attainment of habitual bipedalism (White et al. 2011). An exact date for when our ancestors first experimented with bipedal behavior is unknown, although most researchers agree that by 4 million years ago, our ancestors were reasonably efficient bipeds (Leakey and Walker 2003). The results of the musculo-skeletal adaptations that were necessary for habitual bipedalism transformed virtually the whole skeleton, with particularly dramatic changes occurring in the infracranial skeleton. One of these major adaptive changes occurred in the human foot, as it evolved from a

dexterous grasping appendage, to a much more rigid structure adapted for weight bearing, shock absorption and propulsion (White et al. 2011).

The human foot is a complex system that acclimates to varying forces and strains, such as those experienced while standing, walking, running or jumping (Garcia-Aznar et al. 2009). It normally consists of 28 bones, each with a function to accommodate our bipedalism. Notwithstanding the allometric associations of all the foot bones, the human first metatarsal has had the most significant shift in function, as it lost its abduction and grasping capabilities present in the last common ancestor (LCA) of the genera *Homo* and *Pan*. These structural-behavioural changes are found in fossilized bones of *Australopithecus afarensis,* one of the earliest species in our hominin family.

This species was first identified from the Hadar region of Ethiopia, and was represented by an unusually well-preserved sample of many individuals, which included bones from every region of the skeleton. Though there has been much debate on the exact mode of locomotion of this species, there was little doubt that the infracranial skeleton had distinct evidence of habitual bipedalism (Leakey 1981). In the famous Tanzanian Laetoli site, this was confirmed, as the trails of footprints from three *A. afarensis* hominins were found preserved in hardened volcanic ash, and attested to their bipedal gait some 3.5 to 3.8 million years ago (Leakey 1981). These footprints point towards the presence of a well-developed heel, an adducted converged hallux, and foot-arches that are similar to the modern humans (**Figure 1**). Though considerable debate has occurred on the exact bipedal capabilities of *A. afarensis*, there is currently a consensus that the species was habitually bipedal while on the ground, and would have had a MT1 similar to a segment of our modern first-ray. Obviously, during the subsequent three to four million

2

years, many subtle changes to the human foot, including the first digital ray, have occurred, but the anatomical foundation was clearly established in these early australopithecines.

Figure 1 *A. afarensis* **Footprints.** One of the footprints from Laetoli, in Tanzania. This shows the human foot characteristics – deep heel impression, the arch and of course the depression for the MT1 (arrow). The alignment with the other toes shows the adducted nature of the MT1 (from Jurmain et al. 2017).

1.2   The Genesis of the Hypothesis

The MT1, as noted, has received only sporadic interest in bioarchaeological research. This research has primarily focused on osteobiographical applications, including aging (Scheuer and Black 2004), sexing (Mountrakis et al. 2010; Robling and Ubelaker 1997; Wolpoff and Frayer 1985), stature estimation (Byers et al. 1989; De Groote and Humphrey 2011), morphological variation (Le Minor and Winter 2003) and pathology (Kilmartin et al. 1991). That being said, biomechanical studies (kinesiology) with implications for evolutionary studies are more common than bioarchaeological studies.

The results of these bioarchaeological studies have been limited in terms of providing alternative methods for individuation, or for contributing to skeletal studies at the population level. The purpose of this thesis is to explore the bioarchaeological research potential of the MT1 in areas thus far neglected: Human variation with respect to nonmetric traits and sexual dimorphism, and human bone health research. **The null hypothesis (H_0) tested herein is that the MT1 will not prove to be useful for bioarchaeological research, particularly in the areas of human variation and bone health in antiquity**.

The MT1 samples used in this thesis are from the large Kellis 2 Roman Period cemetery in the Dakhleh Oasis, Egypt. The bones from this site are well preserved with very limited post-mortem destruction, which is ideal for this pilot research. Furthermore, each of the skeletons selected have been profiled for age, sex, morphogenetic traits, and osteopathology. Controlling for these osteobiographical variables is important for testing the efficacy of the MT1 for bioarchaeology research.

It is important to note that the MT1s were initially selected for isotopic and ancient DNA (*a*DNA) research. During the curational process in the Dakhleh Oasis Lab, at the University of Western Ontario, I measured these bones per standard osteometric techniques, and observed them for any pathological changes or osteoscopic nonmetric variations. The latter morphological variations are virtually undescribed in the bioarchaeological literature. As I studied the MT1, the thought of how its micro-structure might have been affected by its weight-bearing function and constitutional factors (i.e., sex and age), and how this might be useful in bioarchaeology ultimately led to this research.

1.3   Previous Research on the MT1: the foundation of the H_0

The MT1s were initially selected for *a*DNA and isotopic research because of their durability, easy transport and storage, and limited value to bioarchaeological research. The latter facilitated their accessibility for sampling from the Egyptian Antiquities organization (Dr. Molto personal communication). As part of the protocol, each of the MT1s were to be photographed and measured before they were to be sampled for the destructive *a*DNA and isotopic research.

As noted above, there was very limited bioarchaeological research on the MT1s, so my initial task was to review the available information and to record on the Dakhleh sample. Since my laboratory sample included both subadults and adults, I used Scheuer and Black (2004) method as a reference to understand the age-related changes/growth and development of the MT1. Due to the fact that the major developmental changes are complete prior to adulthood, it was easy to see why the life-history of the MT1 was not a primary method for aging skeletons, particularly when dental development and other skeletal variations with tested results were available. These aging data, like all other data on the Dakhleh sample were collected in-blind. As none of the standard skeletal manuals (e.g., Bass 1995; Buikstra and Ubelaker 1994) commonly used in bioarchaeology provide osteometric data for the MT1, I followed White et al. (2011) who report on five linear measurements that are described in chapter 3. Various combinations of these measurements, as well as slight variations, were used in several publications trying to determine sex in specific populations (Mountrakis et al. 2010; Robling and Ubelaker 1997; Wolpoff and Frayer 1985). The results, though positive, were generally not useful as they relied on multiple metatarsals, and showed differences between individuals from

different populations. For example, Mountrakis et al. (2010) found the accuracy of their discriminant function equations derived from a Greek cemetery sample to be between 80-90%, depending on the number of metatarsal elements used. Moreover, Robling and Ubelaker (1997) found similar correlations using their discriminant functions based on combined complete metatarsal (1-5) analysis on a sample from the Terry collection and a small cadaver population provided by the University of Missouri. They also found that the discriminant function accuracy varied depending on race. Similarly, Byers et al. (1989) used MT1 measurements on cadavers and attempted to estimate living stature with results that were no more accurate than using fragments of the femoral shaft. Moreover, the fact that all these results are population-specific further compromises their broad use in bioarchaeology, and specifically the Kellis 2 skeletal population.

The clinical literature reports the presence of a lateral facet on the MT1 (Intermetatarsal Facet (IMF)), a nonmetric trait that may have potential for both morphogenetic, functional or pathology-oriented research. I collected and tested this trait but little is known of its compositional (age/sex) association, or its association with foot pathology. Investigation of the latter requires the complete foot for biomechanical analysis, which is not possible to conduct with just the MT1. Concerning pathology, the total foot-bone complex has been studied for degenerative joint disease (DJD) (Kilmartin et al. 1991), but by itself, the MT1 is no different than most other bones used to document DJD. One such pathology, which appeared frequently in the Kellis 2 skeletal population, was osteoarthritis (OA). A case can be seen in **Figure 2**. A visual inspection of this individual (Burial 4) showed only eburnation to the distal surface of the head, while a µCT image was able to fully illustrate the osteoarthritic (subchondral) cyst.
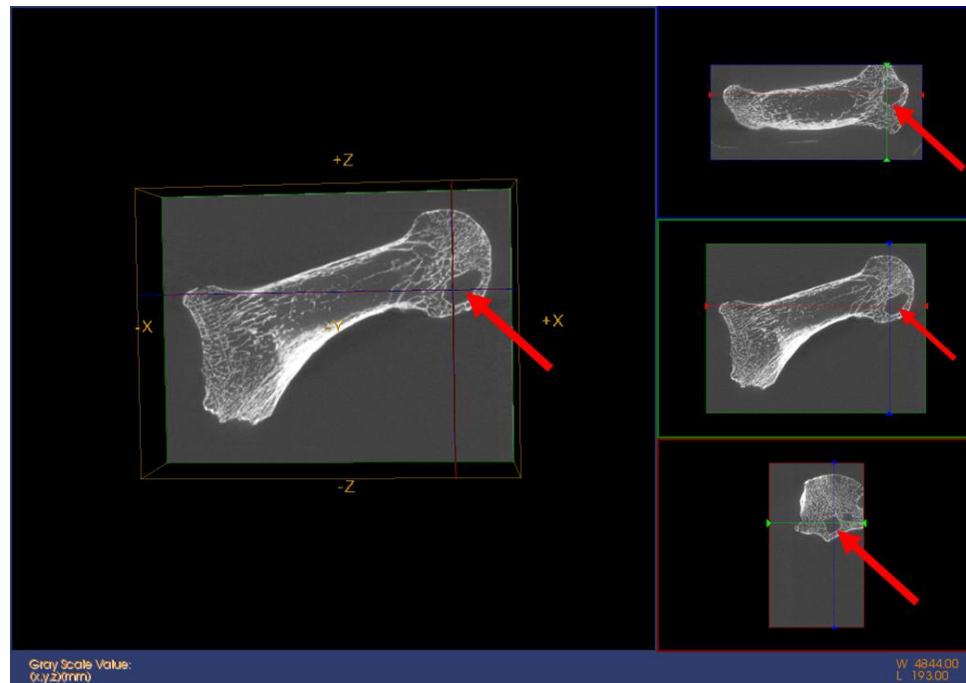
Figure 2 Osteoarthritis of the MT1. Kellis 2 burial #4 diagnosed with Osteoarthritis. Visual inspection showed slight eburnation on the distal surface of the head from exposed and polished trabeculae. µCT imaging allowed for the visualization of osteoarthritic cysts that formed as a result of bone-on-bone agitation and the disappearance of cortical bone. These cysts are indicated by red arrows.

Additionally, another disease also has a high rate of occurrence at the MT1-proximal epiphyseal joint, namely gout (Aufderheide and Rodriguez-Martin 1998). Though gout is a complex disease in terms of etiology, one rather constant characteristic is that, in its chronic phase, which is initiated by massive depositions of uric acid crystals, it normally involves the MT1 phalangeal joint. The crystal build-up results in lytic lesions around the joints, and have been diagnosed without the presence of urate crystals. In paleopathology, there have been very few identified cases (n = 3). One hypothesis for its absence is the fact that water can remove the urate crystals, a diagenic effect illustrating the environmental influence on preservation. However, Rothschild and Heathcote (1995)

report that 5% of their Pacific population in Guam had lytic lesions characteristic of gout. As gout is known in present-day populations in the Far East, this publication probably built on this historical information. Of interest is that one burial from Kellis 2, estimated to be a 55 ± 5 year old male (Burial 213), has extensive deposits around both MT1 phalangeal joints, with sharply defined, periarticular lytic lesions, with overhanging ledges and perilesional sclerosis (see **Figure 3**). SEM testing of the deposits were not positive for urate. This, in addition to the bilateral nature of the lesions, suggests only a provisional diagnosis of gout.   An alternative diagnosis is calcium pyrophosphate deposition disease (CPPD), which is a variety of crystalline arthritis, a form which closely mimics gout (Rothschild and Martin 1993). Also, included in the differential diagnosis is psoriatic arthritis (Rothschild and Martin 1993).

Figure 3 Gout. The metatarsal 1s and proximal and distal phalanges from burial 213, a 55 ± 5 year-old male from the Kellis 2 cemetery in the Dakhleh Oasis, Egypt. These photos show the exuberant build-up of bone, the sharply defined peri-articular lytic lesions with overhanging ledges and perilesion sclerosis, which are suggestive of gout. A

SEM and ICP test for uric acid was negative. The differential diagnosis includes calcium pyrophosphate deposition disease (CPPD) and psoriatic arthritis. Gout is known to involve the MT1s first although usually it is unilateral.

A nonmetric, but functional, trait occurring on the metatarsals, is a dorsal facet that develops from chronic hyperdorsiflexion during kneeling (Ubelaker 1979). This uncommon variant has been described in a small number of research articles from different populations, and all agree that it represents hyperdorsiflexion, but the behavioural contexts vary (Ubelaker 1979; Molleson 1989; Lai and Lovell 1992; Lovell and Dublenko 1999; Molto et al. 2017). Molto (2017, in review) has found this facet in all adult 'working-class' individuals in a Shang dynasty sample from Anyang, China. In this population, the facet develops during childhood and is observed initially on the MT1. Around the 4th decade all metatarsals have the facet (**Figure 4**). Molto et al. (2017) hypothesized that it likely relates to kneeling behaviour while eating, as the population had no tables and chairs, and the kneeling position was used from childhood on. Of course, there were probably other unknown behaviours associated with this development. This facet was completely absent in the Dakhleh Oasis population from Kellis.

Figure 4 Kneeling Facet. Dorsal view of the left metatarsals of an older adult male burial from the Anyang site in China showing facets on the anterior-dorsal surfaces. These facets develop from chronic kneeling and in this population, they are present in all adults. They develop on the MT1s first. These facets are absent in the MT1s from Dakhleh.

This overview showing the limited role of the MT1 in bioarchaeological research was, in retrospect, the ultimate reason for selecting this bone for future biochemical research. However, during my curational research role in this project, I decided to examine the macro- and micro-structure of this weight-bearing bone as a potential method for investigating human variation and bone health in antiquity. I hypothesize that the first metatarsal is an excellent proxy for examining bone density and architectural changes, since it has similar structural and physiological properties as weight-bearing

bones such as the vertebrae, hips and lower limb long bones (see chapter 2), is very similar in structure, development and physiology to the long bones, and it is often preserved in archaeological samples. I hypothesize that its application to bone health will provide an important tool for bioarchaeological research, a process that can be adopted for use in all populations. Though there has been virtually no information on the MT1 in bioarchaeological bone health research, the extant literature on bone density loss with age in both sexes, and predominantly in females in the menopausal years, leads to the null hypothesis that this research will not support the MT1 as a proxy for sex and age-related regressive changes in the bone mineralization and architecture in this past population. As a corollary to this, is the null hypothesis that the MT1 will not be useful in modern clinical contexts for measuring bone density changes. A final research design feature that needs mention is the fact that all this research was done in-blind: I had no knowledge of the age, sex, genetics and pathologies of the individuals analyzed in this Egyptian population.

1.4   Thesis Outline

There are five additional chapters in the thesis. Chapter 2, Literature Review, provides an in-depth analysis of the anatomy, growth and development, biomechanics and neurovascular aspects of the MT1. Additionally, this chapter will review the accepted ways in which bone health, specifically osteoporosis, is typically studied for ancient populations. This information is fundamental for understanding the information in the subsequent chapters. Chapter 3, Materials and Methods, details the skeletal sample used, and describes the data gathering and statistical methods involved in testing the efficacy of the MT1 in the bioarchaeological research. A key aspect of the research, as noted, is the

fact that it was conducted with a 'blind design', in that I had no previous knowledge of age, sex or pathology of the skeletons, and each of the linear measurements were optimized for observer reliability. Moreover, this chapter places this investigation within the larger Dakhleh Oasis Project, and describes the work on the population that was previously conducted. Chapter 4, Results, provides the results of each test used in this dissertation. Chapter 5, Overview, Discussion, Conclusions and Future Considerations, provides a discussion of the MT1 as a means for supplying relevant data for current bioarchaeological research and potentially for clinical assessments of bone health. This chapter also considers the possible future research directions with regards to this skeletal element.

Chapter 2

2 LITERATURE REVIEW: Structure and Function of the Human First Metatarsal and Diagnosing Skeletal Health in Antiquity

2.1 Introduction

Section 2.2 presents a detailed analysis of the anatomy, growth and development, biomechanical, neurovascular, and morphological variation (i.e., nonmetric and metric) characteristics of the MT1. A reference guide of terminology is given in Appendix A. Section 2.3 defines osteoporosis, and details the technological evolution, both in clinical and bioarchaeological research, that has occurred in studying bone health, and specifically osteoporosis. This provides the necessary background information and guide for understanding the information in subsequent chapters.

2.2 Anatomy of the foot: General Comments

As noted, the human foot is uniquely adapted for several functions, namely, weight-bearing, and bipedal locomotion, and the metatarsal 1 is one skeletal element of the foot's functional anatomy. The human foot is composed of 28 bones in three major segments (7 tarsals, 5 metatarsals, 14 phalanges and 2 sesamoid bones). Both of the latter are associated with the MT1. The tarsals and metatarsals form the longitudinal and transverse arches of the foot. These elements are rigid, in terms of their joint articulations, which facilitates the arch to absorb and distribute the energy produced during locomotion from the lower leg, through the foot to the ground.

In anatomical position, plantar refers to the sole of the foot with dorsal being the superior surface. When the foot is flexed (bringing the toes upward) the movement is

therefore called dorsiflexion. Distal refers to the tips of the toes, while proximal is towards the tibial-fibular axis. Medial is towards the midline of the body, while lateral is way from the midline. Moreover, there are terms used to convey the direction of the motion, or action of the muscle groups (i.e., adduction, abduction, flexion and extension).

It is germane to note that though the normal number of bones is 28, there are over 50 reported supernumerary or sesamoid bones that are present in the developing foot but are absent in the mature foot (Scheuer and Black 2004). The specific functions of these sesamoids during development have yet to be elucidated, but they may have some functional significance. The sesamoids that persist into adulthood are found in association with the big toe and are thought to function as small buffer areas. One of these supernumerary elements, if ossified separately, is called *os intermetatarseum*, which is a free ossicle distally and laterally to the medial cuneiform and adjacent to the MTI and MTII. When present in adults it is considered benign with regard to the overall anatomy and function of the foot (Scheuer and Black 2004).

The first metatarsal, or hallux, articulates with the proximal and distal first phalanges. It is part of the first ray of the foot, and with the phalanges also includes the medial cuneiform (White et al. 2011). The first ray of the foot maintains the arch design (lateral and transverse) of the human foot, which helps humans to stand, walk, run and jump bipedally.

2.2.1 The Anatomy and blood supply of the MT1

Figure 5 shows a number of views of the MT1. Although the shortest in absolute length, the MTI is by far the largest of the metatarsals in terms of size, robusticity and strength

(Glasoe et al. 1999; Martini 2001; White et al. 2011). Although small and somewhat featureless, the MT1 has a complex anatomy in terms of its articulations, musculature and ligamentary support systems, as well as its arterial supply. In its general anatomy, the MTI is organized into three segments: The base, the body or shaft, and the head. In this configuration, it closely resembles the long bones of the human skeleton. Additionally, the medial-lateral pinching of the shaft allows for the distinction between the dorsal surface and the plantar surface of the bone (Scheuer and Black 2004). The dorsal surface of the body is flat and smooth, while the plantar surface is convex, creating an arch when viewed from either the medial or lateral sides. In cross-section, the body is prismoid in form, with the dorsal surface being wider than the plantar surface.

Figure 5 Multiple Views of the Human First Metatarsal. Left: Medial view of a right first metatarsal (plantar to the left and dorsal to the right). **Upper-Right:** Distal view of a right first metatarsal (plantar is down and dorsal is up). **Lower-Right:** Proximal view of a right first metatarsal (plantar is down and dorsal is up)(Kellis 2 Burial 274, Photography by Mathew Teeter, 2013).

The MTI consists of a shell of cortical bone of varying thicknesses along its distribution, and trabecular bone located primarily within the head and base, diminishing within the shaft (Muehleman et al. 1999). The differences in the density of this bone throughout its structure will be discussed in the biomechanical section due to the functional aspects of the variation observed. A nonmetric variant of the MT1 is a facet on the lateral aspect of the base, known as the Intermetatarsal facet. This variation is due to articulation with the MT2, and may in fact represent an angulation problem, as it possibly relates to a pathology known as *metatarsus primus varus* (Hyer et al. 2005). Apart from this variant, the MT1, as well as the other metatarsal bones, are without notable nonmetric variants (White et al. 2011).

The MTI articulates proximally with the medial cuneiform, and distally with the proximal end of the first proximal phalanx. The proximal articular surface is reniform or kidney-shaped, while the distal articular surface is rounded and smooth. Occasionally, the MTI will articulate with the second metatarsal on the lateral surface of the base. At this location, in individuals who have this articulation, there will be an oval facet (Intermetatarsal facet) located on the lateral surface of the base of the MTI (White et al. 2011). The head of the MTI is large with two small grooved facets on the plantar surface. These facets articulate with two small sesamoid bones. The sesamoid bones are embedded in the *flexor hallucis brevis* muscle, which extends beyond the head of the MTI and inserts into both the medial and lateral portions of the first proximal phalanx. The sesamoid bones act to distance the *flexor hallucis brevis* from the metatarsophalangeal joint, thus allowing the joint to function properly (Martini 2001; White et al. 2011).

The joint created by the proximal end of the first metatarsal and the distal end of the medial cuneiform is known as a tarsometatarsal joint (TMT), while the joint created by the articulation of the head of the first metatarsal and the base of the first proximal phalanx is called the metatarsophalangeal joint (MTP). The TMT is considered a gliding diarthrodial joint. This joint is quite rigid as it is encased within a ligamentous joint capsule, although some movement does occur. The MTP joint is an ellipsoidal diarthrosis joint that is capable of flexion/extension, and adduction/abduction (Martini 2001).

There are numerous ligaments and muscle tendons associated with the first metatarsal. The ligaments act to anchor the MTI to surrounding elements, while the muscle tendon attachments facilitate movement of the associated MTI joints as well as movement of the elements located distally to the MTI (Martini 2001; White et al. 2011). The base of the MTI is grooved for the insertion of the tarsometatarsal ligaments. There are two sets of these tarsometatarsal ligaments: the dorsal tarsometatarsal ligaments and the plantar tarsometatarsal ligaments. As their name suggests, the dorsal tarsometatarsal ligaments are located on the superior surface of the base of the MTI, while the plantar are located on the inferior surface of the base of the MTI. These ligaments act to bind the MTI to the medial cuneiform creating the stable TMT joint. Unlike the other 4 metatarsals, the base of the MTI is not connected to the base of any other metatarsal for stability. In this respect, it resembles the metacarpal of the hand (Martini 2001). The heads of all of the metatarsal bones, however, are connected by the transverse metatarsal ligament. The articulation of the first metatarsal with the first proximal phalanx is mediated by 3 more ligaments – one plantar ligament, and two collateral ligaments.

In addition to the array of ligaments associated with the MTI, there are a number of tendon attachments for the muscle groups responsible for the movement of the ankle, foot and toes. Two muscles directly insert into the base of the MTI, while 4 tendons run along the MTI and insert into the first proximal phalanx (Martini 2001; White et al. 2011). The *tibialis anterior* muscle originates on the lateral condyle and the proximal shaft of the tibia and inserts in to the medial cuneiform and the medial base of the MTI. This muscle is responsible for the dorsiflexion of the ankle as well as the inversion of the foot. On the plantar surface at the base of the MTI there is a tuberosity that marks the insertion of the tendon of *peroneus longus* (*fibularis longus*) muscle. The *peroneus longus* muscle originates from the head and proximal parts of the fibula and the lateral condyle of the tibia and inserts into the lateral base of the MTI and the lateral side of the medial cuneiform. This muscle is responsible for everting the foot and plantar flexing the ankle.

The *flexor hallucis longus* muscle originates in the distal posterior portion of the fibula, runs along the plantar surface of the MTI, between the grooves of the sesamoid bones (*flexor hallucis brevis*), and eventually inserts into the inferior base of the distal phalanx of the hallux (White et al. 2011). This muscle acts to flex the joints of the hallux. The *extensor hallucis longus* muscle originates on the anterior surface of the distal fibula and inserts on the superior surface of the base of the distal phalanx of the hallux. This muscle is responsible for the extension of the joints of the hallux. The *flexor hallucis brevis* muscle originates on the inferior surface of the cuboid bone, divides into two portions, which run along the medial and lateral surfaces of the MTI, and insert into the medial and lateral surfaces of the first proximal phalanx (Martini 2001; White et al.

2011). This muscle group is responsible for the flexion of the hallux much like the *flexor hallucis longus* muscle. The *extensor hallucis brevis* muscle originates in the calcaneus and runs along the medial and lateral surfaces of the MTI and inserts into the medial and lateral surfaces of the first proximal phalanx. This muscle, again, like the *extensor hallucis longus* muscle, acts to extend the hallux. These muscle groups, their origination sites, insertion sites, and actions are itemized in **Table 1**.

Table 1 Muscle Groups, Origination, Insertion and Action with respect to the First Metatarsal.

Muscle	Origin	Insertion	Action
Tibialis anterior	Lateral condyle and proximal shaft of the tibia	Base of the MTI and medial cuneiform	Dorsiflexion at the ankle; inversion of the foot
Peroneus longus (fibularus longus)	Lateral condyle of the tibia, head and proximal shaft of the fibula	Base of the MTI and medial cuneiform	Eversion of the foot and plantar flexion at the ankle; supports the longitudinal arch
Flexor hallucis longus	Posterior surface of the fibula	Inferior surface of the base of the distal phalanx of the hallux	Flexion of the joints of the hallux
Extensor hallucis longus	Anterior surface of the fibula	Superior surface of the base of the distal phalanx of the hallux	Extension of the joints of the hallux
Flexor hallucis brevis	Inferior surface of the cuboid	Medial and lateral surfaces of the first proximal phalanx	Flexion of the joints of the hallux
Extensor hallucis brevis	Calcaneus	Medial and lateral surfaces of the first proximal phalanx	Extension of the joints of the hallux

Like long bones the blood supply to the MTI varies in the immature and mature states. In the immature, the ends or epiphyses have their own vessels as the nutrient foramen of the diaphysis cannot penetrate the cartilaginous epiphyseal plate of the base. The main blood supply of the MT1 originates from the anterior and posterior tibial arteries as well as the fibular artery (Rath et al. 2009). These larger arterial supplies

branch into a number of smaller arteries which extend distally to the MTI. The base of the first metatarsal is supplied by dorsal and plantar arteries. As noted without these arteries, the base would not receive blood supply through the main nutrient foramen due to the presence of the epiphyseal cartilaginous plate (Rath et al. 2009). The diaphysis of the MTI is fed by the commonly observed nutrient artery. This foramen is normally, but not always, located on the medial side of the diaphysis, directed away from the growing end. Sometimes it is difficult observe and in some diseases, like leprosy, the nutrient foramen can be very enlarged. The head of the MTI is supplied by the first plantar metatarsal artery (Rath et al. 2009). Therefore, each one of the main divisions of the MTI (base, shaft and head) receives separate blood supplies.

2.2.2   Growth and development of the first metatarsal

The formation of the skeleton is a complex and highly controlled system. Many internal and external factors interact in order to achieve the '*normal*' mature skeletal structure. If one of these factors (e.g., timing, genetics, hormone levels, receptor structure, nutrient supply, etc.) is amiss, the whole system breaks down, causing malformations or even death. During the very early developmental stages, there is remarkably little flexibility in terms of the timing of developmental events. This timing, as will be seen, is much less rigid during the later developmental periods. This section examines some of the general aspects of skeletal growth and development, and specifically, the aspects of the growth and development of the first metatarsal.

The appendicular skeleton is formed via endochondral ossification that arises from the mesoderm – one of three primary germ layers of the developing embryo (Scheuer and Black 2004). Endochondral ossification incorporates a cartilaginous

precursor, which differs from the process of intramembranous ossification that is present in the skull. Once formed, the skeletal system actively remodels throughout life in order to adapt to the constant and changing forces to which it is exposed (Muehleman et al. 1999). The developed bones deform during stress, and this deformation stress, followed by periods of relaxation, results in the formation and remodelling of bone. The response of developing bone to mechanical (and other stressors) is the fundamental tenet of Wolff's law (Muehleman et al. 1999).

Prior to the formation of the recognizable skeleton and the dynamic process of remodeling, many developments happen in the embryonic stage including cell differentiation and migration. This generally occurs top to bottom, that is head to torso, and ending with the areas that will become the hands and feet (Martini 2001; Scheuer and Black 2004). Due to this proximodistal temporal organization of the development of the human embryo, the development of the foot lags behind that of even the hand. This lag is already approximately 5-6 days behind from the onset of embryonic development (Scheuer and Black 2004). With respect to the development of the foot and associated MTI, at approximately 37 days after fertilization and the beginning of intrauterine life, the footplate begins to develop on the caudal end of the lower limb bud. By the time the foot plate is visible, the tibial nerve has already penetrated into the region (Scheuer and Black 2004).

On approximately the 41st day of embryonic development, the tarsal region can be visualized. Moreover, by this time the tibial nerve has reached the plantar surface of the foot (Scheuer and Black 2004). By the 44th day, distinct digital rays can be seen and each tarsal and metatarsal has begun chondrification. The latter is the process of creating

21

cartilage from the undifferentiated mesodermal cells. At approximately the same time, interdigital notches begin to form, separating the eventual toes from one another. This process is accomplished by selective cell necrosis (apoptosis) in the ectodermal and underlying mesodermal interdigital zones, which results in the formation of 5 separate toe structures (Scheuer and Black 2004). This process is similar in both the hands and the feet of the developing embryo.

By the end of the 57th day of intrauterine life, the foot has reached the end of its embryonic development. The soles of the feet face medially and dorsally and the toes of one side of the body are usually in contact with the toes of the other side (Scheuer and Black 2004). This position is known as '*praying feet*'. The reason they face somewhat dorsally is that the angle of the ankle has not developed at this stage, which causes the foot to approximately be aligned with the rest of the leg.

Not including the supernumerary bones and sesamoids, it is generally agreed that there are potentially 46 separate centres of ossification in the foot (Martini 2001; Scheuer and Black 2004). Of these, 26 are primary centres, and 20 are secondary centres of ossification. Many of the primary centres of ossification arise during the early fetal period, while the remainder develop postnatally. The secondary centres arise interspersed between the sequential appearance of the primary centres, and therefore the term secondary may be confusing (Scheuer and Black 2004). There is no linear temporal relationship between the two types of ossification centres unless when referring to the same skeletal element. There is a great deal of individual variation when it comes to the exact timing of the development of these centres, and when genetic ancestry as well as environmental factors are considered, the timing of their appearance and fusion is quite

variable (Scheuer and Black 2004; White et al. 2011). This results in large age ranges for these developmental events.

In terms of fetal development (9-12 weeks until birth), ossification commences in the metatarsals, followed by the distal phalanges and proximal phalanges, and finally the middle phalanges. The primary centres of ossification are located on the shafts of the metatarsals and generally appear between 8-10 weeks prenatally, but the first metatarsal may be delayed up until the 12th week of development (Scheuer and Black 2004). While the secondary centres of ossification, which form the epiphyses, are located near the heads of the 4 lateral metatarsals, it is located in the base of the MTI. Consequently, the base of the MTI develops from a secondary ossification centre, while the shaft and distal articular surfaces are formed by the primary centre (Scheuer and Black 2004). As a general rule, all metatarsal epiphyses may develop from more than one centre of ossification. This is highly variable, and as many as eight centres have been observed in the first metatarsal. They will, however, begin to consolidate at ~4 years of age, so that only a single secondary centre is present (Scheuer and Black 2004).

Generally, the time of appearance of the secondary centre of ossification in the epiphysis of the base of MT1 is between 18-20 months in females and 26-31 months in males. The epiphysis at the base of the MTI is quite different from all other metatarsal epiphyses, so much so, that it is often discussed separately in the current literature (Scheuer and Black 2004). The basal surface of the epiphysis is well developed by the age of 6-7 years (Scheuer and Black 2004). Around this time, the proximal surface is roughly ovoid and slightly thicker at the plantar margin. The lateral border is straight in appearance, while the medial boarder is rounded when viewed from the proximal end. By

8 years of age, the proximal epiphysis has its classic kidney-shaped appearance, with the concave margin facing laterally. The latter is a key visualization for siding the MT1s. The articular margins of the epiphysis are well formed by the age of 10, and the *peroneus longus* muscle attachment site is also visible (Scheuer and Black 2004). By approximately 12 years of age, the epiphysis has adopted its adult morphology. Interestingly, so called '*pseudo-epiphyses*' are often described on the MTI. They tend to appear as clefts or notches in the normally non-epiphyseal distal end of the bone. These are thought to arise from the invasion of the primary centre into the head of the metatarsal and may appear at approximately 4-5 years of age (Scheuer and Black 2004).

Fusion of the base of the MTI occurs at approximately 13-15 years of age in females, and 16-18 years of age in males (Scheuer and Black 2004; Weiss et al. 2012). The timing of the fusion of the epiphysis of the MTI can be confusing as often an *epiphyseal scar remains*, which is the remnant of the growth plate. Weiss et al. (2012) note that the persisting scar can result in age assessment errors as a closed epiphysis and recorded as unfused.

In summation, the appearance of the primary centre of ossification in the MTI appears mid-shaft at approximately 12 weeks prenatally. The appearance of the secondary site of ossification on the epiphysis at the base appears between 2 and 3 years of age. Epiphyseal fusion occurs at 13-15 years old for females and 16-18 years old for males. Beyond the fusion of the calcaneal epiphysis (15-16 for females and 18-20 for males), the fusion of the MTI is the last to occur in the foot (Scheuer and Black 2004). The age ranges given for the timing of specific events in the development of the MTI represents one of the classic problems in the area of studying growth and development in

24

past populations. The inability to sex juvenile human skeletal remains confounds the study of growth and development in that there are already significant differences between the two sexes in the timing of developmental events. This does not allow researchers to create accurate estimations of the critical developmental stages in terms of timing with respect to the two sexes.

2.2.3   First metatarsal biomechanics

As noted, the foot is a very complex anatomical and biomechanical structure that allows for the transfer of force from the lower limb to the ground during movement and at rest (Dawe and Davis 2011). The science of biomechanics examines the forces, and their effects, on a biological structure. This section examines the biomechanics of the first metatarsal both as part of the larger pedal organ, and as an element of that larger structure. The exact mechanics of this may vary from person to person depending on their personal gait. This section describes the mechanics of a '*normal*' gait. Although the biomechanics of the foot are researched quite often, the biomechanical function of the first metatarsal by itself is dramatically understudied. This is in part due to the inability to develop viable methods to study the MTI *in situ*, separately from the rest of the foot. There is little doubt that foot problems are one of the many scars of human evolution that are a consequence of the stresses our bipedal gait places on our feet (e.g., plantar fasciitis, over pronation etc.), both in movement and when stationary. Foot and gait problems have spawned the field of podiatry.

The force distribution during normal walking or jogging begins with lateral heel pressure called the *heel strike*. As the foot plantar-flexes from the heel towards the ball of the foot, this force is then transmitted up the lateral border of the foot to the heads of the

metatarsals, where it is dispersed, with the largest of the loads going to the MTI-sesamoid complex, followed by the second metatarsal (Adelaar 1986; Chen et al. 2010; Gross and Bunch 1989; Pan et al. 2006). Interestingly, the disorder *hallux valgus* causes less load to be carried by the MTI-sesamoid complex due to sesamoid rotation. This rotation causes some of the load normally absorbed by the head of the MTI to be redistributed to the heads of the other metatarsals which may cause pain and stress lesions (Garcia-Aznar et al. 2009; Gross and Bunch 1989; Kirby 2000; Pan et al. 2006).

With respect to the TMT joint, the movement of the first metatarsal is very limited during walking and jogging. There is roughly only between 3.5 degrees of motion during flexion/extension and 1.5 degrees of motion during pronation/supination. This is considerably less with respect to the other TMT joints, where there is approximately 9 degrees of flexion/extension and pronation/supination (Cornwall and Mcpoil 2002; Dawe and Davis 2011). Thus, the TMT joint contributes very little to mid-foot flexibility and is somewhat rigid, but is useful in the energy absorption. This joint stability is reinforced by very strong ligamentous support previously noted (Dawe and Davis 2011; Adelaar 1986). Thus, the MTP joint is much less rigid than the TMT joint. The normal range of motion at the MTP joint is 30 degrees in plantarflexion and 90 degrees in dorsiflexion. This amount of flexibility is essential for the function of the foot during bipedal locomotion and full dorsiflexion is essential for a normal gait (Dawe and Davis 2011). The phases of dorsiflexion followed by plantarflexion represent the last two stages in which the foot is in contact with the ground. The remaining energy from the heel strike is passed into the ground, and propulsion from the action of the foot and its muscles commences. The

inflexibility of the TMT joint and the highly flexible nature of the MTP joint facilitates this progression to transpire.

The ball of the forefoot, which consist of the heads of the metatarsals, support a significant proportion of the body weight during rest and locomotion. As protection, this area is covered with fleshy pads which help to absorb some of the energy. This serves as a pivotal point during the push-off phase of locomotion. The force that is applied to each individual metatarsal is difficult to estimate, and most studies have only looked at the combined force across the ball of the forefoot (Chen et al. 2010). The greatest force is measured at the point of contact of the ground and the head of the first and second metatarsals (Gross and Bunch 1989). The measurements from beneath the heads of the metatarsals show that 30% of the force is under the MTI, and 28% of the force is under MTII (Pan et al. 2006).

Muehleman et al. (1999) found that the pressures exerted on the heads of the MTI and the other metatarsals caused structural changes in terms of bone density. They found that the heads of the metatarsals were denser (as measured by the cortical density) than the bases. This was in response to the repeated stress of striking the ground during motion, as well as the forces due to gravity that were exerted on the balls of the feet during periods of rest. They also found that the dorsal surface of the MTI was denser than the plantar surface (Muehleman et al. 1999). This, in part, is due to the arch shape of the shaft of the bone, which transfers compression stress to the dorsal surface while the bone flexes. This action works as part of the shock absorbing properties of the foot, and specifically the MTI. The final difference noted by Muehleman et al. (1999) was that the lateral surface of the MTI was denser than the medial surface. This again was as a result

of bone flexing in response to stress directed towards the lateral portion of the shaft during motion. The arch-shape bone structure as well as the adaptive nature of bone to stress allows the MTI to contribute to the overall absorptive properties of the foot and the transverse and lateral arches during mechanical stress.

The complex structure of the first metatarsal and its associated elements facilitates its significant contribution in bipedal locomotion. Its elegant arch design, differential bone density, and intricate ligament and tendon insertions are micro-witnesses to its major role in our bipedal gait. It functions as part of our overall pedal unit, a smaller first ray, and as a discrete skeletal element towards this goal. A major part of this research will focus on the micro-structure of the MT1 using µCT will facilitates a three-dimensional visualization of the complex structures of this bone and the forces that combine to make them.

2.2.4   Neurovascular influence of the structure of the MT1

The importance of the weight-bearing function and its effect on the microstructure of the MT1 needs emphasis. **Figure 6** shows a µCT parasagittal section of an MT1 from a ~45 year old adult female (burial #19) from the Kellis 2 cemetery, Dakhleh Oasis, Egypt. The ample cortical bone especially on the inferior surface is clear, as is the abundant trabecular bone in the proximal and distal ends. Both the thickness of the cortical bone and the diffuse trabecular pattern reflect its weight-bearing function.
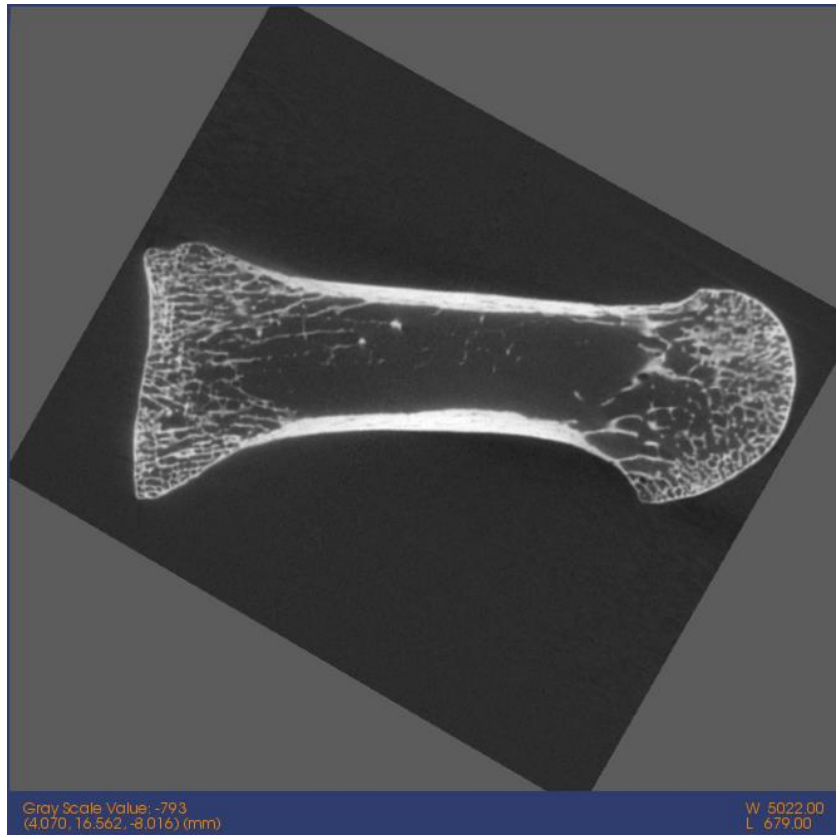
Figure 6 µCT Parasagittal section of Burial 19, Left MT1, Kellis 2 Cemetery, Dakhleh, Oasis, Egypt. Note the thick cortical bone of the dorsal and plantar surfaces, as well as the complex network of trabeculae throughout the head and the base.

In addition to the mechanical role of weight-bearing, it is important to emphasize that bone structure is maintained by an intricate balance of the neurovascular system. The arterial supply of the foot, including the hallux, is derived from the anterior and posterior tibial and peroneal arteries, and their numerous branches. They are responsible for the structural maintenance of all skeletal elements nurtured by them, including the MT1. The arterial control is accomplished by a sophisticated homeostasis between the sympathetic and parasympathetic systems, whereby there is a balance between osteoblastic and osteoclastic activities which enables the maintenance of skeletal function. When there is a

dysfunction either by disuse atrophy (DA), metabolic diseases, or in diseases that alter the neurovascular function (e.g., leprosy), bone structure and function can be severely affected.

In terms of DA, the overall diameter of the bone may be maintained but the cortex becomes thin and osteoporotic, and is associated with a relative increase in the diameter of the medullary cavity, as well as a reduction in quality and number of trabecular structures. The autonomic control is hypothesized to be maintained, but the lack of use disrupts the osteoclastic-osteoblastic homeostasis, thus the structural change noted is a direct consequence of the reduced stress load (note, stress does not have a positive or negative connotation).

In terms of neurovascular disruption and its role in bone structure, the presence of diaphyseal remodeling in lepromatous leprosy is instructive (Andersen et al. 1992). In diaphyseal concentric remodeling there is a progressive loss of the diameter of the metatarsals, metacarpals and proximal phalanges. The cortical bone is maintained while the medullary cavity progressively decreases to the point where only cortical bone is present in the distal diaphysis and the medullary cavity vanishes. This results in a drastically increased risk of fracture (**Figure 7**). Andersen et al. (1992) hypothesized that the changes occur because of sympathetic neuropathy concomitant with the alteration of the peripheral vascular bed dynamics which selectively stimulate extracortical osteoclastic and endosteal osteoblastic activity. Thus, the disruption of the sympathetic-parasympathetic balance in arterial control by this autonomic neuropathy alters the osteoblastic-osteoclastic homeostasis. Noteworthy in leprosy is that the MT1 is the least affected bone, which may reflect its weight bearing role relative to the other metatarsals,

despite the presence of this neuropathy. As the Kellis 2 sample has several individuals
with leprosy, these comments have significance for understanding bone dynamics.

Figure 7 Leprosy. The remaining foot elements of an individual (burial 116) from the
Kellis 2 cemetery, Dakhleh Oasis, Egypt. Note the concentric remodeling of most of the
bones, as well as the overall "untouched" appearance of the first metatarsals.

2.2.5   Morphological Variation

As noted, there has been a limited number of studies of morphological variation of the
MT1 apart from its use as a means of studying the evolution of bipedality. Ironically, in
the anatomical position there is limited direct contact between the MT1 and MT2,
although occasionally there is a distinct facet (intermetatarsal facet) on the lateral margin
of the base (**Figure 8**). This facet has been studied for its prevalence in some populations
(approximately 30%) and its possible association with foot disorders (e.g., *metatarsus*

primus varus leading to hallux valgus) (Hyer et al. 2005; Le Minor and Winter 2003). Other than these few studies, the intermetatarsal facet has had limited attention in contemporary studies, let alone bioarchaeological studies. There is another facet which can occur on the dorsal portion of the head, a kneeling facet, which is the result of constant kneeling with the toes of the foot hyperextended, and can be considered a Measure of Occupation Stress type variation. This variation will be discussed in a later section (Chapter 4) as it does not occur in the Dakhleh Oasis population, which, in itself, is an interesting observation.

Figure 8 Intermetatarsal Facet, Kellis 2, Dakhleh Oasis, Egypt. Intermetatarsal Facet, Kellis 2, Dakhleh Oasis, Egypt. Left: Left MT1, burial #107, no facet present. **Middle:** Left MT1, burial #30, slight intermetatarsal facet present. **Right:** Left MT1, burial #16, full intermetatarsal facet present (Pictures taken by Ed Eastaugh, Department of Anthropology, The University of Western Ontario, 2017).

2.2.6   Summary

The null hypothesis (H_0) examined in this thesis is that the MT1 will not prove very useful for osteobiographical research, particularly bone density and sexing. The morphological variation reported has to be seen in the light that researchers have not used the MT1 as an alternative when other methods are available. Despite its limited use in bioarchaeology, the MT1 was selected because it is often well preserved, and being a weight-bearing bone, it should have potential for bone density research. This in-depth review of the anatomy, growth and development, biomechanics and neuro-vascularity of the MT1 is an aid to understanding the information in the following chapters, particularly for bone density research.

2.3   Clinical and Bioarchaeological Investigations of Osteoporosis

The study of human diseases in the past has been a long-standing research interest within anthropology and bioarchaeology. These studies allow us to investigate not only the evolution of disease and disease pathogens, but also the role of contributing factors such as the environment, social status, genetics, sex, and age on disease risk and prevalence. Different populations, and the individuals within those population, have varying disease profiles and risks to certain diseases due to those contributing factors. One such disorder which appears throughout human history (to varying amounts) is osteoporosis. No matter the population, or the environment in which they live, this disorder appears in the older age-cohorts (particularly females) throughout human existence. The ubiquitous nature of this disorder throughout time, as well as the current and past societal costs of osteoporosis, warrants extensive research into the at-risk populations, the disorder's prevalence and contributing causes. Indeed, much study, both clinically and into the past,

has focused on this systemic disorder. With emerging technologies and methodologies, these studies have evolved over time in order to establish the varying presentations of osteoporosis, differences in prevalence seen between populations and between segments within those populations, as well as some of the contributing factors of osteoporosis.

The focus of this section is not only to define osteoporosis, but also the changes in the technologies and methodologies used in its study. This refers to studies that have taken place both clinically and in studies of populations and individuals in the past.

2.3.1   Osteoporosis – Definition, impact and etiology

Osteoporosis, or the loss of bone density resulting in an increased risk of bone fracture, is a serious disorder that has plagued human societies for millennia and is most likely part of our human legacy (Dequeker et al. 1997; Molto and Sheldrick 2010; WHO 2003). The association between bone loss and an increased risk of fracture was first noted over 160 years ago, by Sir Astley Cooper (Cooper 1999). Moreover, the term '*osteoporosis*' first came into use during the 19th century to describe the histologically porous appearance of bones sampled from older individuals by French and German physicians (Holroyd et al. 2008; Jordan and Cooper 2002). This term was then adopted to describe the current understanding of the disorder.

The prevalence of osteoporosis is highly dependent on constitutional factors, particularly innate bone density, age and sex, as well as having associations to varying environments, levels of activity and diet (Grynpas 2003; Holroyd et al. 2008; Molto and Sheldrick 2010). Peri- and post-menopausal females are at risk for Primary Type I osteoporosis which primarily involves the loss of trabecular bone, while both sexes are at

risk of Primary Type II (senile) osteoporosis, which has a later onset and involves both compact and trabecular bone. Again, females are at a much greater risk of developing this type (2:1) (Jordan and Cooper 2002; WHO 2003).

Specifically, osteoporosis is a systemic disorder of the skeleton that results in reduced bone density and an increased risk of low-impact fractures. Hip and wrist fractures, as well as vertebral compression deformities, are the most common injuries associated with osteoporosis (Cooper 1999; Holroyd et al. 2008; Jordan and Cooper 2002; WHO 2003). The most serious complications of osteoporosis are hip fractures which contribute to the greatest risk of morbidity and mortality. Modern clinical data estimate that between 2 and 3 pints of blood are lost as a consequence of a hip fracture. This amount of blood loss can be very detrimental to the body's systems, especially with respect to the older age-cohorts. It has been estimated that 3% of females and 8% of males over the age of 50 will die while hospitalized for an osteoporotic-related hip fracture (Brickley 2002; Holroyd et al. 2008). These numbers may be misleading as fewer males have osteoporotic-related hip fractures in the 50+ age-cohort, but it does illustrate that males are less likely to survive the effects of such a fracture. Moreover, the 1 year mortality rate in these individuals is 36% and 21% for males and females respectively (Brickley 2002; Holroyd et al. 2008). Morbidity and mortality rates in past populations undoubtedly were much higher due to a lack of medical treatment knowledge and the limited technology available. With the increased life expectancy of contemporary Western populations, osteoporosis is increasing in incidence and prevalence and is a major health problem both from the standpoint of quality of life and costs (Holroyd et al. 2008; Mays and Stevenson 1998; WHO 2003). Modern studies have estimated that

osteoporosis affects more than 75 million people in Europe, Japan and the United States, while accounting for more than 2.3 million fractures annually in Europe and the United States alone (WHO 2003). It is also estimated that the United States spends more than 10 billion dollars per year as a result of this disorder (Mays and Stevenson 1998).

There are three subcategories of osteoporosis. The first is known as Primary Type I. This form has been seen to affect post-menopausal women and is identified as a marked decrease in trabecular bone density and microarchitecture (Brickley and Agarwal 2003). It is thought that Primary Type I osteoporosis is the result of a reduction in the production of estrogens by the ovaries. These hormones are essential for maintaining bone homeostasis; therefore, without them the bone strength is compromised.

The second subcategory is known as Primary Type II or senile osteoporosis. This type affects both females and males (2:1) and is usually seen in the later years of life (70+). This type is identified as a marked decrease in both cortical and trabecular bone density and microarchitecture (Brickley and Agarwal 2003; WHO 2003). This category, like Type I, is brought on by the failure of the body to naturally maintain bone density and architecture due to the aging system and the reduction in hormone production resulting in instability in the synergy between osteoblastic and osteoclastic maintenance (Parfitt 2003).

The final subcategory is known as Secondary osteoporosis, and like Primary Type II, this disorder affects both the trabecular and cortical bone density and microarchitecture. This disorder can happen during any age, and affects both males and females equally (WHO 2003). The proximate cause of this form is from being in a

chronic diseased state resulting in bone destruction. The disease state can be brought on by environmental deficiencies such as lack of sunshine for vitamin D production, dietary deficiencies such as lack of vitamin C or protein, lack of exercise or even metabolic disorders or wasting diseases such as cancer – or any combination of the above. This form is exacerbated in modern populations by the use of certain medications, such as glucocorticoids, which are used in the treatment of many other disorders (WHO 2003). Unlike the primary types, secondary osteoporosis affects all age and sex cohorts equally. This category of osteoporosis will not be discussed further as it has very different causes and presentations when compared to the primary types of osteoporosis.

The reduction in bone density and microarchitecture that is seen in cases of primary osteoporosis can only be understood through the synergy of the basic-multicellular unit (BMU) and the way in which it produces and maintains bone. Historically, bone physiology was often thought of as two opposing forces – the osteoblasts vs. the osteoclast. These two types of cells were often thought of as working independently from one another. In reality, these two cell types work in cooperation as part of the BMU for the purposes of creation, redistribution, repair and replacement of bone (Frost 2003; Parfitt 2003). From growth until maturation, the modelling of bone by BMUs results in a net gain of ossified material. Once a mature state is reached, bones will remodel throughout life in order to redistribute material (i.e., calcium), repair the current structures (micro-damage), strengthen areas under stress, as well as replace old bone with new (Parfitt 2003). This does not mean that the processes of modelling and remodeling are exclusive from one another. Remodeling begins to occur once bone is formed, and

continues throughout life. Modelling, however, stops with the cessation of growth and the formation of the bones.

The BMU consists of a leading osteoclast (cutting cone in compact bone and hemicone in trabecular bone) and trailing osteoblasts (closing cone in compact bone and closing hemicone in trabecular bone). In compact bone, the osteoclast moves through the bone removing material creating an empty '*cylinder*'. The osteoblasts move in behind and refill the void left by the osteoclast. Occasionally, this results in osteoblasts being embedded in the newly formed bone matrix, which results in the creation of an osteoblast and the associated osteon or Haversian system (Parfitt 2003).

A similar process occurs in trabecular bone, but the complex three-dimensional nature of this bone makes the visualization of the process more complex. The osteoclast, instead of moving through the bone as was seen in compact bone, moves along the surface carving a trench (hemicone). The osteoblasts again follow behind replacing the material that was removed (Parfitt 2003). The distinction between the two different types of bone with regards to remodeling is important. The amount of surface area in trabecular bone is much higher than seen in compact bone. This may be the reason that bone loss is usually seen to occur in trabecular bone first, and why in general, the turnover rates of trabecular bone are much higher when compared to compact bone (Brickley and Agarwal 2003).

If the BMU is working properly, a zero net of bone gain or bone loss should be seen, and therefore bone loss indicates disordered remodeling. The latter is clearly the case with primary osteoporosis. The synergy between the osteoclasts and osteoblasts

forming a BMU can be disrupted in one of two ways: the first is osteoclast-mediated bone loss, which is excessive depth of osteoclast resorption. The excessive depth cannot be replaced by normal osteoblastic activity. This results in bone loss. The second way is osteoblast-mediated bone loss. This means that the resorption cavity is normal, but the osteoblasts do not replace it fully with new bone. Again, this results in bone loss (Parfitt 2003).

The distinction between these two types of bone loss processes is important for understanding some of the contributing factors of osteoporosis, as well as the distinction between the two types of primary osteoporosis. Primary Type I osteoporosis is thought to be the result of declining estrogen during the cessation of menses or menopause (WHO 2003). A decline in estrogen has been seen to increase both the life span and production of osteoclasts (Gruber et al. 1985; Parfitt 2003). This means that there are more osteoclasts and they are removing more material than was seen during normal bone maintenance, resulting in osteoclast-mediated bone loss. Conversely, Primary Type II (senile) osteoporosis is thought to be the consequence of a naturally declining number of osteoblasts due to the aging system (Parfitt 2003), which results in osteoblast-mediated bone loss. Osteoclast-mediated Type I osteoporosis is inherently a faster process which has been seen to affect primarily the trabecular bone (Gruber et al. 1985; WHO 2003). This is because of the nature of trabecular turnover, which was discussed above. Trabecular bone has a faster turnover rate because it has much more surface area for the BMUs to act upon. This is not to say that Type I osteoporosis does not affect the cortical bone; it is just less noticeable during the short time frame of peri-/post-menopause. Conversely, Type II osteoporosis is due to a slower and natural decline in osteoblast

numbers and osteoblastic activity, and thus, it is seen to detrimentally affect both the trabecular and cortical bone over a much longer time frame (adult peak bone density until death) (Brickley and Agarwal 2003).

2.3.2   Diagnosis, methods and technology

The methods and technologies for studying osteoporosis are usually not exclusive to either clinical research or studies of the past. Many of the same approaches and technologies have been used by both disciplines in order to diagnose and study the disorder. As discussed previously, primary osteoporosis is seen to affect trabecular bone (1^0 Type I) and whole bone (1^0 Type II). Due to this difference, diverse methodologies have been developed, and approaches employed, for the study of trabecular bone, cortical bone, and whole bone. This section will discuss the developments in visual analysis (gross analysis and histology), followed by methods that use imaging (X-ray, CT, etc.) to look at trabecular bone, cortical bone, and finally whole bone.

The diagnosis of osteoporosis is complex and multifactorial. Currently, many approaches and technologies are utilized to aid in the diagnosis of osteoporosis. Historically, diagnosis was made based solely on the physical appearance of the bone, as noted with Sir Astley Cooper and the physicians of 19th century Germany and France (Cooper 1999; Holroyd et al. 2008). Moreover, until relatively recently, the occurrence of an associated low-impact fracture to the at-risk skeletal sites was the only requirement for clinical diagnosis (Cooper 1999). This fracture-based diagnosis was simple and straightforward, but was not useful when discussing epidemiology and the at-risk population, as well as the skeletal changes that contribute to an increased risk of fracture. This approach to diagnosis has also been seen in bioarchaeological research with case

studies, and research into prevalence and risk assessed from the amount of associated fractures observed in a skeletal population (Bartonicek and Vicek 2001; Dequeker et al. 1997; Molto and Sheldrick 2010). This approach to diagnosis can be problematic. Although it correctly assesses individuals who present with osteoporotic-related fractures as osteoporotic, it does little to account for the at-risk population and those individuals who are subclinical. Not everyone who has osteoporosis will have a related fracture, thus skewing the reported prevalence of the disorder. Moreover, this method of diagnosis cannot factor in changes to bone on the micro-level.

In order to correct the shortcomings seen in a strictly visual or fracture-related approach to diagnosis, the World Health Organization developed a standard definition for use in the diagnosis of osteoporosis (WHO 2003) that estimates bone strength and identifies individuals who are at a greater risk of osteoporotic-related fractures. WHO suggests the use of Bone Mineral Density (BMD) as the standard for diagnosis. Therefore, beyond the presentation of an associated fracture, BMD measurements are the current standard for assessing bone fragility in clinical studies, as well as in most studies of individuals and populations in the past (Brickley and Agarwal 2003). WHO (2003) defines osteoporosis as any individual who falls 2.5 standard deviations or more below the BMD of the healthy adult-cohort of that same population (Holck 2007; Holroyd et al. 2008; Jordan and Cooper 2002; WHO 2003). Moreover, while a marked decrease in this density increases the risk of associated fractures, this new standard implies that the associated fractures are not necessary for the diagnosis of osteoporosis.

An important distinction to make is that of bone strength vs. the standard measures of bone loss that are used in clinical and bioarchaeological research, such as

bone mineral density (BMD). There is no way to measure bone strength on living individuals in a clinical setting. In order to measure this, force must be applied and measured to the point of structural failure. This is not feasible with living people. Moreover, in a bioarchaeological context, although this method is possible, it would result in the loss of bone material, which is ethically questionable. Additionally, dry bone is much more brittle when compared to normal active bone, which again makes the comparison between the past and present difficult in terms of bone strength. Furthermore, one objective of studying the past is to compare the results to the present. This means that bioarchaeological studies that directly measure bone strength could not be compared to current studies on living individuals. For these reasons, the use of surrogate measures such as BMD as well as microarchitectural changes to bone are employed to diagnose osteoporosis and estimate the risk of fracture (Grynpas 2003). As it stands, BMD does seem to be a relatively good proxy for bone strength. It has been estimated that between 75-90% of bone strength is associated to BMD (Jordan and Cooper 2002). Moreover, the risk of fracture has been estimated to be 1.5-3.0-fold more for every standard deviation below that of the healthy adult population (Holroyd et al. 2008). This would mean that a post-menopausal female whose BMD is 1 standard deviation below the normal healthy adult population has a roughly 30% greater risk of fracture over the course of her life (Jordan and Cooper 2002). This indicates that BMD is useful in the diagnosis of osteoporosis and the identification of individuals who are at a greater risk of sustaining an osteoporotic-related fracture.

Although BMD is strongly associated to the risk of fracture, it does not account for the entire risk. This is one problem with the standard diagnosis definition developed

by WHO (2003). BMD is a measure of the quantity of bone mineral within a predefined area. This, however, does not give any information as to the quality of the bone. Studying the micro-architecture of bone reveals information about the quality of the bone present, which also contributes to understanding the risk of osteoporotic-related fractures (Brickley and Agarwal 2003). Micro-architectural assessments of bone include trabecular number per defined area, as well as their thickness and their connectivity with other trabeculae. As one would expect, bones at low risk of osteoporotic related fracture tend to have high trabecular numbers, with little space between adjoining trabeculae. Conversely, bones with low trabecular numbers, and large amounts of negative space between adjoining trabeculae are at a much greater risk of osteoporotic-related fractures.

In summation, when diagnosing osteoporosis there are three important criteria. The first is the presentation of an associated fracture. This approach is still used in clinical and bioarchaeological diagnoses for obvious reasons. The presence of a low-impact osteoporotic-related fracture is the most direct way in which to diagnose poor bone strength, and thus osteoporosis. This approach, however, is unable to diagnose those individuals who are osteoporotic that do not present with a related fracture – the at-risk population. Moreover, any estimations of prevalence or risk are made entirely on fractures present vs. not present in a study population (whether living or bioarchaeological). This inherently would discount those with osteoporosis who do not have an associated fracture from the study. The second criterion, as set out by the WHO (2003), defines osteoporosis as any individual who falls 2.5 standard deviations or more below the BMD of the healthy adult cohort of that same population. This approach allows for the diagnosis of individuals who do not have an associated fracture, but are at a much

higher risk than the rest of the population to develop one. This is the gold standard of the diagnosis of osteoporosis in both clinical and bioarchaeological research when a fracture is not present. The problem with this approach, as mentioned above, is that it only accounts for bone quantity and not quality, both of which contribute to bone strength. If BMD was quantified on a compressed vertebra, it would undoubtedly give a high and erroneous result. This is the reason for the development of the third criterion, which is bone quality assessment through micro-architectural analysis. This approach relies on the density and connectivity of trabeculae within bone. It is a reasonable measurement of bone quality and therefore supplements the BMD measurement of bone quantity in order to diagnose osteoporosis. The downside to this approach is that it only measures trabecular bone, which makes up only approximately 20% of dry bone by weight (Brickley and Agarwal 2003; Parfitt 2003). Moreover, trabecular bone is not present everywhere throughout the skeleton, and thus on its own, may provide a poor assessment of a systemic disorder like osteoporosis.

When these criteria are used in combination, an accurate diagnosis of individuals with osteoporosis, and the estimation of the prevalence within a population are possible. The assessment of osteoporotic-related fractures in both clinical and bioarchaeological settings is apparent and needs no more discussion in terms of methodology and technology. The assessment of the other two criteria (bone quantity and quality) is much more complicated, and has changed with emerging technologies. Early assessments of these bone strength proxies used visual inspection of the bone both macroscopically and microscopically through histology. More recently, imaging technologies have been employed in the assessment of these associated measurements of bone strength.

As previously stated, the study of osteoporosis has a long history. The association between age-related bone loss and fractures was first described by Sir Astley Cooper in his publication *Dislocations and Fractures* (1822) (Cooper 1999). Even though the mechanisms of senile and post-menopausal bone loss were unknown to Cooper, he noted that bones from individuals in the older age-cohorts seemed less dense (Cooper 1999; Holroyd et al. 2008; Jordan and Cooper 2002). He associated '*less dense*' bone with the increased prevalence of certain fractures such as hip fractures and vertebral compression deformities in those cohorts. This is an example of early visual diagnosis of bone quantity. Currently, this is usually done by investigating fragility-related fractures of the spine, wrist and hip in archaeological bone. Simply feeling the weight of the bone to determine how heavy or light it is (as Cooper did), is not sufficient for diagnosing osteoporosis. This type of evidence is unsound and makes repeatability difficult. Other lines of evidence can be added to a visual examination such as the age and sex of an individual, the location of the fracture, and any other pathological changes to the skeleton (Brickley and Agarwal 2003). Some problems with this type of examination in bioarchaeology, even though it is direct, are determining when the fracture took place if one is present (peri-mortem, post-mortem, etc.), and distinguishing between a traumatic fracture and a low-impact fragility fracture. Moreover, bone quantity/quality may be altered in the burial environment (Schultz 2003), thus making a strictly unaided visual assessment difficult.

The use of histology helps to lessen this impediment. By studying the microstructures of bone, an assessment not based merely on '*experience*' is possible. Moreover, the use of standardization can increase the reliability and repeatability of these

assessments. The early studies of the 19th century conducted by French and German physicians using histology were purely descriptive (Cooper 1999; Holroyd et al. 2008). Being as such, they are not the histological methods that are utilized today in order to assess osteoporosis and bone quality. Histological methods have been used on both cortical bone and trabecular bone. One such method used for cortical bone assessment is known as cortical histomorphometry (Parfitt et al. 1987). While a basic visual examination of bone using histology can examine general bone loss and porosity, histomorphometry is the quantitative examination of these changes at both the tissue and cellular level. Although this technique is often utilized as an aging technique, it has also come into use for determining bone remodeling and loss (Brickley and Agarwal 2003). This method uses thin sections (most often from the femur or rib) and measurements, such as the number and size of secondary osteons and their associated canals, in order to derive osteonal population density, mean wall thickness, porosity, and rates of turnover. These measurements and derived calculations are taken manually or with the aid of computer software (Brickley and Agarwal 2003). The caveats of this examination are that it is destructive, relies on accurate chronological age assessments, and only deals with one two-dimensional section of a whole unit. In order for this last concern to be addressed, multiple bones should be investigated, and multiple sites within that bone should be studied. Moreover, this technique cannot be used in clinical settings, thus, does not allow for cross-comparisons between past and contemporary populations.

Histological assessment of trabecular bone has been used, but is much more diverse with less standardization. Trabecular bone consists of many tiny strut-like structures that function to support the bone during both normal and external forces. For

46

this reason, it is no surprise that most of the osteoporotic-related fractures occur in areas with a large amount of trabecular bone, such as the femoral neck, vertebral bodies, and the distal ends of the long bones in the forearm (Brickley and Agarwal 2003). When these struts are lost during metabolic disorders such as osteoporosis, the strength of the bone in those regions is drastically compromised. In fact, changes to bone density and strength can usually be identified in trabecular bone first because it is more metabolically active when compared to cortical bone. On a gross scale, observations concerning trabecular bone loss and cortical thinning can be made, while on a microscopic scale, features such as free-ending struts and the callus formation associated with micro-fractures or damage can be observed. These observations, however, cannot be quantified in this method, and therefore, cross-comparisons either between individuals within a population, or between populations, are very difficult.

A related histological study of trabecular structures known as stereometry has been developed, although it is not widely used (Jayasinghe et al. 1994; Brickley and Howell 1999). The authors found that analyzing the three-dimensional structure of trabecular bone was a good assessment of trabecular quality. They found that both horizontal, and to a smaller degree, vertical structures decreased in number with age, and that vertical struts became elongated with the removal of horizontal structures. There are a few caveats when using this method. First, it is destructive, requiring sections of bone to be made. This is an undesirable approach in bioarchaeology. Secondly, these sections are then imaged by making stereo-pair photographs and analyzed on a stereocomparator, both of which are not widely available. Finally, again, this method cannot be used in a clinical setting, thus not allowing for the cross-comparison of information concerning

past and present populations (Brickley and Agarwal 2003; Brickley and Howell 1999). This method does, however, begin to address the idea of using a three-dimensional approach toward studying bone loss. This is important, especially when concerning the complex structure of trabecular architecture, as opposed to the previously standard measures which could only visualize bone on a two-dimensional plane.

Beyond visual/gross examination and histology, osteoporosis has mostly been diagnosed with the use of imaging equipment such as radiography with film exposure, and more recently, complex analyses using detectors and computer imaging software to create three dimensional images from radiographical information. The advantage in using many of these methods is that they can be used in both clinical and bioarchaeological research which allows for the comparison of individuals from the past to those of the present. However, some of these techniques (i.e. μCT) are again restricted to use on human remains and are not suitable for clinical assessment. In the case of high-energy radiographic methods such as μCT, the radiation exposure is much too high for the use on living tissues. The use of x-ray radiography, specifically those using film, marked the next step in the technological advancement concerning imaging and the diagnosis of osteoporosis.

Standard radiography can be used to assess both the cortical index, and the trabecular architecture. The cortical index is ascertained by measuring the thickness of the cortical bone in long bones as well as the medullary cavity from standard radiographs. One specific method that measures the cortical index using standard radiography is metacarpal radiogrammetry. This is a non-destructive method that relies on the calculation of cortical bone present in a metacarpal from standard radiographs (Ekenman

et al. 1995; Mays 1996; Mays 2000; Mays 2001). This methodology utilizes the second metacarpal as suggested by Virtama and Helela (1969) and Meema and Meema (1987). The approach derives a cortical index by subtracting the medullary width from the total width of the metacarpal and dividing it by the total width. This number is then multiplied by 100 in order to establish the cortical index. The cortical index represents the percentage of bone width that is represented by the cortex of the bone. This method is straightforward, and is easy to replicate and compare between populations. An advantage of this technique is that, before Duel Energy X-Ray Absorptiometry (DEXA/DXA) became the popular methodology in clinical research, this method was used, so there were data from current populations that could be used in comparison to those in the past (Brickley and Agarwal 2003). The criticisms are that inclusions will skew the results (important in archaeological samples), only cortical bone is considered which does not account for trabecular change in architecture and density, it assesses a non-weight bearing bone, and it does not measure an area of the skeleton that is typically affected by fragility fractures (Brickley and Agarwal 2003).

A method to assess trabecular quality using standard radiographs is called the Singh Index (Singh et al. 1970). The Singh index uses measurements taken from radiographic images of the proximal end of the femur. Trabecular structure is assessed at a landmark known as '*Ward's Triangle*' using 6 stages of change to the trabecular structure. In terms of repeatability (both intra- and inter-observer) this method is difficult. The middle stages of trabecular loss are problematic (Brickley and Agarwal 2003). However, the extreme ends of the scale seem to be quite repeatable, which is promising for determining the extremes of osteoporotic bone deterioration.

In addition to the above standard radiographic techniques for measuring qualities of either compact bone or trabecular bone, there are techniques that utilize sophisticated detectors and analysing equipment to measure radiographic information for trabecular bone and whole bone. The first is known as quantitative histomorphometry of trabecular bone, developed by Weinstein et al. in 1981. It has been demonstrated that image analysis of sex- and age-related changes in trabecular architecture can be quantitatively examined in archaeological bone (Brickley and Agarwal 2003). Earlier, this was done using x-ray images of thick sections in archaeological examinations (Brickley and Agarwal 2003) as well as thin sections in clinical investigations (Garrahan et al. 1986; Thomsen et al. 2000). CT images have since been used in this type of method by Gordon et al. (1998). It should be noted that the different methods, although not directly comparable, do provide similar information. Image analyses from x-rays are usually taken from sections, and only provide a two-dimensional representation of a three-dimensional structure. CT on the other hand can be done on a whole element and provides a three-dimensional picture of trabecular architecture. From the analysis of these images, measurements such as connectivity, trabecular bone volume, average trabecular thickness, trabecular number and separation can be calculated. Bone quality can be assessed by using these data, especially when discussing aspects such as connectivity.

The final category of methods that are used in the diagnosis of osteoporosis are those that measure whole bone using modern radiographic imaging. Specifically, these are methods that assess bone mass and density in order to assess fracture risk using both trabecular and compact bone values. These include quantitative CT and ultrasound techniques (Genant et al. 1996). Bone mass, however, can also be assessed using

absorptiometric methods based on the absorption of radiation by tissues such as bone or muscles etc. The key advantage to these techniques is that they are non-invasive, and non-destructive. Moreover, they provide more diagnosis criteria, thus providing a more holistic approach to diagnosing osteoporosis (Brickley and Agarwal 2003).

The first method is known as optical or photo densitometry. This method is used to assess the density of a whole bone. The bone of interest (clinical and archaeological) is radiographed along with an object of known density. This is often a step wedge made from aluminum. Each step represents a known density. The density of this bone can then be estimated using an optical densitometer. A number of these images are usually taken and averaged in order to determine the average density. In a clinical setting, this has been done with the wrist and hand (Bland et al. 1989). One caveat to this technique is that due to the presence of soft tissue in clinical research, this approach cannot be used to compare with archaeological samples unless a soft tissue proxy is utilized. Archaeological samples can, however, be compared to one another (Brickley and Agarwal 2003). Moreover, when using archaeological samples, one must also be cautious. Diagenetic changes to the structure of crystals and mineral content can alter the density of an object. Therefore, assessments of the types and amounts of diagenetic changes should be made prior to using this method.

Another approach for assessing osteoporosis in whole bone that will be discussed is Duel-Energy-X-ray-Absorptiometry (DEXA). This technique is by far and away the gold standard in clinical research for the diagnosis of osteoporosis without the presentation of an associated fracture (Brickley and Agarwal 2003). Moreover, it has become the standard used in bioarchaeology in order to be able to make cross-temporal

comparisons between contemporary and past populations. DEXA was originally designed

for clinical practice, and is currently widely used to assess bone density in that setting.

This method uses a stable x-ray source that bombards the tissue (both soft and skeletal)

with two beams of x-rays at different energy levels. A detector then analyses the

absorption of those and estimates the density of the study area. DEXA has also been used

extensively in archaeological research concerning mineral content, bone density and

osteoporosis (Brickley and Agarwal 2003). Again, one of the problems when using this

method on skeletal populations is the lack of soft tissue. These machines and software

were designed for clinical practice where soft tissue is accounted for and absorbs some of

the energy. In order to address this problem, some machines have been designed with a

'*no-tissue*' or '*small animal*' setting. Moreover, stand-ins for soft tissue such as rice,

water, or other substances have been used to increase the accuracy and ability to compare

archaeological and clinical results (Brickley and Agarwal 2003). The data retrieved from

these scans estimate the amount of hydroxyapatite and the areal density of the bone in

two dimensions. This again assumes no diagenesis, so testing should be conducted with

archaeological samples. Moreover, the scanning area is small, so the use of sections or

small bones is required for archaeological research. The advantages of this technology

are the short scanning time and reproducible results (Brickley and Agarwal 2003).

Osteoporosis is a complex and multifactorial disorder that has been present

throughout human history. The fractures associated with this disorder are costly both in

terms of societal costs and the quality of life of individuals who sustain them. Early

diagnoses were made strictly based on the occurrence of the associated fracture, which

fails to identify all of the individuals with the disorder, as fractures are only the extreme

presentation of osteoporosis. With changes in technology and the methodologies used in the diagnosis of osteoporosis, we can now better assess individuals with the disorder. These non-fracture-based diagnoses have had a huge impact on the clinical assessment of the disorder. They have enabled the introduction of preventative medicine to take place with regards to osteoporosis. As discussed previously, there are many contributing factors that lead to systemic bone loss including diet and activity level. These factors can be controlled, and thus, with early diagnosis of the disorder, mitigating actions can help to lower the risk of fractures in the future for many individuals. In bioarchaeology, the advancements in the methods and technologies used in the diagnosis of osteoporosis have allowed for the movement beyond a fracture-based diagnosis. This breakthrough has allowed for a more thorough understanding of the prevalence of osteoporosis in the past, as well as the risk of fractures for those who had the disorder. Moreover, the diagnosis of individuals who did not have a fracture allows for a better understanding of the etiology of osteoporosis and the many different presentations and stages of progression for the disorder.

Future studies of osteoporosis seem to be headed towards more advanced imaging techniques, such as three-dimensional analyses using CT in clinical research, and high energy radiography using μCT in bioarchaeology. One such study by Cooper et al. (2006) showed that a three-dimensional approach was much better for visualizing the complexities of bone than the previously used two-dimensional methods. Moreover, the three-dimensional techniques seem to be much more reproducible, and therefore more reliable for a scientific approach to studying bone and bone loss. These techniques are of

great importance as they will be able to study the true structure of bone, unlike the previously used two-dimensional techniques.

Studies of individuals of the past have an advantage over those on living people. The use of high energy radiation, as well as sectioning and destructive methods allows for better resolution and understanding of the minute changes that take place throughout the progression of osteoporosis. These types of studies cannot take place in clinical practice. Therefore, the research being done in bioarchaeology is of extreme importance for understanding the disorder not only from a historical standpoint, but the progression of the disorder in living individuals and the preventative measures that can be taken by current and future populations. Like the technological advancements that were developed in the study of ancient DNA, the need for more sensitive and advanced equipment by bioarchaeologists for the study of human remains have pushed the technological evolution forward, and both clinical and studies of the past have benefited and will undoubtedly continue to do so in the future.

Chapter 3

3 MATERIALS AND METHODS

3.1 Introduction

As noted previously, the MT1 samples analyzed herein come from the Kellis 2 (K2) cemetery in the Roman Period occupation of the Kellis town site in the Dakhleh Oasis, Egypt. This chapter provides the context for this research. Section 3.2 details the basic (geography, climate, human history) background of the Dakhleh Oasis, including information on the Kellis 2 cemetery. Section 3.3 details the Dakhleh Oasis Project (DOP) bioarchaeological research strategy including a brief history of its development and some key findings. This is followed by a description of the methods used in the collection of data for the MT1s (section 3.4). Section 3.5 details the various statistical tests and strategies used for analysis of the MT1s. Section 3.6 provides a brief summary of the chapter.

3.2 The Oasis, The Village and the Kellis Sample

Dakhleh, meaning 'inner' in Arabic, is one of five major oases in Egypt's Western desert (**Figure 9**). It is somewhat kidney-shaped and is approximately 70 kilometers east-west and 20 kilometres north-south at its greatest width (Mills 2010). Geographically, it is the most isolated of the major Oases, with its eastern border being approximately 300 kilometres from, and at the same latitude as, Luxor (Mills 2010). Before modern transportation it took minimally two weeks to travel by camel from the Nile region to Dakhleh. As much of the distance was across the Sahara, water was key to successful passage. Successful passages utilized the Kharga Oasis with its dependable surface

waters. This isolation was gradually lessened over time as Dakhleh became important in Egypt's agrarian economy, particularly during the late Ptolemaic and Roman periods. Today, the Oasis can be reached by car along the Nile highway and across the desert in ~ 9-12hours. Egypt Air has a daily flight that takes under an hour from Cairo to Dakhleh, which is located near Mut (Mout in Arabic) in the central part of the Oasis. This provides an invaluable service for the ~75,000 people living in the Oasis today and helps minimize its isolation.
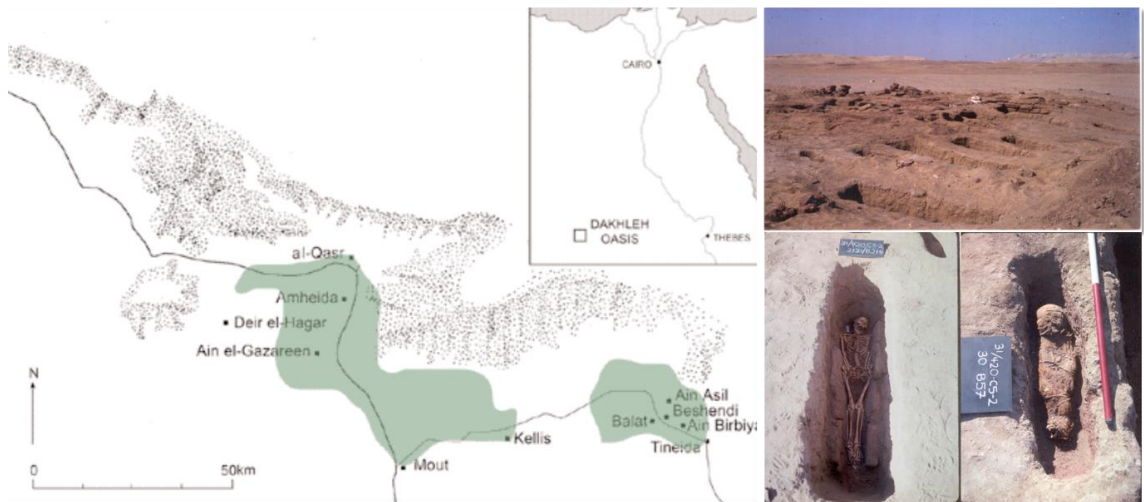
Figure 9 Dakhleh Oasis, Egypt. Dakhleh Oasis, Egypt. The location of the Dakhleh Oasis in Egypt's western desert. The town of Kellis, which was occupied continuously from early Ptolemaic to later Roman times, is located approximately in the centre of the Oasis. It was abandoned in ~ 450 CE The MT1 samples analyzed in this thesis are from the large K2 cemetery located just north and east of Kellis. Over 700 individual burials have been excavated and partially analyzed. For the most part the preservation is excellent and there was limited postmortem bone diagenesis. The burials shown indicate the typical preservation.

The archaeology of the Oasis was virtually unknown until the late 1970s when initial systematic surveys were conducted by the Dakhleh Oasis Project (DOP). The DOP

is a multidisciplinary program that, for the most part, has been directed by Professor Tony Mills under the auspices of the Royal Ontario Museum in Toronto, Ontario, Canada and the Society for the Study of Egyptian Antiquities (SSEA). The purpose of the DOP is to investigate human bio-cultural adaptations to this challenging desert ecology over the millennia (Mills 1999). From approximately 4000 years ago, with the arrival of the first wave Nile region migrants, until the present, the people of the Oasis, the Dakhlans, have pursued an agrarian lifestyle (Mills 1999). Rainfall in the region has been negligible (< 1 mm/year) since that time. Despite the hyperaridity, the Oases have been habitable because they have accessibility to one of the largest aquifers in the world (Schild and Wendorff 1977), the Nubian Sandstone Acquifer (Dahab et al. 2001). During the early phases of human adaptations to Dakhleh (e.g., late Paleolithic to early Pharonic times) surface water was found in areas where artesian pressure resulted in natural spring mounds or vents (Schild and Wendorff 1977). Schild and Wendorff (1977) note that rudimentary well digging has been documented as early as the Paleolithic, but over time the Dakhlans refined their hydrology skills. Thanheiser et al. (2002) note that by the Ptolemaic period (circa BCE305-50) irrigation techniques improved substantially with concomitant increases in the amount of arable land and the indigenous population. Under this foreign influence (Greeks) trade to Oasis increased.

It was during Dakhleh's Roman period (circa 50-600CE) that the population and agricultural productivity increased substantially (Mills 1999). The Romans introduced many new agricultural technologies, particularly the water wheel, which facilitated the expansion of irrigation and the concomitant increase of arable land. Evidence of the impact of the Roman Period on the Oasis is shown throughout the current landscape,

57

including the village of Kellis (Ismant el-Kharab in Arabic), which sits as an almost haunting vestige of the Oases' past.

Kellis is located in the south-central part of Dakhleh, just east of the town of Mut (see **Figure 9**), and was first systematically studied in 1981 (Birrell 1999; Knudstad and Frey 1999). The initial research involved surveying and mapping of the entire settlement and later test excavations of key architectural structures (house structures, churches, temples, tombs etc.) were conducted. Kellis was continuously occupied from the Ptolemaic period to the late Roman period (Hope 1995; Thurston 2012). The Ptolemaic remnants of the village have been largely replaced over time and most of the archaeological presence of the site, which have been researched by Dr. Colin Hope and his team from Australia since the early 1980s, derive from the Roman period occupation. Dr. Hope has determined that Kellis was abandoned in ~450CE (Hope 1995).

There are many hypotheses advanced to explain why Kellis was abandoned, with most favouring desert encroachment and/or exhaustion of water resources (Hope 1995; Mills 2010). It has been estimated that the village increased in size (perhaps up to 2000 people), which would have placed additional stress on the immediate environment and its resources. There is little doubt that by the late 3rd or early 4th century that Kellis was at its zenith in terms of population size, administrative and religious functions (Molto 2002). In terms of the latter, the Kellans experienced the end of the Ptolemaic influence and the origins of Christianity. A major archaeological find in Kellis is the oldest Christian church in Egypt and the introduction of the Christian mortuary pattern, which is present in the Kellis 2 cemetery.

Mortuary complexes associated with Kellis were found within the town itself, and in two cemeteries northwest (Kellis 1) and north-east (Kellis 2) of the village (Molto 2001, Birrell 1999, Hope and McKenzie 1999; Knudstad and Frey 1999). In terms of mortuary customs, from the late Ptolemaic and early Roman periods, the Kellans interred their dead in rock-cut tombs in Kellis 1 which is located in low rising hills immediately northwest of the settlement (Birrell 1999). These tombs reflect longstanding late Pharonic traditions evidenced by anthropogenic mummification, cartonnage, iconography and grave inclusions (Birrell 1999, Molto 2001). Birrel notes that the tombs appear to have been used continuously, as later burials were often placed on top of earlier ones, or the latter were moved to make space for the new ones (Birrell 1999). Virtually all the mummies and skeletonized remains have been disturbed. The mummies of K1 have been studied by several researchers over a ten-year period (Cook 1994; Aufderheide et al. 1999). Molto (2001) suggests that the tombs represent familial groups. To date, most of the tombs from K1 are from the early Roman period, which is expected as it was during this period that the Oasis was transformed in terms of agricultural pursuits, trade and theology. Sometime during the early Roman period the Kellans switched their mortuary program to Kellis 2 (K2), which is located less than a kilometre east of K1. The change likely reflects a major shift to Christianity from the pagan beliefs that dominated from Pharonic to early Roman times (Bowen 1998).

It is not known exactly when K1 was abandoned, but it is likely K1 was still in use when K2 was gradually developing. The change probably involved native Dakhlans and immigrants, as well as a number of new religious belief systems (e.g., Manichean, as

well as, Coptic). The change was, however, dramatic and significant, both in terms of structure and symbolism, as no later Roman period tombs have been found in K1.

The K2 burials are invariably single, east-west extended inhumations with the head to the west, with limited grave inclusions and no evidence of anthropogenic mummification (see **Figure 10**). This is consistent with early Christian burial customs (Birrell 1999, Hope and McKenzie 1999, Molto 2003). Excavation and survey of the K2 remains have been continuously conducted from 1991 to the present, although in the past few years, with mounting troubles in the Middle East, and Egypt specifically in this case, field work has been suspended. To date, over 750 burials have been excavated and partially analyzed.
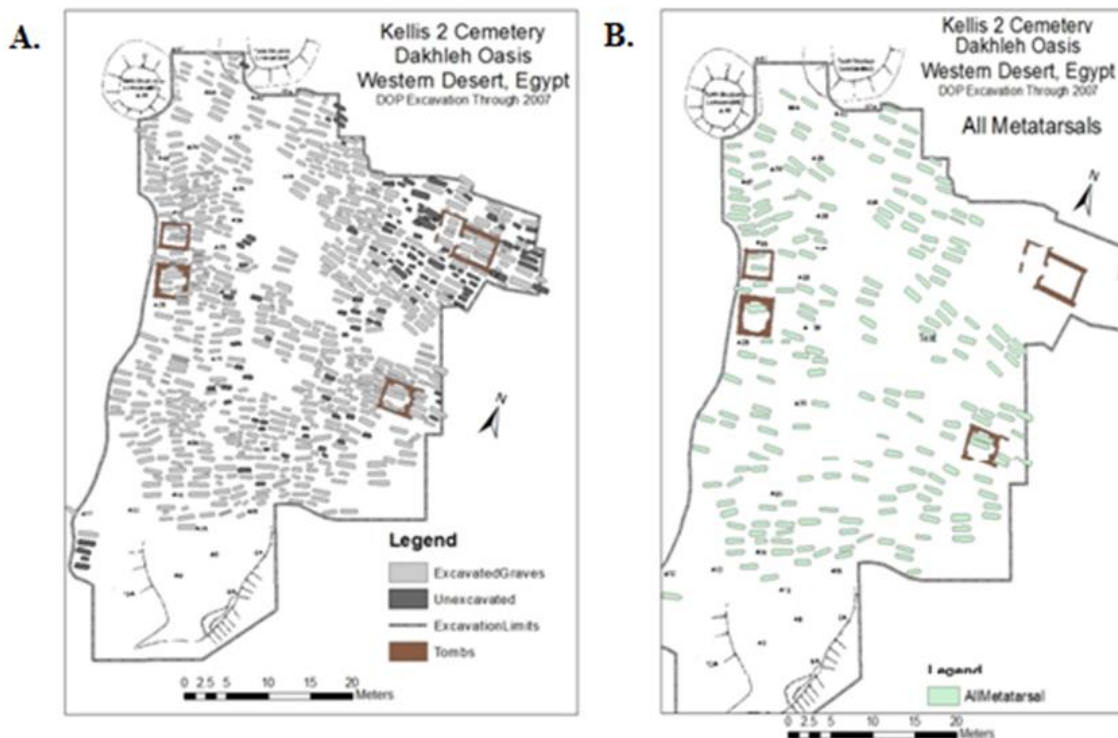
Figure 10 Kellis 2 Cemetery. A. Site map of the Kellis 2 Cemetery, Dakhleh Oasis, Egypt. The occupation of this cemetery has been radiocarbon dated to between 50-450CE. **B.** Map of the 1st metatarsals available from excavation (maps created by James Keron, Department of Anthropology, The University of Western Ontario, London Ontario).

The K2 burials are generally well-preserved and intact, though many have been disturbed and often key elements, particularly the skulls, have been disturbed or looted (Molto 2001). With permission from the Supreme Council of the Egyptian Antiquities, skeletal elements (including MT1s) for radiocarbon dating, isotope and ancient DNA (*a*DNA), have been sampled. Of significance is that 21 K2 burials have been AMS radiocarbon dated and suggest with 100% confidence that this cemetery was in use from 50-450CE (Stewart et al. 2006). The upper-range agrees with the archaeological data that, as noted, indicate the village was abandoned in the mid-5th century. However, the

61

archaeological data, including coins and papyri excavated from the village, are at variance to the lower-range (i.e., 50CE), suggesting that the Kellis cemetery dates from circa 265CE (Bowen 1998). Stewart et al. (2006) favour the science of AMS radiocarbon dating and suggest that the burial position found at Kellis is among the first symbolic religious expressions of the Kellans to avoid persecution until Christianity became more accepted, as witnessed by Christian names, which became more prevalent after circa 265CE. The dating controversy at Kellis is an ongoing conundrum for the DOP (Molto 2005; Molto personal communication 2016).

From the above illustration of the Kellis 2 cemetery, three aspects of Figure 10 stand out. First, there are a number of superstructures within and around that the individual burials are organized. Molto (2002) suggests that when the decision to change their mortuary program was implemented based on the emergence of Christian beliefs, individual families selected areas to inter their dead, and focused around the developing 'familial' superstructures. This builds on the tradition of familial burial areas in pre-Christian times (Molto 2001, Molto 2002). Recall that at Kellis 1, families buried their dead in family crypts cut into the gebel. Initial support for this hypothesis is that burials in and around the K2 superstructures span the time period defined by the AMS dates (50-450CE). Secondly, the burials in and around the superstructures shared genetic affinities to each other, as witnessed by rare morphogenetic traits (Molto 2002). Though this hypothesis is still under investigation, the results to date have been supportive of this assumption (Molto 2002; Edwards 2005; Haddow 2012; Keron 2015).

Finally, the burials are placed at angles which may coincide with the angle of the sun; the solar arc hypothesis (Williams 2009). Though the solar arc hypothesis is not

strictly associated with Christianity (Morgan 1990), it does have significant implications for interpreting certain aspects of the skeletal data produced by the bioarchaeology program of the DOP such as paleodemography, paleopathology and season at death.

3.3   DOP Bioarchaeological Research Program

At the first Dakhleh Oasis Symposium held in Durham, England, 1994, Molto presented a paper that outlined the objectives and research strategies, as well as the early findings, of the bioarchaeology component of the DOP. These were later published (Molto 2001). A key problem outlined was the fact that, because most of the research had to be conducted in the field, the skeletal database needed to be streamlined and the data collected had to be analyzed for observer reliability, or done in-blind. In terms of streamlining, sex determination used only the Phenice method (Phenice 1969), as most of the burials had pelves, and this method has proven to be reliable on all populations studied to date. Inter-observer reliability testing of the Phenice method between Dr. Sheldrick, Dr. Molto and Dr. Fairgrieve proved to have absolute concordance on the 50 randomly selected hip bones.

Dr. Fairgrieve was conducting his research on amino acid residue analysis of the Ain Tirghi and Kellis material. Dr. Fairgrieve, then a PhD student at the University of Toronto, produced the second PhD thesis on Dakhleh material in 1993 entitled "Amino acid residue analysis of type 1 collagen in human hard tissue: An assessment of *cribra orbitalia* from tomb 31, site 31/435-D5-2, Dakhleh Oasis, Egypt." Over the last twenty-five years the bioarchaeology team has produced a large number of undergraduate, Masters and PhD theses, as well as numerous refereed publications in the top journals in

biological anthropology and many presentations and posters at major conferences. Throughout this time, the research team has expanded, which was a major objective of the project (Molto 2001). The following is a **partial list** of some of the key findings from the skeletal biological research from K2 that was conducted previously to this research:

1. The antibiotic tetracycline has been found in the remains of third Intermediate-Late period and Kellis 2 skeletons, mainly from femoral mid-shaft samples (Cook et al. 1989, Maggiano et al. 2003).

2. Amino acid residues were extracted from Ain Tirghi and Kellis samples and for the first time molecular evidence was used to support the anemia hypothesis for porotic hyperostosis (Fairgrieve 1993). As a follow up to this, Fairgrieve and Molto (2000) were the first to note that the extensive porotic hyperostosis found in Ain Tirghi and Kellis could represent a response to megaloblastic anemias (from folic acid and vitamin B12 deficiencies), as well as, iron deficiency anemia.

3. In 1989 Dr. Molto was the invited keynote speaker for the first ever Spina Bifida and Hydrocephalus Association of Canada conference held in Edmonton, Alberta. This hour-long presentation before over 700 people, including medical clinicians and epidemiologists, detailed the research on spina bifida at Ain Tirghi. More important the medical community in Canada became aware of the importance of paleoepidemiological research in documenting the natural history of spina bifida. This lead to a major grant from the Spina Bifida and Hydrocephalus Association of Canada.

4. Stable isotopes and dental pathology have been used to reconstruct the paleodiet of the ancient Dakhlans (Dupras 1999). Moreover, the isotopic data have been used to reconstruct the time of weaning in the Kellans (Dupras et al. 2001).

5. Leprosy has been identified in several skeletons from K2 (Molto 2002). Additionally, several individuals had co-infections with leprosy and tuberculosis using ancient DNA (Donoghue et al. 2005). This is the first time these mycobacterial diseases have been confirmed in a single population and in the same individuals.

6. Six individuals have been diagnosed with cancer, with one from K2 being the first case of leukemia identified in the Old World (Molto and Sheldrick 2014).

7. There are four cases of *humeral varus* deformity that likely represents evidence of birth trauma associated with the practice of mid-wifery (Molto 2000).

8. A possible case of child abuse from K2 (Wheeler et al. 2013).

9. The first successful extraction, amplification and sequencing of *a*DNA from Egyptian skeletal remains (Graver et al. 2000, Parr 2002). Recently, the MT1 from burial 124 from Kellis 2 has yielded the complete mitochondrial genome (16,569 base-pairs) This individual skeleton has also been radiocarbon dated to 1780 $\pm$ 50 years BP with a 100% probability of falling between 129-385 CE (paper accepted July 2017).

10. The material from the DOP has lead to refinements in several techniques, including stable isotopic and *a*DNA methods. The isotope data were used to show that some of the K2 lepers actually lived away from the Oasis, and probably returned home to the town of Kellis and it appears that they were not being

ostracized. Also, noted, Williams (2009) used isotopic data from the Kellis 2 cemetery to show the seasonality associated with grave positions at K2. This is the first test of the solar arc hypothesis in an Egyptian cemetery.

3.4 Data collected for Kellis MT1s

It is important to emphasize that the data produced on the MT1s in this thesis were done in-blind. No information about the burials, including age, sex, genetics and pathology were provided. As noted, sex determination of all the adult burials was based on the Phenice method (Phenice 1969). Age determinations for adolescents and adults were based on multiple methods outlined in the *Standards for Data Collection from Human Skeletal Remains* (Buikstra and Ubelaker 1994). Procedurally, the skulls were labelled and then stored in sequence on shelves in the bioarchaeology lab at team dig house near Mut. Dental attrition and pathology were initially scored and recorded for each skull. As well, general bone condition for each infracranial skeleton was noted separately. Key infracranial elements (hip bone, ribs and sacra) that involve specific aging methods were then taken and given random numbers. These include the left hip bones (scored for symphysis pubis morphogenesis (Brooks and Suchey 1990) and iliac crest fusion (Buikstra and Ubelaker 1994), the sacra (fusion of the centra, particularly the stage of S1-S2 fusion), and the right 4th ribs (5th or 6th if the 4th was not preserved) (modified from Iscan et al. 1984, and 1985). Age determination of these bones were also done separately. Later the results were compared to come up with a consensus age. Following the data collection on the MT1s, I was given the consensus age and the sex for each corresponding individual. Later, when the quantitative analyses were completed, other

aspects of each burial were given. In particular, identification of bone diseases that could impact density, such as leprosy, and trauma were provided.

Initially the MT1s were sampled for future ancient DNA and isotopic research because it was assumed they had limited use in bioarchaeological research and they are small, durable and readily stored (Molto personal communication 2013). The K2 MT1 sample is 377 – representing 113 females, 81 males and 18 individuals of unknown sex (mostly subadult) (N=212).

It is worth repeating that the epiphyseal fusion of the MT1 is completed by the mid- to late-teens (approximately 13-15 years of age in females, and 16-18 years of age in males), and as such, they reach skeletal maturity in size, but not necessarily density, at a much younger age than the long bones. Only 1 individual, burial # 207 (female with an estimated age of 60 years), was not preserved well enough to be included in this study. This speaks to the excellent preservation of the K2 sample. As part of the curational process they were photographed, measured and observed for nonmetric traits and pathological changes. They have been stored at room temperature. This started the large MT1 data base, which is a component of the larger bioarchaeological data base of the DOP.

These data, as noted, were initially recorded without any osteobiographical information. Early experimental research indicated that they may be more useful to bioarchaeology than previously thought, which led to the current research. The first part of this section describes the basic information collected on the MT1s including osteometrics, nonmetrics and pathology. The second part expands the data from the

osteometric component for sex determination and includes the development of osteometric volume measures and the use of µCT for measuring bone density for osteoporosis research.

3.4.1   Scoring of the Intermetatarsal Facet

The only nonmetric variants that have been described for the MT1 in the literature are a facet on the dorsal surface just proximal to the head, and a facet on the proximal-lateral surface, distal to the articular surface of the base (Intermetatarsal Facet – IMF). The former is a developmental variant that has been described for the ancient inhabitants of the Hacienda Ayalan site in Ecuador, and five other New World samples (Ubelaker 1979), and a population sample from Anyang, China, dating to the late Shang dynasty (1300-1027 BCE) (Molto and Chemm 2006). This functional facet, shown in **Figure 4**, represents chronic hyper-dorsoflexion from squatting. It is totally absent in the K2 collection. The IMF (see above, **Figure 8**) is a common variant, which is present in the K2 population sample. This intermetatarsal facet represents an articulation with the MT2. Though many assume that because the MT1 is non-abducted in *Homo*, these MT bones are always in contact. In reality, the non-abduction of the human foot involves numerous ligaments, tendons etc., which keep these bones in close proximity, with the facet representing a variant in some individuals. The facet is not described in the literature on the great apes. The scoring of this trait is given in **Table 2**. It can be hypothesized that if the facet is a developmental variant, rather than a heritable feature of a given foot architecture, the full expression should statistically be more common in older cohorts, and perhaps show a sex bias.

Table 2 Intermetatarsal Facet Scoring.

Score	Expression	Description
0	Absent	Absent
1	Slight	Smooth surface with no defined borders
2	Partial	At least one defined and raised border and a smooth surface
3	Full	The whole facet is well defined with all raised borders either separate or merged with the proximal base facet

3.4.2   MT1 Osteometrics

Five linear measurements, which are reported in the published literature (White et al. 2011), were calculated on each K2 MT1. There is no reference in that text for inter- or intra-observer errors. The measurements were made using a Mitutoyo Digimatic Caliper (Model Number NTD12-6"C). These measurements, shown in **Figure 11**, are: maximum physiological length (MPL), maximum head height (MMH), maximum head breadth (MMB), maximum base height (MBH) and maximum base breadth (MBB). In addition to these metrics, the mass of every MT1 was also recorded. The mass estimates were made using the Ohaus Adventurer SL balance (Model Number AS 312). These metrics were used for both sex determination, and to calculate volume and density estimates (osteo-volumetric density research), that are novel in bioarchaeology.
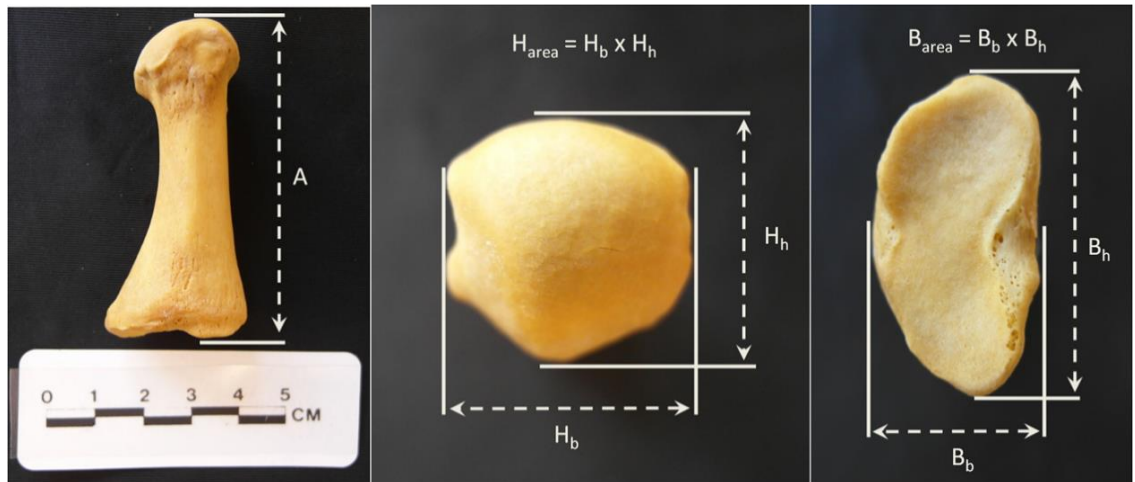
Figure 11 Metric Measurements of the MT1. Left: Medial view of a right first metatarsal (Kellis 2 Burial 274). "A" Determining the metatarsal Physiological length (MPL). **Middle:** Distal view of a right first metatarsal (Kellis 2 Burial 274). Determining the area of the metatarsal head. H_h is the maximum head height (MHH). H_b is the maximum head breadth (MHB). **Right:** Proximal view of a right first metatarsal (Kellis 2 Burial 274). Determining the area of the metatarsal base. B_h is the maximum base height (MBH). B_b is the maximum base breadth (MBB). Measurements are as outlined by White et al. 2011 (Photography by Mathew Teeter, 2013).

The density measurement utilized an engineering method for estimating volume etc. in complicated structures – those that are not squares, rectangular, etc. The results of the osteo-volumetric density provided a baseline model for further analyses of the bone density using µCT, which will be described below. For this part of the study a selection of ~44 MT1s was used. It required both a '*healthy sample*' versus one known to have pathology that would affect bone density. The latter subsample was determined as part of the blind design.

3.4.3   Sexing of the MT1 using metric measurements

The sexing methodology developed in this thesis uses the same metric measurements described above, which again will be used for the osteo-volumetric density calculations (e.g., physiological length, base breadth and height, head breadth and height, and mass). This was done in order to streamline the process and maximize the amount of information obtainable for osteobiographies using the same skeletal element.

3.4.4   Osteo-volumetric Analysis of the MT1

The measurements described in **Figure 12** were used to estimate bone volume. The volume was calculated using the frustum formula shown in Figure 12. The approximate volume of each MT1 was estimated using these formulae. The volume of a frustum both closely approximates the MT1 in terms of shape, and is easy to calculate – therefore it was suitable to act as a <u>proxy</u> for the MT1 in this study. The volumes obtained, though not true MT1 volumes, are close approximations of a close-fitting frustum unique to each individual. Creating a standardized measurement for each sample allows for comparisons to be made between individuals.
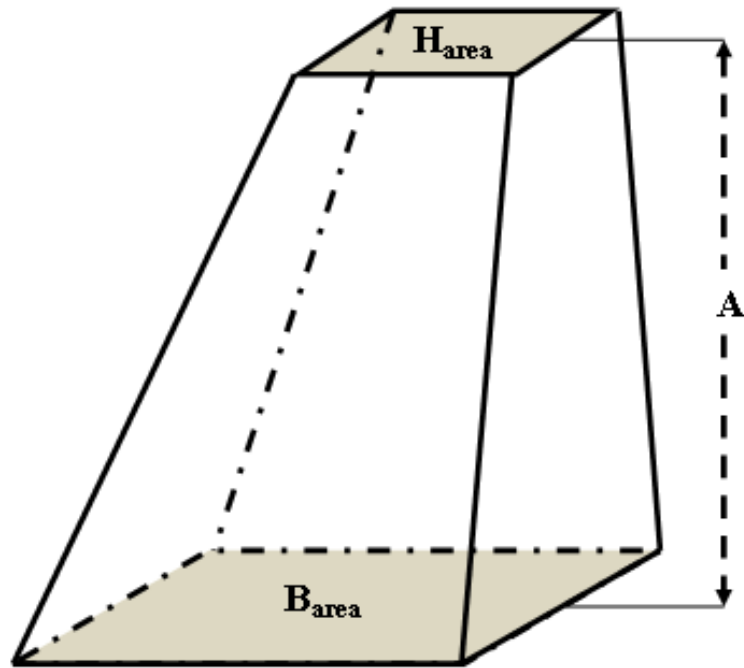
Figure 12 Estimating the volume of a MT1. Determining the volume of a frustum (apex-truncated square pyramid). Volume of a frustum = $A/3((H_{area} + B_{area}) + \sqrt{} (H_{area} * B_{area}))$.

Once the approximate volumes were calculated for each bone, MT1 mass was determined. Using the volume and mass of the MT1 facilitates the estimation of the density of the close-fitting frustum. This value was determined by dividing the mass by the volume (i.e., mg/cm^3). This estimated osteo-volumetric density does not represent, and is not equivalent to, the bone mineral density obtained using imaging techniques (i.e., DEXA, μCT). This estimated density only represents the amount of mass per unit volume of the entire frustum, and therefore does not account for differences in density throughout different regions of the bone. For this reason, the calculated osteo-volumetric density is more analogous to bulk density estimations, but where the volume is static and still includes voids. The estimated osteo-volumetric density is considered a standard measurement allowing for the comparison of individuals. This approximate density

reduces bone size and weight biases (i.e., bones that are larger tend to weigh more) to a standard score much like the coefficient of variation. Thus, the comparisons between the MT1s are standardized as being based on mass per unit volume. This method is similar to that used by Brickley (1997) to obtain base-line density values. However, instead of using bone-sections, the osteo-volumetric density is an estimation of the entire bone, which is more desirable, as the destruction of skeletal materials can be reduced or eliminated.

3.4.5   Sample Selection and μCT Analyses of the MT1

3.4.5.1   Sample Selection

As part of this pilot study involves testing the efficacy of the MT1 for future bioarchaeological bone quantity studies, it was not feasible to scan all of the MT1s from the K2 skeletal population (n=377). Moreover, because it is known that the decline in bone density with age is more common in females, this part of the research involves a subsample of this cohort. The results of the research conducted pertaining to the osteo-volumetric density of the K2 skeletal sample guided the selection of a sub-sample (n=44) of the K2 female MT1s used herein. Twenty-eight females estimated to be below 50 years of age were randomly selected using a random number generator to represent the "*healthy*" adult female cohort. A necessary caution, or caveat, in the "*healthy*" designation pertains to the Osteological Paradox – healthy but dead (Wood et al. 1990). This is unavoidable when using skeletal populations in Biological Anthropology, as every individual represented has died, but must be acknowledged.

Additional samples were selected for the μCT analysis in order to more closely study reduced bone density and architecture in Kellan females – Female burials with hip

fractures were selected. In K2, 9 females in the 50+ age cohort suffered osteoporosis-related fractures (Molto and Sheldrick 2010). **Table 3** details the individuals and the type of osteoporosis-related fracture(s) present. An additional 7 females were chosen randomly from the 50+ age-cohort, using a random number generator. This resulted in a sample of 44 K2 Females. Additionally, for the cortical index (CI) section of this analysis, one more female was available for analysis (burial 440, 20 years old). This brought the sample size to 29 for the "healthy" adult female population (n=45) for the CI analysis.

Table 3 K2 females with osteoporosis-related fractures used in this study. Diagnosis based on the occurrence of one, or multiple, low-impact fractures relative to age- and sex-cohort data (i.e., older females), site of the fracture (e.g., wrist, hip, vertebrae, etc.), and occurring peri-mortem to avoid cumulative fracture effects.

Burial	Sex	Age	Fracture
5	F	55	R. Hip, Sacral Compression and 7 Ribs
8	F	72	R. Hip and R. Colles
41	F	60	L. Hip
72	F	65	Sacral Compression
261	F	70	L. Hip, Sacral and Vertebral Compression (L1)
275	F	55	L. Colles
438	F	65	L. Hip and Rib (L10)
459	F	55	L. Hip, and R. Colles
D7-3	F	60	R. Hip

It should be noted that fractures accumulate with age. Thus, only individuals in the upper age-cohorts with fractures that were in osteoporotic high-risk areas of the skeleton (i.e., hip, vertebra, and distal upper limb), and were either peri-mortem (fresh or in a state of healing at the time of death), or a result of compression (e.g., vertebral or sacral compression deformities) were considered in this study.

3.4.5.2   Micro-CT imaging

Micro-CT imaging of the bones was done using *eXplore speCZT scanner* (GE Healthcare, London, ON, Canada). The scan protocol consisted of an x-ray source, which operated at an x-ray tube voltage of 90 kV and a tube current of 40 mA. The x-ray source and the gantry rotated around the object, and 900 views of data were acquired at an angular increment of 0.4 degrees. Each view was exposed for 16 ms and the scan time was approximately 5 minutes per sample. Data were acquired at isotropic voxel size of 50 µm and reconstructed into a 3D volume image at the same voxel size using a modified cone-beam algorithm. The images were rebinned at 100 µm voxel size to increase the signal-to-noise ratio. Images were calibrated in Hounsfield units using image values of air and water. A calibrating phantom consisting of air, water and SB3 (synthethic cortical bone-mimicking epoxy) was scanned together with the metatarsal bones. Using the image values of water and air, all image data were linearly rescaled (using a custom software program) so that water image had a mean value of 0 HU and air -1000 HU. Analyses were done in *MicroView* with the *Advanced Bone Analysis Application* software add-in (Version 2.1.2, GE Healthcare Biosciences, London, ON). In the following subsections, the methods used for specific µCT analyses using *MicroView* are outlined.

3.4.5.3   Bone Mineral Density and Bone Volume Fraction analyses

Three cylindrical volumes of interest (VOI), measuring 175x175x50 pixels were chosen along the shaft of the MT1. These represented proximal, mid, and distal shaft locations. Additionally, a cylindrical VOI measuring 175x175x175 pixels was chosen to represent the entire shaft, as seen in Figure 13. Bone mineral density and bone volume fraction measurements were taken at all four locations using *MicroView* with the *Advanced Bone Analysis Application* software add-in (Version 2.1.2, GE Healthcare Biosciences, London, ON).
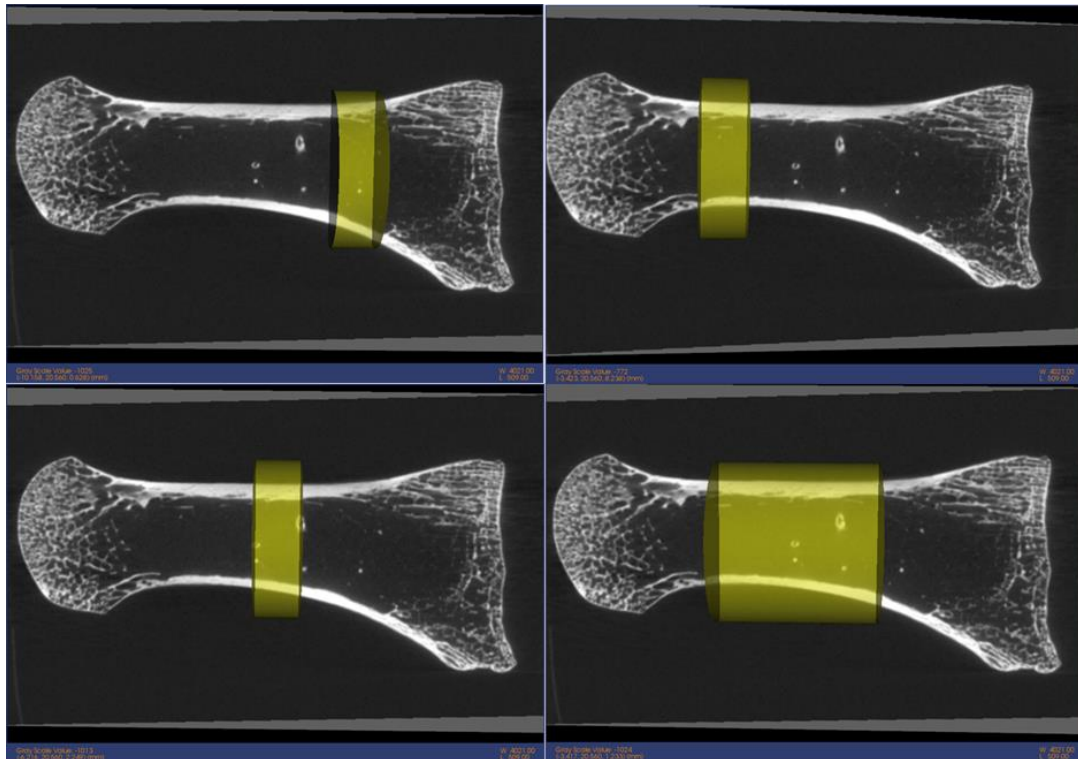
Figure 13 Cortical Volumes of Interest. Burial #68, Female (~30 years old). **Upper-Left**: The location of the proximal volume of interest used to estimate BMD and BVF. **Lower-Left**: The location of the mid-shaft volume of interest used to estimate BMD and BVF. **Upper-Right**: The location of the distal volume of interest used to estimate BMD

and BVF. **Lower-Right**: The location of the whole shaft volume of interest used to estimate BMD and BVF.

3.4.5.4 CI analysis

Cortical index measurements were taken mid-shaft on each MT1 by manually delineating both the endo- and ecto-dorsal and –plantar cortical surfaces, as seen in Figure 14. Three-dimensional coordinates were reported for each point, and Pythagorean calculations were made in order to determine the distance between each position for all metatarsals. The calculation given in **Figure 14** was used to determine the cortical index.
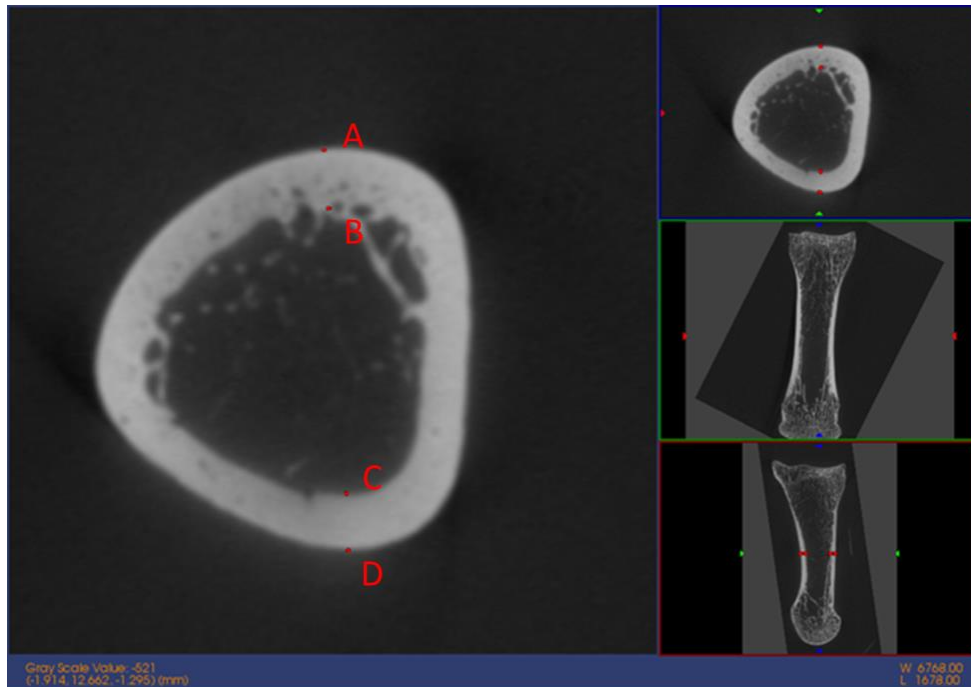
Figure 14 Cortical Index. Calculating the cortical index for the human first metatarsal at the mid-shaft region (Burial 131). 'A' is the ecto-dorsal surface. 'B' is the endo-dorsal surface. 'C' is the endo-plantar surface. 'D' is the ecto-plantar surface. Distances were calculated between AD and BC (dorso-plantar). The calculation of cortical index is:

$$\text{C.I.} = \frac{\left(\overleftrightarrow{AD}\right) - \left(\overrightarrow{BC}\right)}{\left(\overleftrightarrow{AD}\right)}.$$

3.4.5.5   Trabecular Microarchitecture Analysis

Two cubic volumes of interest (VOI), measuring 50x50x50 pixels were investigated. One was located midline in the region occupied by cancellous bone within the base of the MT1, and the other was located midline in the cancellous region within the head of the MT1 (See **Figure 15**). No measurements were taken within the shaft of the MT1 (medullary cavity), as this region is typically devoid of trabecular bone.
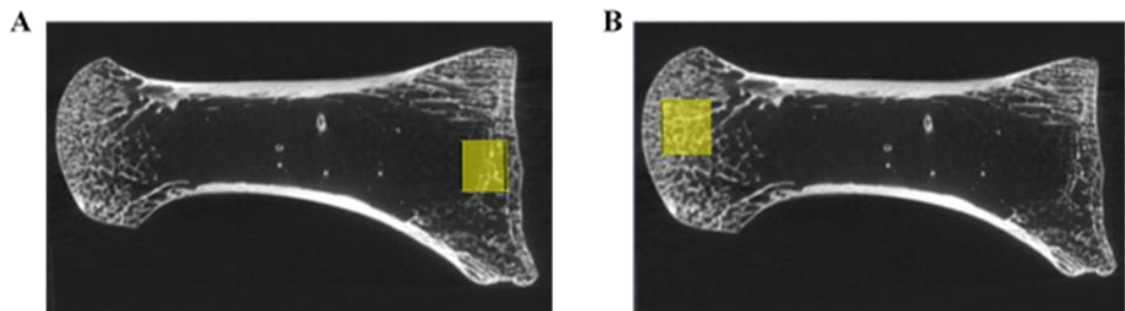
Figure 15 Trabecular Volumes of Interest. Burial 68 (Female, 30) **A.** The location of the cubic (50x50x50 pixels) volume of interest used to estimate the trabecular architecture in the base of the MT1. **B.** The location of the cubic (50x50x50 pixels) volume of interest used to estimate the trabecular architecture in the head of the MT1.

The following data were collected relating to the trabecular quantity and quality in the base and head of the MT1s: Trabecular Bone Volume Fraction (BVF), Trabecular Bone Mineral Density (BMD), Trabecular Thickness (TbTh), and Trabecular Spacing (TbSp). These data were collected using *MicroView* with the *Advanced Bone Analysis Application* software add-in (Version 2.1.2, GE Healthcare Biosciences, London, ON).

3.5   Statistical Analyses

There are numerous statistical tests used throughout this dissertation and to mention them all now would not benefit the reader. The additional specific tests will be outlined and

discussed in the result chapter. Described here are general comments that can be made about the statistical approach. With the exception of logistic regression (predictive) used for sexing, all other statistics used were either descriptive, prevalence, or frequentist hypothesis testing.

The sample population, as well as sub-samples (e.g., different age- and sex-cohorts), were tested for normality before the appropriate hypothesis test was selected, and variances were compared using F-tests when comparing to sample, or sub-sample means. The tests used for each sample and sub-sample can vary depending on the observational data and descriptive findings, therefore they will be discussed when presented in the results. It should also be noted that even though the volumetric methodology described is new when applied to male–female tests, one-tailed tests are used as we know from current literature on bone density and health that males generally have higher density values. The remainder of this section will outline the rationale behind the statistical approach used in the various experiments discussed in this dissertation concerning the efficacy of the MT1 in bioarchaeological research.

3.5.1   Prevalence of the Intermetatarsal Facet

Basic descriptive statistics were employed to assess the prevalence of this non-metric trait within the whole population. Variation between different segments of this population (i.e., between males and females, younger and older age-cohorts, etc.) was also examined.

3.5.2 Inter- and Intra-Observer Reliability/Reproducibility Test-Retest Statistical Analyses

Measurements and calculations were conducted by the primary author (MT) on two different occasions (2013 and 2014). The re-measuring was used to determine intra-observer test-retest reliability. In addition, measurements and calculations were also conducted by a secondary author, Isabella Graham, in-blind, to judge inter-observer test-retest reproducibility. The primary statistical tests used for determining intra- and inter-observer reliability and reproducibility was the Wilcoxon Signed-Rank test for paired samples ($\alpha=0.05$) (for general agreement), the Concordance Correlation Coefficient (CCC), and the Intraclass Correlation Coefficient (ICC).

3.5.3 Sexing of the MT1

Using the measurements taken for the MT1 metric recording described earlier, a binary logistic regression model was created. This model was used to estimate the probability of an individual being either male or female, given the measurements of their MT1.

3.5.4 Osteo-volumetric Density

A fundamental component of this methodology requires the determination of a '*healthy adult population*' in order to compare the relative bone densities of all the skeletons. Obviously, the Osteological Paradox (Wood et al. 1992) raises a concern for defining '*healthy*' in bioarchaeological samples, so care must be taken in order to assess each skeleton. The MT1s in burials with pathologies known to influence bone densities (e.g., leprosy) were eliminated from the '*healthy*' population. In addition to eliminating individuals with pathologies, a number of additional considerations were required to establish the '*healthy*' adult population. First, symmetry bias was determined using the

paired two-sample t-test. Second, sex- and age-cohort testing were conducted using the two-sample t-tests. In order to examine bone density loss with age, we decided to divide the '*healthy population*' into two age-cohorts: those 40 and below, and those above 40 years of age.

Though somewhat arbitrary, this cut-off has some physiological reality, especially for females, since it is well known that the loss of bone density accelerates in the fourth decade with the approaching peri- and menopausal periods. Additionally, it has been shown that peak bone density is established within the third decade of life (Plato et al. 1994; WHO 2003; Bartl and Frisch 2004; Camacho and Miller 2007). The same age-cohorts are used for both males and females. Of course, we acknowledge the problem of a cut-off age when aging adult skeletal remains; some individuals aged in their mid to late 30s could in reality be in their 40s and vice versa. The significance and validity of the 40 cut-off were tested using standard t-tests (or non-parametric equivalents).

With the '*healthy population*' established, each individual can be visualized using a regression scatter-plot. In order to determine at-risk individuals, we followed the World Health Organization standard. For bone mineral density values (BMD) of the hip, they define osteoporosis as those individuals who are more than -2.5 standard deviations below the mean of the healthy adult population (WHO 2003; WHO 2007). Although their criteria use a different region of the skeleton and different measurement data, we believe the approach is suitable for this research. A deficit of -2.5 standard deviations is a significant departure for an individual to be below the healthy adult population mean. In our study, the MT1 osteo-volumetric density data for each burial is compared to the population mean using a T-Score (see below). Several authors (e.g., WHO 2003; Bartl

81

and Frisch 2004; Camacho and Miller, 2007) note that one of the caveats in modern clinical diagnoses is the lack of population and sex-specific standards. This approach addresses their concerns. Moreover, though modern clinicians have the ability to conduct longitudinal studies, today individuals are compared to cross-sectional standards, not their own longitudinal values. In our research, as is the case in clinical, we can assume most individuals as they aged would have declining bone density from their own peak density values. Again, this is usually established by the early 30s (Plato et al., 1994; WHO, 2003; Bartl and Frisch, 2004; Camacho and Miller, 2007). While there are likely cases where density values would not change with advancing age, these would be rare.

In summary, as the methodology is new, the measurements used first underwent intra- and inter-reliability and reproducibility testing. Standard hypothesis tests were then conducted to evaluate the amount of symmetry, to test the differences between the sexes, and to validate the division of age-cohorts, both between and within the sex-cohorts. This facilitated the development of mean osteo-volumetric density values for the '*healthy*' adult population, which was then used to calculate T-scores for the remainder of the skeletal sample. Osteoporosis-related low-impact fracture data were correlated with these T-scores for the purposes of evaluating the <-2.5 SD standard, and to establish if the MT1 is in fact a suitable element for the study of bone health and osteoporosis in antiquity.

3.5.5   μCT Density and Trabecular Architecture

3.5.5.1   μCT Density.

In order to examine the usefulness of the MT1 in bioarchaeological bone health studies, two null hypotheses were tested. The first null hypothesis is that the bone quantity of the MT1 is independent of biological age. The second null hypothesis is that the quantity of

bone in those individuals with osteoporosis-related fractures is not significantly lower than the "*healthy*" adult population mean. In order to test the first hypothesis a simple linear regression analysis between age and the previously stated surrogate measures of bone strength provides some insight into their relationship. The second hypothesis was investigated by developing a population-specific female standard, using the "*healthy*" adult female sub-sample from K2 (<50 years old), and estimating T-Scores for those individuals with osteoporosis-related fractures. It should be noted that the term "*healthy*", used herein, refers to individuals who were absent of any pathological skeletal evidence, but makes no assumptions as to the actual health-status of the individual. The individuals clearly had died from something, but there are no signs as to the cause of death on the skeleton. This is the "*healthy but dead*" paradox (Wood et al. 1992), and is unavoidable when using bioarchaeological remains. Although the sample population used herein is somewhat small, it again, should provide us some insight into the efficacy of the MT1 for the study of diseases of systemic bone loss such as osteoporosis.

3.5.5.2   μCT Trabecular Architecture

In order to examine the usefulness of the MT1 in bioarchaeological trabecular bone health studies, a number of null hypotheses were tested. The first null hypothesis is that there is no difference between the various trabecular measures used in this study with regards to the two different VOIs (base and head) from the same individual. The second null hypothesis is that trabecular bone quantity and quality of the MT1 is independent of biological age. The third null hypothesis is that the trabecular bone quantity and quality of the MT1s associated with individuals with osteoporosis-related fractures will not be significantly lower than the '*healthy*' adult female population mean.

In order to test the first null hypothesis, standard paired (repeated measures) parametric testing, or the non-parametric equivalent, were conducted for all quantity and quality measurements for comparison between the two VOIs for each MT1. The second null hypothesis was investigated using multiple linear regression (dependent variables BVF, BMD, TbTh, and TbSp) with respect to biological age. The final null hypothesis was tested using a T-Score approach that compares the individuals with osteoporosis-related fractures to the '*healthy*' K2 adult female population mean. All data analyses were generated using Microsoft Excel (2016 MOS) with the Real Statistics Resource Pack Software (Release 4.3) add-in.

3.6   Summary

This chapter has briefly described the history and geography of the Dakhleh Oasis Project, and placed the bioarchaeological research program in this context. A key advantage for bioarchaeological research in the Dakhleh Oasis is the excellent preservation and context of the Kellis 2 sample. In advance I will note that only a single MT1, of the 377 analysed, was eliminated because of preservation problems. Moreover, though not a part of the methodology's research design, following my data (measurements, and statistics detailed in this chapter), the osteo-volumetric data were plotted by burial in the K2 cemetery to determine if there were any biases in bone density that may reflect diagenic concerns. This research was based on a sophisticated spatial statistical program developed by Dr. Jim Keron, and was the basis of a recently completed PhD thesis on Kellis (Keron 2015). The test of my data resulted in H_o being accepted. Diagenic changes in the MT1 samples described in this chapter, particularly bone density, were not affected by post-environmental degradation on an intra-cemetery

level, which is always a major concern of researchers working on bone density. This again will be mentioned in Chapter 4.

Chapter 4

4   RESULTS

4.1   Introduction

This chapter presents the results of the statistical tests that were described in Chapter 3, section 3.6. Section 4.2 presents the prevalence results of the occurrence of the Intermetatarsal Facet in the Kellis 2 population. Section 4.3 is the results from the inter- and intra-observer reliability/reproducibility Test-Retest statistics. Section 4.4 presents the results from the use of the MT1 for sexing individuals from the Kellis 2 cemetery. Section 4.5 presents the results from the Osteo-volumetric density analyses. Section 4.6 presents the results of the μCT analyses concerning MT1 cortical bone density. Section 4.7 presents the results from the analyses concerning trabecular architecture. It should be noted that because there were many different types of analyses used in this thesis to test the many applications of the MT1 in bioarchaeological research, that a small discussion will follow each results section in order to discuss those observations and methods specifically. A general discussion of the use of the MT1 in bioarchaeology, and future considerations in this area of research are saved for Chapter 5, Discussion.

Additionally, it should be noted that a spatial analysis was conducted by the Author and Jim Keron (PhD, Western University, London Ontario), which tested the distribution of individuals with low osteo-volumetric density within the K2 cemetery in order to see if there was differential preservation within the site. Since this was co-authored and relied on both investigators equally, it will not be included within this dissertation. The conclusions of this analysis failed to reject the null hypothesis, and

authors conclude that the distribution of MT1s with low osteo-volumetric density does not indicate any localized intra-cemetery environmental factors resulting in differential preservation from a spatial perspective. Consequently, there are no areas of the site with differential preservation.

It should also be noted when analyzing the µCT data I could select known values for bone. This means that I could exclude all values below (e.g., water, air, etc.) and above (e.g., sediment, etc.) those acceptable for bone, which could have caused erroneous results. Inclusions from the surrounding environment did not contribute to the data and analyses. Finally, all raw data are included in Appendix B.

4.2   Intermetatarsal Facet Prevalence

The scoring of the Intermetatarsal Facet (IMF) followed the outlined descriptions found in **Table 4**. A total number of 214 (n=214) individuals from the Kellis 2 cemetery was observed for the IMF nonmetric trait. When scoring a presence (score of 1, 2, or 3) it was found that 60 of the 214 individuals (P=28%) had IMF present on at least one of their MT1s. Moreover, it was found that of those 60 individuals, 41 of the individuals (68%) had bilateral expression, while 10 individuals were unobservable because of a missing MT1.

Table 4 Intermetatarsal Facet Scoring. This table describes the scoring criteria for the IMF that was used to investigate the prevalence of the trait in the Kellis 2 population.

Score	Expression	Description
0	Absent	Absent
1	Slight	Smooth surface with no defined borders
2	Partial	At least one defined and raisedborder and a smooth surface
3	Full	The whole facet is well defined with all raised borders either seperate or merged with the proximal base facet
N/O		Missing MT1

While scoring the IMF trait, it was found that the distinction between 0 and 1 was particularly difficult to state with certainty, so in another analysis these two categories were combined and considered absence of the IMF trait. When approaching the analysis using these categories (A = 0 and 1, P = 2 and 3) it was found that IMF was present in 41 of the 214 individuals (P=19%), and had bilateral expression in 19 of the 41 individuals (46%), while 7 individuals were unobservable because of a missing MT1.

If the presence of the IMF was developmental, its prevalence should increase with increasing age. This was found to not be the case. Both methods of scoring were used and are presented in **Figure 16**. The distribution of the IMF does not seem to be related to age.
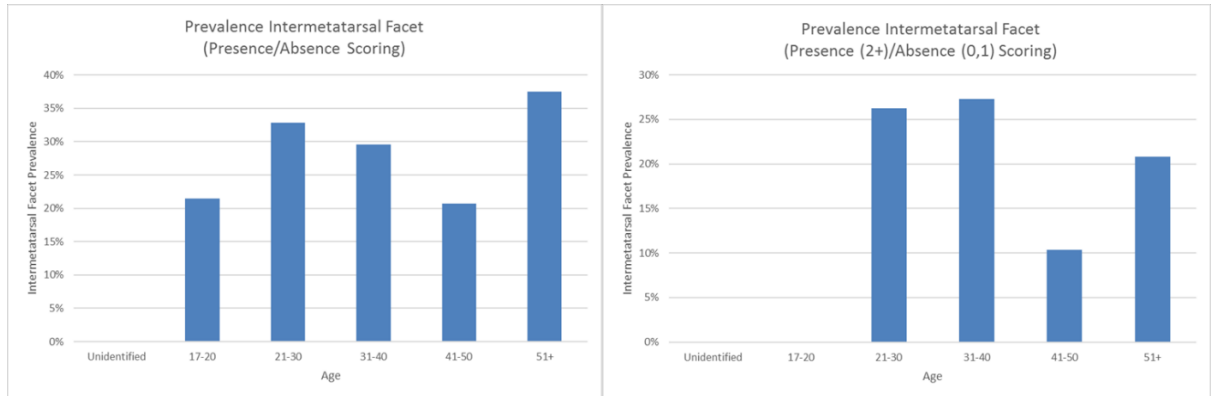
Figure 16 Prevalence of Intermetatarsal Facet within Various Age-Cohorts. The distribution of the IMF trait does not appear to be age-related when using either of the scoring methods.

The K2 population was also analyzed to see if the presence of the IMF trait was correlated with the sex of an individual. It was found that there is no apparent relationship between the prevalence of IMF and sex within the K2 population, as seen in **Figure 17**. In summary, the prevalence of the Intermetatarsal Facet in the K2 population was between 19% and 28%, which was dependent on the scoring criteria for presence and absence. Moreover, there was no evidence to support that the presence of IMF was related to either age or sex in the K2 population.
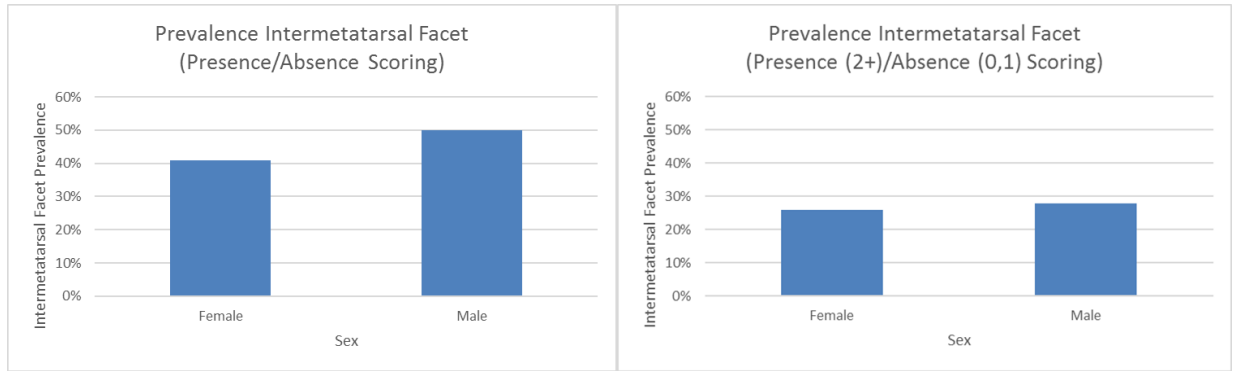
Figure 17 Prevalence of Intermetatarsal Facet within Various Sex-Cohorts. The distribution of the IMF trait does not appear to be sex-related when using either of the scoring methods.

4.3 Inter- and Intra-Observer Reliability/Reproducibility Test-Retest

All scientific data are required to be precise and accurate in order to test hypotheses (Molto 1979). For any new methods, like the one presented herein, this requirement carries increased weight. Statistical testing of the osteo-volumetric density measurements, described above, for intra- and inter-observer reliability and reproducibility primarily used the Wilcoxon Signed-Rank test for paired samples (α=0.05) (the data sets were not assumed to be normally distributed), the Concordance Correlation Coefficient (CCC), and the Intraclass Correlation Coefficient (ICC).

The testing of intra-observer error by the author (MT) compared the densities of 106 randomly selected MT1s – measured and calculated twice over a one-year period (2013-14). The null hypothesis was accepted, as there was no significant difference between the estimated osteo-volumetric density calculated between the 2013 ($\bar{x}_{2013}$=230.74 mg/cm^3, SD=56.80) and 2014 ($\bar{x}_{2014}$=230.74mg/cm^3, SD=56.76) MT1s

from the same individuals (T (105) =2534, p=0.525). Additionally, coefficient measures of CCC=0.9966 and ICC=0.9966 were found between the two sets of observations.

Additionally, the measurements and the osteo-volumetric density values for 269 MT1s were tested between the author MT and Isabella Graham (IG) – the latter being a graduate student in the Anthropology Department, Western University. The null hypothesis was accepted, as no significant differences occurred between the estimated osteo-volumetric density calculated by Teeter ($\overline{x}_{Teeter}$=247.22mg/cm^3, SD=53.52) and Graham ($\overline{x}_{Graham}$=247.82mg/cm^3, SD=57.02) for the same MT1s (T (268) =16467, p=0.355). Furthermore, CCC=0.9692 and ICC=0.9693 were found between the two sets of observations. Intra- and Inter-observer reliability and reproducibility tests were all statistically concordant in accepting the null hypothesis. The osteo-volumetric density calculations used herein are highly reliable and reproducible.

4.4 Sexing of the MT1 using Metric Measurements

Authors such as Robbling and Ubelaker (1997) and Mountrakis et al. (2010) used discriminant function analysis of osteometric data from metatarsals to create a sexing method. This method relied upon all metatarsals, and as a consequence to the type of analysis, also assumed that the independent variables were normally distributed for each level of the grouping variable. Both of these conditions made the use of their method untenable in this investigation. In order to bypass the assumptions necessary for a discriminant function analysis to make a method more usable by researchers with many different types of data or single skeletal elements, it was decided to use logistic regression analysis.

There are two different approaches when using this type of analysis. The first is what can be termed as "the kitchen sink" approach. This is when as many types of independent variables as possible, measurements in this case, are used to predict a binary response or dependent variable. The second approach is more selective and only uses those independent variables that have significant p-values from the initial analysis. Both methods are given below in **Tables 5-8**.

Table 5 "Kitchen Sink" Logistic Regression. Results from the logistic regression analysis for the MT1 using all independent variables that were measured. The model categorizes females as 0 and males as 1 with respect to the dependent variable. This model correctly classified females and males ~89% of the time.

Predictor	coeff b	s.e.	Wald	p-value	exp(b)	lower	upper
Intercept	-18.211	4.94427	13.56635	0.00023	1.23E-08		
Weight	1.254658	0.255842	24.04957	9.39E-07	3.506638	2.123821	5.789804
Max. Length	-0.17901	0.093852	3.638156	0.056469	0.836095	0.695615	1.004946
Head Width	-0.39011	0.300664	1.683532	0.194456	0.676979	0.375534	1.220397
Head Height	0.676142	0.330496	4.185454	0.040772	1.966277	1.028788	3.75806
Base Height	0.20359	0.257284	0.626165	0.428766	1.225796	0.740317	2.029638
Base Width	0.528621	0.296679	3.174795	0.074783	1.696592	0.948514	3.034667

Chi-Sq	123.9841	Hosmer	325.7625
df	6	df	163
p-value	2.37E-24	p-value	6.31E-13
alpha	0.05	alpha	0.05
sig	yes	sig	yes

Classification Table			
	Suc-Obs	Fail-Obs	
Suc-Pred	57	7	64
Fail-Pred	11	90	101
	68	97	165
Accuracy	0.838235	0.927835	0.890909
Cutoff	0.5		

Table 6 Selective Logistic Regression. From Table 5, only MT1 weight and Head Height were significant in contributing to the prediction of the dependent variable (female or male). When a logistic regression was run only using these two independent variables it was found that the model could correctly classify sex in ~88% of the K2 population.

Predictor	coeff b	s.e.	Wald	p-value	exp(b)	lower	upper
Intercept	-19.0172	3.823901	24.7331	6.58E-07	5.51E-09		
Weight	1.027822	0.196861	27.25943	1.78E-07	2.794971	1.900243	4.110982
Head Height	0.633517	0.207082	9.359065	0.002219	1.884226	1.255638	2.827493

Chi-Sq	114.4141	Hosmer	237.2673
df	2	df	163
p-value	1.43E-25	p-value	0.000131
alpha	0.05	alpha	0.05
sig	yes	sig	yes

Classification Table			
	Suc-Obs	Fail-Obs	
Suc-Pred	55	7	62
Fail-Pred	13	90	103
	68	97	165
Accuracy	0.808824	0.927835	0.878788
Cutoff	0.5		

Table 7 "Kitchen Sink" without Weight Logistic Regression. Due to the fact that bone weight can be highly affected by bone disorders such as osteoporosis, it was decided to run a logistic regression without a weight independent variable. When using all other independent variables, it was found that the model could correctly classify sex in ~82% of the K2 population.

Predictor	coeff b	s.e.	Wald	p-value	exp(b)	lower	upper
Intercept	-25.0831	4.260376	34.66301	3.92E-09	1.28E-11		
Max. Length	-0.0482	0.075276	0.40998	0.52198	0.952944	0.822228	1.104441
Head Width	0.092538	0.245793	0.141744	0.706554	1.096955	0.677593	1.77586
Head Height	0.640902	0.245599	6.809731	0.009066	1.898193	1.172967	3.071812
Base Height	0.300607	0.207898	2.090718	0.148196	1.350678	0.898646	2.03009
Base Width	0.287006	0.209811	1.871231	0.171334	1.332433	0.88319	2.010187

Chi-Sq	77.97912	Hosmer	212.7656
df	5	df	163
p-value	2.22E-15	p-value	0.005338
alpha	0.05	alpha	0.05
sig	yes	sig	yes

Classification Table			
	Suc-Obs	Fail-Obs	
Suc-Pred	52	13	65
Fail-Pred	16	84	100
	68	97	165
Accuracy	0.764706	0.865979	0.824242
Cutoff	0.5		

Table 8 Selective Logistic Regression without weight. From Table 7, only Head Height was significant in contributing to the prediction of the dependent variable (female or male). When a logistic regression was run only using that independent variable, it was found that the model could correctly classify sex in ~81% of the K2 population.

Predictor	coeff b	s.e.	Wald	p-value	exp(b)	lower	upper
Intercept	-20.8832	3.335966	39.1879	3.85E-10	8.52E-10		
Head Height	1.091595	0.176668	38.17753	6.46E-10	2.979023	2.107142	4.211666

Chi-Sq	68.62022	Hosmer	200.5693
df	1	df	157
p-value	1.19E-16	p-value	0.01075
alpha	0.05	alpha	0.05
sig	yes	sig	yes

Classification Table			
	Suc-Obs	Fail-Obs	
Suc-Pred	50	14	64
Fail-Pred	18	83	101
	68	97	165
Accuracy	0.735294	0.85567	0.806061
Cutoff	0.5		

In summary, it was found that when using various metrics of human MT1 as independent variables, that the correct sex category (female = 0, male = 1) could be predicted between ~81-89% for the K2 population using logistic regression modelling. Very little difference was found between the "kitchen sink" method and the more selective methods relying on only those independent variables that were found to be statistically significant. Moreover, when bone mass was included as an independent variable, the predictive model was much better (~88-89% compared to ~81-82%).

4.5   Osteo-Volumetric Density

4.5.1   Symmetry

Symmetry between the left and right MT1 was tested on one hundred randomly selected individuals using a random number generator provided by Microsoft Excel 2007. Only those individuals that had both MT1s recovered were included in this analysis. The data met the parametric parameters and the assumption of a normal distribution. The null hypothesis was accepted using a paired two-sample for means t-test (hypothesized mean difference = 0). There were no differences between the estimated osteo-volumetric density values for the left ($\overline{x}_{Left}$=238.853mg/cm^3, SD=54.88), and right ($\overline{x}_{Right}$=239.42 mg/cm^3, SD= 55.11) MT1s from the same individuals (t(99) =1.17, p=0.244). Thus, asymmetry was not a research concern when only a left or right MT1 was available for a given burial. For skeletons with both MT1s present, the mean density value was computed to minimize any bias.

4.5.2   Sex and Age Statistics

A two-sample t-test (equal variances, hypothesized mean difference = 0) was used to test the mean osteo-volumetric densities for K2 females (n=112) and males (n=81) (the data sets met the requirements for parametric testing). The null hypothesis was rejected – statistically significant differences occurred between the sexes at K2 (t(191)=4.88, p=2.24E-06; ($\overline{x}_{Females}$=227.56mg/cm^3, SD=55.14) ($\overline{x}_{Males}$=264.38mg/cm^3, SD=46.61)). The regression of the estimated osteo-volumetric values against age for both males and females also supports this conclusion (see **Figure 18**). Note that in these figures, the

osteo-volumetric patterns differ significantly between males and females with increasing age. The inverse relationship (decreasing density with increasing age) in females is much more pronounced than is seen in males. The R^2 coefficients of determination of 0.5248 and 0.1251 for females and males, respectively, demonstrate the enormous disparity that age has on the female osteo-volumetric density values, relative to males. Although the female R^2 appears to be low, as it only explains approximately 52% of the variation, it is quite significant given the complex multifactorial nature of bone density loss. Regardless, it is quite clear that female and male osteo-volumetric densities require separation for creating the '*healthy*' adult population standard. Consequently, individual cases should be compared to the respective male/female sub-populations.
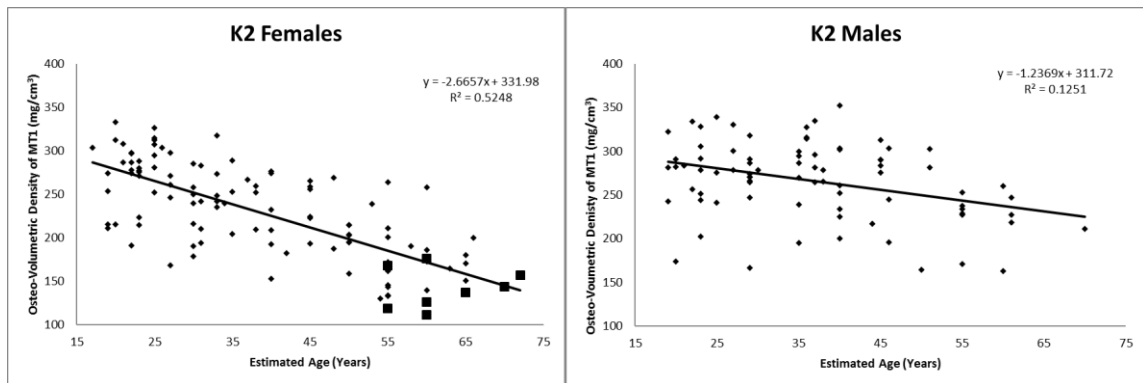
Figure 18 Female vs. Male Regression. Left: A regression consisting of Osteo-Volumetric Density of the first metatarsal with age in females of the K2 cemetery population. '■' denotes the 8 females with hip fractures that MT1s were available for in this research. **Right:** A regression consisting of Osteo-Volumetric Density of the first metatarsal with age in males of the K2 cemetery population.

Quite clearly the older-adult cohort data have a profound influence on the overall data and, therefore, may obscure our understanding of the pattern of bone loss in the younger adult males and females. To test this effect requires that the latter cohort data be

treated separately. This is tested using a two-sample t-test (equal variances, hypothesized mean difference = 0). The data sets met the requirements for parametric testing. The null hypothesis – there is no difference between the mean osteo-volumetric densities between young-adult (< 40 years) females and males – is rejected in the Kellis 2 population (t(104)=2.98, p=0.0036); ($\bar{x}_{\text{Females}<40}$=260.84mg/cm^3, SD= 39.85) ($\bar{x}_{\text{Males}<40}$=282.35mg/cm^3, SD=32.39). Bone density appears to be lower in K2 females even before the 4$^{\text{th}}$ decade.

A two-sample t-test (equal variances, hypothesized mean difference of = 0) of the older-adult cohorts, not unexpectedly, resulted in the rejection of the null hypothesis of estimated osteo-volumetric densities between females (40+) ($\bar{x}_{\text{Females40+}}$=189.16mg/cm^3, SD=44.42) and males (40+) ($\bar{x}_{\text{Males40+}}$=249.03mg/cm^3, SD=45.74) of the K2 cemetery population (t (82)=5.93, p=6.89125E-08). This clearly shows that beyond having lower bone density during young-adulthood, there is also an exponential bone loss in females relative to males after the 4$^{\text{th}}$ decade.

In order to examine this exponential nature of bone density loss in the females, a two-sample t-test (equal variances, hypothesized mean difference = 0) was conducted comparing the younger (n=60) and older female (n =52) cohorts. Again H$_0$ was rejected, as the following values show ($\bar{x}_{\text{Females}<40}$ = 260.84mg/cm^3, SD=39.85; $\bar{x}_{\text{Females40+}}$=189.16mg/cm^3, SD=44.42; K2 cemetery population (t(110)=9.00, p=7.60195E-15)). This result seems to support our seemingly arbitrary selection of the 40-year-old cut-off point, at least for the female sub-population. As will be discussed,

there is considerable bone density variation among the healthy females in both cohorts. A summary of the statistics used can be found in **Table 9**.

Table 9 A summary of the statistical tests conducted. '*n*' is the number of individual MT1s used in the statistical test. '*df*' is the degrees of freedom. '*p*' is the probability. '*HMD*' is the hypothesized mean difference. '*t-crit*' is the critical values used to determine significance.

Purpose	Test	n	df	Level	Result	Critical Value	p	Significant
Asymmetry	t-test: Paired two sample for means	100	99	HMD = 0	t=1.17	t-crit=1.98	0.244	no
Female/Male	t-Test: Two-Sample Assuming Equal Variances	112/81	191	HMD = 0	t=4.88	t-crit=1.97	2.24E-06	yes
Female (<40)/ Male (<40)	t-Test: Two-Sample Assuming Equal Variances	60/46	104	HMD = 0	t=2.98	t-crit=1.98	0.0036	yes
Female (40+)/ Male (40+)	t-Test: Two-Sample Assuming Equal Variances	52/32	82	HMD = 0	t=5.93	t-crit=1.99	6.89E-08	yes
Female (<40)/ Female (40+)	t-Test: Two-Sample Assuming Equal Variances	60/52	110	HMD = 0	t=9.00	t-crit=1.98	7.60E-15	yes

4.5.3 Osteoporosis-related fracture pattern

Given the age and sex statistical results, it was decided to create a '*healthy*' adult population from only the younger female cohort for use in a T-score evaluation (Z-score if the individual was a member of the 'healthy' adult cohort). Using the formula (x_i-$\bar{x}$)/SD), the T-score/Z-score values were determined for all females (where x_i = individual osteo-volumetric density; $\bar{x}$ = mean of the '*healthy*' female (<40) population; SD = the standard deviation of the '*healthy*' female population). These values were then correlated with known fracture pattern and osteobiographical data. Of the 112 females sampled in this study, 17.9 % (n =20) had osteoporosis-related low-impact fractures (hip, colles',

sacral, rib, and vertebral compression). Moreover, it was found that all individuals with ORFs had negative T-score values ranging from -0.04 to -3.71. Of these, all but two females were lower than -1.5 SDs from the '*healthy*' female adult mean.

There were no individuals below the age of 40 years of age (n=60) with an ORF – all 20 that occurred were in the older age-cohort for a prevalence of 38.5% (20/52). Of the 40+ females, two, or 13% (2/15), in the 40-50-year-old age-range, had ORFs (n=15, prevalence of ~13%). Low-impact fractures were respectively present in 32% (7/22) and 73% (11/15) of 50-60-year-old and 60+ female populations. Clearly the risk of fractures rises exponentially in the older age-cohorts. Moreover, individuals with hip fractures (n=8) for which we had MT1 data, the most serious of the osteoporosis-related fractures, all had T-scores less than -2.1 standard deviations below the healthy adult female population mean (See **Table 10** for fracture data). Of the 27 females who fell below -2SD from the healthy adult population, 15 had osteoporotic low-impact fractures (prevalence of ~58%), and eight of those were hip fractures (~31%) (See **Table 11** for all females below -2SD from the healthy adult population). For females between -2 and -3SD below the healthy adult mean, 10 of 18 (~56%) had ORFs. Of the females below -3SD, 5 of 8 (~63%) had ORFs.

Table 10 A summary of all of the osteoporosis-related fractures (ORFs) from the K2 cemetery sample. T-scores were determined by comparing the estimated osteo-volumetric density of each individual with the healthy adult female mean. Note, all of the hip fractures occur in individuals with T-scores less than or equal to -2.1 standard deviations and an estimated range of 55-72 years of age. '*VCD*' is the occurrence of vertebral compression deformities.

Burial	Side	Age	Sex	Osteo-Volumetric Density (mg/cm^3)	T-Score	Colles	Hip	Sacrum	VCD	Ribs
41	A	60	F	111.63	-3.7142	0	1	0	0	0
459	A	55	F	119.17	-3.5258	1	1	0	1	0
D7-3	R	60	F	125.99	-3.3557	0	1	0	0	0
266	R	55	F	133.71	-3.1628	0	0	0	1	1
438	A	65	F	137.41	-3.0706	0	1	0	0	1
275	L	55	F	143.51	-2.9183	1	0	0	0	0
261	A	70	F	143.78	-2.9116	0	1	1	1	0
530	A	40	F	153.25	-2.6752	0	0	0	1	0
8	A	72	F	156.87	-2.5847	1	1	0	0	0
377	A	55	F	161.58	-2.4671	0	0	0	1	0
44	A	63	F	164.56	-2.3929	1	0	0	1	0
5	A	55	F	167.84	-2.3109	0	1	1	0	1
443	A	60	F	173.02	-2.1817	0	0	0	1	0
82	A	60	F	176.46	-2.0959	0	1	0	0	1
72	A	65	F	180.09	-2.0052	0	0	1	0	0
470	A	50	F	194.82	-1.6374	1	0	0	0	0
458	A	50	F	195.18	-1.6284	1	0	0	0	0
202	A	66	F	200.46	-1.4966	1	0	0	1	1
294	A	45	F	222.7	-0.9415	0	0	0	0	1
280	L	60	F	258.43	-0.0496	1	0	0	1	1

Table 11 Fractures present in females with T-Score/Z-Scores lower than -2 SD from the healthy adult population mean. VCD = Vertebral Compression Deformity.

Burial	Age	Sex	T-Score/Z-score	Fracture
41	60	F	-3.74	Hip
459	55	F	-3.55	Colles', Hip, VCD
D7-3	60	F	-3.38	Hip
210	54	F	-3.27	None
528	55	F	-3.2	None
266	55	F	-3.19	VCD, Ribs
438	65	F	-3.1	Hip, Ribs
452	60	F	-3.03	None
275	55	F	-2.94	Colles'
261	70	F	-2.94	Hip, Sacrum, VCD
165	55	F	-2.88	None
541	65	F	-2.77	None
530	40	F	-2.7	VCD
8	72	F	-2.61	Colles', Hip
76	50	F	-2.57	None
377	55	F	-2.49	VCD
91	55	F	-2.46	None
44	63	F	-2.42	Colles', VCD
5	55	F	-2.33	Hip, Sacrum, Ribs
413	27	F	-2.32	None
306	65	F	-2.26	None
20	55	F	-2.23	None
443	60	F	-2.2	VCD
82	60	F	-2.12	Hip, Ribs
540	30	F	-2.06	None
72	65	F	-2.03	Sacrum
141 a	42	F	-1.97	None

4.5.4   Osteoporosis diagnosis

Using the definition of <-2.5SD, as suggested by WHO (2003) for hip BMD, I found that of the 60 females below the age of 40, none would be diagnosed with osteoporosis. Moreover, in the 40-49 age-cohorts (n=15) only one individual (~7%) would be diagnosed. In the 50-59 age-cohorts (n=22), nine individuals fell below -2.5 SDs (~41%),

while in the 60+ age-cohort (n=15), seven individuals fell below -2.5 SDs from the female healthy adult mean (~47%). In total, within the 50+ age-cohorts (n=37), 15 would be diagnosed with osteoporosis (~41%) using the definition provided by WHO (2003). The total female population that fell below -2.5 standard deviations (n=112) was 17 (~15%). In addition to the T-score evaluation, we must also include those individuals who did not meet this density criterion, but were determined to have ORFs nonetheless, for a more accurate representation of prevalence. An additional 11 females had ORFs, but were within -2.5SD of the healthy adult female osteo-volumetric density mean. This increases the overall prevalence of osteoporosis in the K2 females from 17 to 28 individuals (25%).

I believe that in the case of the osteo-volumetric density method for the MT1 that the <-2.5SD, as recommended by WHO for hip BMD, is a conservative benchmark. Our results indicate that all hip fracture sufferers, which as discussed are the most dangerous of the ORFs, were greater than -2SD below the healthy female adult mean (see **Table 11**). Additionally, 78% (7/9) of vertebral compression deformities appear in individuals with osteo-volumetric density values that are less than -2SD below the healthy adult mean. If we were to use this more moderate standard, as opposed to the -2.5SDs, the results are quite different. For females <40 (n=60), there are two individuals less than -2SD (~3%). In the 40-49 age-cohort (n=15), two females would be diagnosed (~13%). In the 50-59 age-cohort (n=22), 11 females would be diagnosed with osteoporosis (50%). In the 60+ age-cohort (n=15), 12 females would be diagnosed with osteoporosis (~80%). Therefore, the overall number of females (n=112) that would be diagnosed with osteoporosis would rise to 27 individuals (~24%). Additionally, there are five females

who have ORFs who do not meet the -2 SD criterion, increasing the overall prevalence to 28.5%. See **Table 12** for summary of osteoporosis prevalence results.

Table 12 Summary of the prevalence of osteoporosis in K2 females. This table includes the data for <-2.5 standard deviations and <-2 standard deviations diagnostic criteria. ORFs = Osteoporosis-related Fractures.

<2.5 Standard Deviations			
Age-Cohort	P	n	P/n
<40	0	60	0%
40-49	1	15	7%
50-59	9	22	41%
60+	7	15	47%
Total	17	112	15%
Total + ORFs > -2.5SD	28	112	25%
<2 Standard Deviations			
Age-Cohort	P	n	P/n
<40	2	60	3%
40-49	2	15	13%
50-59	11	22	50%
60+	12	15	80%
Total	27	112	24%
Total + ORFs > -2SD	32	112	29%

4.6 µCT Analysis of the MT1

4.6.1 µCT Density, Bone Volume Fraction, and Cortical Index Analyses of the MT1 Results

Bone mineral density and bone volume fraction measurements were taken for all individuals (n=44) using 4 different VOIs; proximal shaft, mid-shaft, distal shaft and the whole shaft – using the VOI dimensions described in the methods section. All sub-populations were determined to be normally distributed using residual and normal probability plots (Q-Q plots). The residual plots showed no discernible patterns, while the normal probability plots were linear, positive, and had no indications of skewing, and therefore the BMD and BVF data were treated accordingly during analyses.

The linear regression models developed for all VOIs performed well, and were very similar to one another, as seen in **Table 13**. All Models were significant (F(1,42) = ranging from 25.8 to 41.1, p= ranging from 8.3E-6 to 7.0E-7) for predicting BMD and BVF with respect to biological age. Examples of the regression plots for the proximal shaft are given in **Figures 19-20**. All other regression plots were very analogous in their visual appearance and interpretation. The BMD adjusted R^2 values for each model ranged from 0.37 (fig. 19) for the proximal shaft to 0.43 for the mid-shaft. This indicates that between approximately 37% and 43% of the variation in BMD could be accounted for using age alone. This lower value is not unexpected as bone maintenance and loss is a multifactorial process that includes genetics, diet, health, and activity, among other factors. An additional factor, of course, is the reality that accurate aging of older adults is very problematic with bioarchaeological samples. Moreover, the BVF adjusted R^2 values for each model ranged from 0.39 for the distal shaft, and 0.48 for the mid-shaft

estimations. Again, this indicates that between 39% and 48% of the variation in BVF can be accounted for using biological age alone. As **Table 13** illustrates, there were slight variations between the different VOIs in terms of BMD and BVF.

Table 13 Results from the linear regression tests conducted for both BMD and BVF. The results are shown for all VOIs, as well as for the average between the values for the proximal, mid-, and distal shaft measurements.

MT1 Location	Dependent Variable	n	ANOVA				Linear Regression				
			df	F	F sig	Adjusted R^2	Independent Variable	Coefficients	SE	t Stat	P-value
Proximal	BMD	44	1, 42	25.8	8.30E-06	0.3656	Intercept	176.6969	12.9464	13.6	4.90E-17
							Age	-1.4592	0.2874	-5.1	8.30E-06
	BVF	44	1, 42	31.8	1.30E-06	0.4176	Intercept	0.2285	0.01113	20.5	1.60E-23
							Age	-0.0014	0.00025	-5.6	1.30E-06
Mid-Shaft	BMD	44	1, 42	34	7.00E-07	0.4342	Intercept	203.4179	14.5494	14	2.10E-17
							Age	-1.8832	0.32298	-5.8	7.00E-07
	BVF	44	1, 42	41.1	1.00E-07	0.4822	Intercept	0.2428	0.01168	20.8	1.00E-23
							Age	-0.0017	0.00026	-6.4	1.00E-07
Distal	BMD	44	1, 42	32.6	1.00E-06	0.4236	Intercept	208.3628	16.6553	12.5	9.40E-16
							Age	-2.1112	0.36973	-5.7	1.00E-06
	BVF	44	1, 42	28.2	3.80E-06	0.3877	Intercept	0.2661	0.01416	18.8	4.60E-22
							Age	-0.0017	0.00031	-5.3	3.80E-06
Average	BMD	44	1, 42	32.6	1.00E-06	0.4237	Intercept	196.1592	14.3381	13.7	4.50E-17
							Age	-1.8179	0.31829	-5.7	1.00E-06
	BVF	44	1, 42	37	3.00E-07	0.4557	Intercept	0.2458	0.01166	21.1	5.90E-24
							Age	-0.0016	0.00026	-6.1	3.00E-07
Whole	BMD	44	1, 42	33.9	7.20E-07	0.4332	Intercept	833.5924	59.9941	13.9	2.60E-17
							Age	-7.7496	1.33181	-5.8	7.20E-07
	BVF	44	1, 42	39.7	1.50E-07	0.4736	Intercept	0.2854	0.01405	20.3	2.40E-23
							Age	-0.002	0.00031	-6.3	1.50E-07
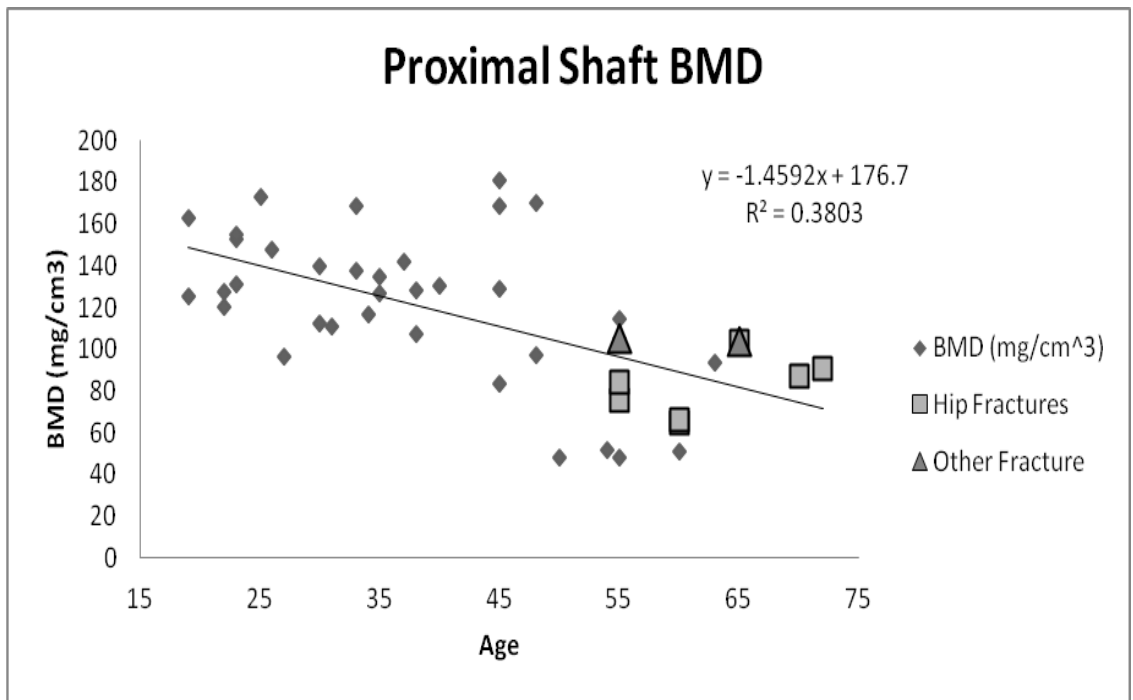
Figure 19 Regression plot of BMD of the proximal shaft of the first metatarsal with estimated mean biological age for K2 females.
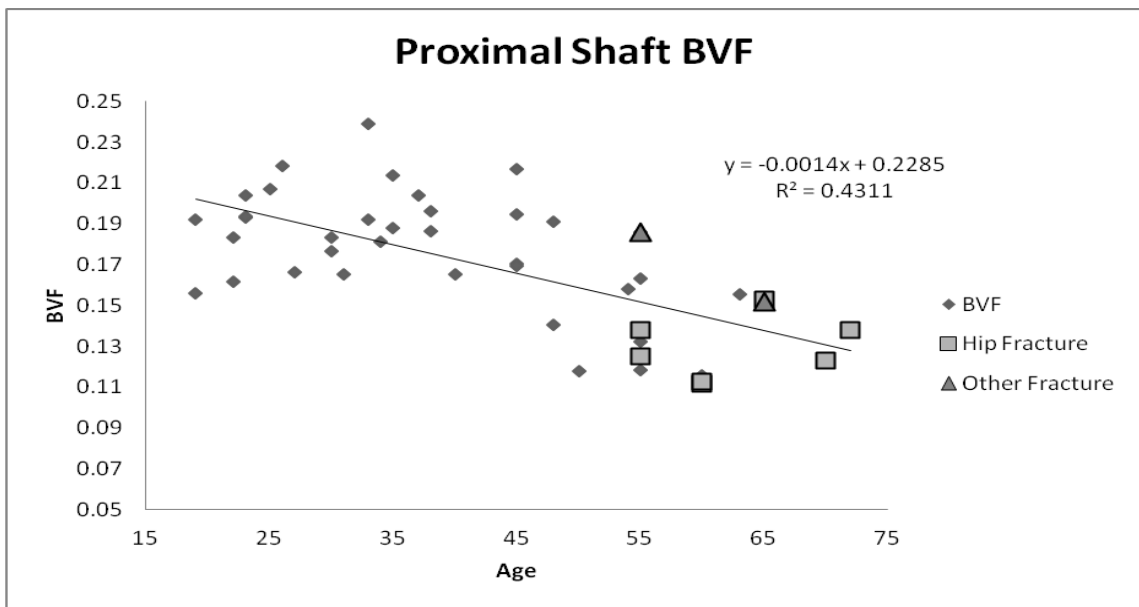
Figure 20 Regression plot of BVF of the proximal shaft of the first metatarsal with estimated biological age for K2 females.

In the proximal shaft of the MT1 there was an average BMD decrease of ~1.5mg/cm3 for every year. This value is slightly less than the ~1.9mg/cm3 per year, and ~2.1gm/cm3 per year, as seen in the mid-shaft and distal shafts respectively. This pattern holds true when BVF is observed. There is an average BVF decrease of ~0.0014 for every year at the proximal shaft VOI, while there was an average decrease of ~0.0017 for every year in both the mid-shaft and distal shaft regions. From these observations, we can conclude the bone, on average, is lost quicker with increasing biological age in the mid- and distal shaft when compared to that of the proximal shaft in this sample population.

Cortical index estimations were made for all individuals (n=45) at the mid-shaft cross-section in the dorso-plantar direction. Again, there was one more individual available for this analysis, which is why the sample size is different from all the other µCT analyses. The estimations were determined to be normally distributed using residual and normal probability plots (Q-Q plots). The residual plots showed no discernible patterns, while the normal probability plots were linear, positive, and had no indications of skewing, and therefore the cortical index estimations were treated accordingly during analyses.

Table 14 summarizes the results of a linear regression analysis. The adjusted R^2 value (0.5845) indicates that ~58% of the cortical index variation observed in the female sub-population can be accounted for by merely using estimated biological age. This is a large amount for a multifactorial system like bone maintenance and loss. **Figure 21** is a visual representation of the regression analysis. This pattern is similar, but more extreme than was seen using either BMD or BVF. The average cortical index loss is ~0.0035/year.

Table 14 Linear regression analysis of the cortical index of the human first metatarsal. Cortical measurements were taken at the mid-shaft (dorso-plantar) for 45 MT1s from the K2 female population.

Dependent Variable	n	ANOVA			Linear Regression					
		df	F	F sig	Adjusted R^2	Variable	Coefficients	SE	t Stat	P-value
Cortical Index	45	1, 43	62.9	5.96E-10	0.5845	Intercept	0.3403	0.0199	17.1386	7.83E-21
						Age	-0.0035	0.0004	-7.9299	5.96E-10
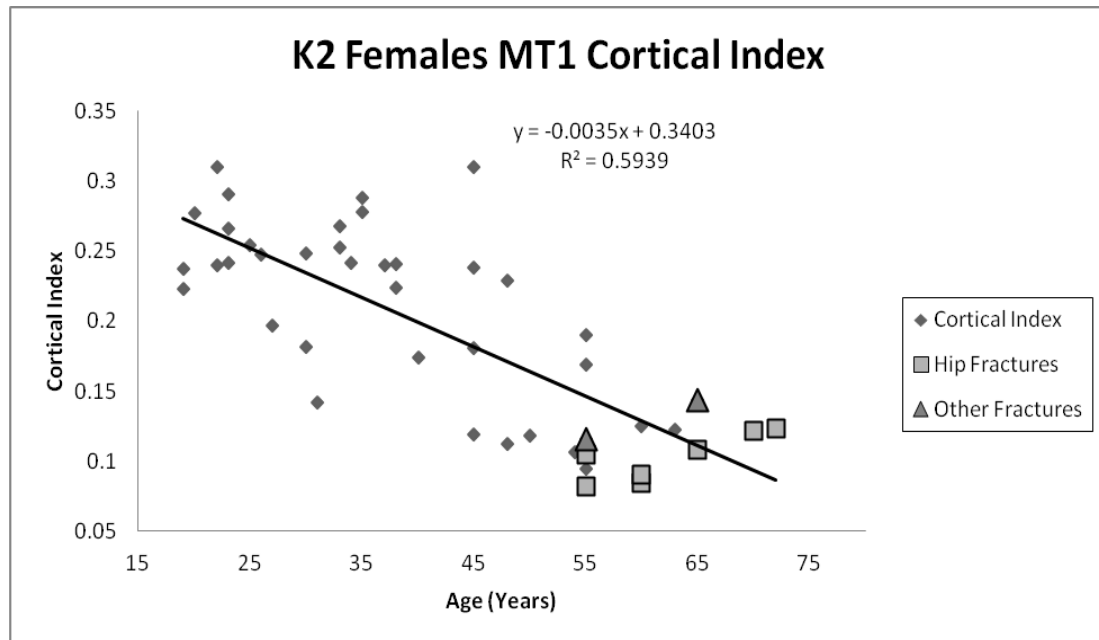
Figure 21 Cortical index of the first metatarsal with mean estimated age for K2 Females. The cortical index decreases on average 0.35% for every year.

4.6.2   T-Score

T-score values were estimated for all of the K2 females that had osteoporosis-related fractures (ORF) (n=9). The estimations were made for both BMD and BVF for all; MT1 shaft VOIs, the average of the MT1 shaft VOIs, and the whole shaft. T-scores were also determined using the cortical index estimated from the mid-shaft cross-section in the dorso-plantar direction (see **Tab. 15**).

All T-scores for individuals with ORFs were found to be negative, indicating that all of those individuals were below the "*healthy*" adult population mean for all of the observed bone quantity measurements. The T-scores varied by individual and by BMD/BVF VOI and CI, as seen in **Table 15**.

Table 15 T-Score values for both BMD and BVF for each VOI, average VOI, and cortical index for the K2 female population with osteoporosis-related fractures.

Burial	Age	T-Score											Average T-score*	Fracture
		PS BMD	PS BVF	MS BMD	MS BVF	DS BMD	DS BVF	AS BMD	AS BVF	WS BMD	WS BVF	CI		
5	55	-2.35	-2.91	-2.19	-2.33	-2.03	-2.12	-2.25	-2.6	-2.29	-2.55	-2.53	-2.37	R. Hip, Sacral Compression and 7 Ribs
8	72	-1.76	-2.32	-2.15	-2.68	-1.77	-2.87	-1.96	-2.86	-2.09	-2.57	-2.16	-2.26	R. Hip and R. Colles
41	60	-2.79	-3.52	-2.78	-3.64	-2.41	-2.71	-2.73	-3.5	-2.74	-3.41	-2.93	-3	L. Hip
72	65	-1.25	-1.67	-1.2	-1.32	-1.5	-1.55	-1.38	-1.63	-1.4	-1.53	-1.76	-1.46	Sacral Compression
261	70	-1.91	-3	-2.24	-3.47	-2.02	-3.78	-2.14	-3.73	-2.16	-3.42	-2.2	-2.7	L. Hip, Sacral and Vertebral Compression (L1)
275	55	-1.17	-0.06	-1.45	-1.17	-1.49	-0.5	-1.44	-0.64	-1.45	-1.12	-2.31	-1.19	L. Colles
438	65	-1.23	-1.62	-0.89	-1	-1.19	-0.89	-1.14	-1.22	-1.05	-0.88	-2.45	-1.24	L. Hip and Rib (L10)
459	55	-2.02	-2.31	-1.91	-2.25	-1.8	-2.14	-1.96	-2.4	-1.9	-2.31	-2.97	-2.18	L. Hip, and R. Colles
D7-3	60	-2.72	-3.48	-2.61	-3.48	-2.37	-2.86	-2.63	-3.49	-2.62	-3.31	-2.81	-2.92	R. Hip
Average T-Score		-1.91	-2.32	-1.93	-2.37	-1.84	-2.16	-1.96	-2.45	-1.97	-2.35	-2.46		

*Average T-score did not include Average Shaft BMD or BVF	
PS	Proximal Shaft
MS	Mid-Shaft
DS	Distal Shaft
AS	Average Shaft Value
WS	Whole Shaft
CI	Cortical Index

4.7 Trabecular Architecture Analyses of the MT1 Results

4.7.1 Bone Volume Fraction

Bone volume fraction (BVF) measurements were taken for all individuals (n=44) at both VOIs. The sub-population data did not support the normality assumptions using the Shapiro-Wilk test at α=0.05 ($\bar{x}_{base}$ = 0.247, SD = 0.150, W=0.959, p=0.115; $\bar{x}_{head}$=0.513, SD=0.158, W=0.981, p=0.012). The null hypothesis was rejected using the Wilcoxon Signed-Rank Test for Paired Samples at α=0.05 ($T_{(44)}$=0, p=7.88E-09). Furthermore, all BVF observations were higher in the head of the MT1, indicating that there was more trabecular bone present in that region throughout the entire study population.

4.7.2 Bone Mineral Density

Bone mineral density (BMD) measurements were taken for all individuals (n=44) at both VOIs. The sub-population was found to violate the normality assumptions using the Shapiro-Wilk test at α=0.05 ($\bar{x}_{base}$ = 55.37mg/cc, SD = 41.79, W=0.934, p=0.014; $\bar{x}_{head}$=115.81mg/cc, SD=54.66, W=0.948, p=0.048). The null hypothesis was rejected using the Wilcoxon Signed-Rank Test for Paired Samples at α=0.05 ($T_{(44)}$=1, p=8.45E-09). Moreover, all but one observation was higher in the head of the MT1(burial 184), indicating that the BMD of the trabecular bone of the head was higher throughout the entire study population.

4.7.3 Trabecular Thickness (TbTh)

Trabecular thickness (TbTh) measurements were taken for all individuals (n=44) at both VOIs. The sub-population was determined to violate normality assumptions using the Shapiro-Wilk test at α=0.05 ($\bar{x}_{base}$ = 2.18 pixels, SD = 0.957, W=0.877, p=0.0002;

$\bar{x}_{\text{head}}$=2.49 pixels, SD=0.864, W=0.934, p=0.015). The H_0 was rejected using the Wilcoxon Signed-Rank Test for Paired Samples at α=0.05 ($T_{(44)}$=285, p=0.024).

4.7.4   Trabecular Spacing (TbSp)

Trabecular spacing (TbSp) measurements were taken for all individuals (n=44) at both VOIs. The sub-population was again found to violate normality assumptions using the Shapiro-Wilk test at α=0.05 ($\bar{x}_{\text{base}}$ = 10.84 pixels, SD = 7.53, W=0.838, p=2.2E-05; $\bar{x}_{\text{head}}$=3.27 pixels, SD=1.13, W=0.832, p=1.59E-05). The H_0 was also rejected using the Wilcoxon Signed-Rank Test for Paired Samples at α=0.05 ($T_{(44)}$=0, p=7.88E-09). Furthermore, all TbSp observations were higher in the base of the MT1, indicating that the average trabecular strut spacing was consistently higher throughout the entire study population – therefore there are fewer trabecular structures within the base compared to the head.

4.7.5   Trabecular Bone and Biological Age

Multiple regression analysis was undertaken to predict age based on BVF, BMD, TbTh, and TbSp measurements in the base of the MT1. A significant regression equation was found (F(4,39)=8.68, p=4.11E-05), with a Multiple R of 0.686. Predicted age is equal to 96.67-319.69 (BVF) + 0.97 (BMD) – 85.11 (TbTh) – 10.17 (TbSp), where BVF is a ratio, BMD is measured in mg/cc, and TbTh and TbSp are measured in millimeters. Bone volume fraction, BMD, TbTh and TbSp were all significant predictors of age (p = 5.7E-4, 0.001, 0.022, and 0.047, respectively) in the base of the MT1.

Multiple regression analysis was undertaken to predict age based on BVF, BMD, TbTh, and TbSp measurements in the head of the MT1. During the analysis, it was found

that both TbTh and TbSp were not significant predictors of age (p = 0.311, and 0.939) and were therefore not used in the regression model. A significant regression equation was found (F(2,41)=12.60, p=5.42E-05), with a Multiple R of 0.617. Predicted age is equal to 90.61 – 185.04 (BVF) +0.40 (BMD), where BVF is a ratio, and BMD is measured in mg/cc. Bone volume fraction and BMD were both significant predictors of age (p = 5.99E-04, and 0.0076, respectively).

4.7.6   Individuals with Osteoporosis-Related Fractures

A summary of the T-Score analyses can be seen in **Table 16**. Twenty-eight females (<50 years old) were used to establish the 'healthy' adult population mean for each measure, at each VOI. Individual T-Scores were created using $T = (x_j - \bar{x})/SD_{HAP}$, where 'T' is the T-Score, x_j is the individual's value for each analysis, $\bar{x}$ is the healthy adult population mean (n=28), and SD_{HAP} is the standard deviation of the healthy adult population. It was observed that in almost all cases, throughout all trabecular bone measures of quantity and quality, individuals determined to have osteoporosis-related fractures also had corresponding negative T-Score values.

Table 16 A summary table of the K2 females with osteoporosis-related fractures and individual T-Score values for all measures from each VOI. Trabecular Spacing is multiplied by -1 because there is a negative relationship between increased spacing and bone health, unlike the other measures.

Burial	Age	Fracture	BVF (Base)	BVF (Head)	BMD (mg/cc) (Base)	BMD (mg/cc) (Head)	TbTh (mm) (Base)	TbTh (mm) (Head)	TbSp (mm)(*-1) (Base)	TbSp (mm)(*-1) (Head)	Average T-Score	Average T-Score (Base)	Average T-Score (Head)
5	55	R. Hip, Sacral Compression and 7 Ribs	-0.35	-1.1	-0.42	-1.26	-0.82	-1.39	0.39	0.09	-0.61	-0.3	-0.92
8	72	R. Hip and R. Colles	-1.46	-2.73	-1.33	-1.84	-1.36	-1.75	-0.02	-4.04	-1.82	-1.04	-2.59
41	60	L. Hip	-2.19	-2.99	-1.75	-2.24	-1.57	-2.1	-1.1	-2.18	-2.02	-1.65	-2.38
72	65	Sacral Compression	-0.24	-0.15	-0.16	-0.21	-0.66	-0.81	0.35	0.76	-0.14	-0.18	-0.1
261	70	L. Hip, Sacral and Vertebral Compression (L1)	-2.17	-0.19	-1.69	0.15	-1.11	0.63	-2.76	-1.52	-1.08	-1.93	-0.23
275	55	L. Colles	-1.66	-1.85	-1.46	-1.72	-1.08	-1.36	-1.13	-0.64	-1.36	-1.33	-1.39
438	65	L. Hip and Rib (L10)	-2.33	-2.98	-1.82	-2.33	-1.33	-2.02	-3.49	-3.16	-2.43	-2.24	-2.62
459	55	L. Hip, and R. Colles	-2.37	-2.56	-1.84	-2.16	-1.6	-2.18	-3.74	-0.54	-2.12	-2.39	-1.86
D7-3	60	R. Hip	-2.23	-3.5	-1.78	-2.49	-1.56	-2.24	-1.19	-2.92	-2.24	-1.69	-2.79
Average			-1.67	-2.01	-1.36	-1.57	-1.23	-1.47	-1.41	-1.57	-1.54	-1.42	-1.65

Chapter 5

5 OVERVIEW, DISCUSSION, CONCLUSIONS, and FUTURE RESEARCH

5.1 Introduction

This chapter summarizes the results of this dissertation, particularly as it pertains to its relevancy to bioarchaeological research and clinical applications. As a general statement, the <u>overall</u> hypotheses that the MT1 will not prove useful for studying human variation and bone health in antiquity are clearly rejected. However, there are many research caveats, with respect to confounding variables, which had to be addressed in order to properly test the hypotheses. Some confounding variables were controllable, such as testing the data for observer reliability and eliminating individuals with diseases that are known to affect bone density values, or in the case of sexing, not including immature skeletal remains. In the well-preserved bones from Kellis, a number of individuals with skeletal evidence of leprosy had to be eliminated from developing the '*healthy*' male sub-population. However, one caveat which is inescapable is the "Osteological Paradox" (Woods et al. 1992), which challenges the use of the term '*healthy*' – as all the burials represent people who died, and the cause of death can rarely be determined. Another confounding variable is the fact that all skeletal studies are, by nature, cross-sectional (Waldron 2009). Ironically, in clinical diagnoses of osteoporosis using bone density, the studies are also cross-sectional. Why this is the case, and how it can be addressed from the results of this research, will be further discussed in a later section.

This chapter is further divided into five sections. Section 5.2 is an overview of the research to refresh the key aspects of the research design. Section 5.3 discusses the results that were found when looking at human variation (i.e., intermetatarsal facet, and sexual dimorphism) using the MT1. Section 5.4 discusses the results of the bone health research (i.e., Osteo-volumetric Density, µCT analysis) of the MT1 in terms of its value, or influence, on bone health research in bioarchaeology, and potential clinical applications. Section 5.5 provides the main conclusions of the research and addresses the overall potential of this pilot study for future research in both bioarchaeology and clinical medicine. Finally, Section 5.6 provides some succinct conclusions and future research directions.

5.2 Overview

In Chapter 1 I noted that the use of the human first metatarsal in bioanthropological research has primarily been in paleoanthropology, particularly as it relates to the evolution and functional biology of the foot. In the same chapter, I noted that there have been attempts to apply the MT1 in osteobiographical research for determining age (Scheuer and Black 2004), sex (Mountrakis et al. 2010; Robling and Ubelaker 1997; Wolpoff and Frayer 1985), and stature (Byers et al. 1989), although the success of those methods have been case/population specific, and therefore, limited. For example, the use of discriminant function analysis in the case of Mountrakis et al (2010) and Robling and Ubelaker (1997) for sexing using this skeletal element assumes that all samples and sub-samples be normally distributed. This was not possible when using the data from Kellis 2. Moreover, the use of the discriminant function in all research is population specific.

The interpretation that research using the MT1 was lacking in the literature arose from the observation of the sparse number of citations and research applications published in bioarchaeology. Even our commonly used texts, and/or manuals on skeletal biology (e.g., Bass 1994; White et al. 2005; Ubelaker 1989; and Swartz 2007), which we as researchers use when looking for standards for creating osteobiographies, only report on the anatomy (including siding etc.), and sometimes the growth and development of the MT1 in conjunction with the general skeletal anatomy of the foot. None provide methodological uses for this skeletal element despite its complex nature and important role in the evolution of human bipedality. This brought about chapter 2, which provides a detailed background of the complex anatomy and physiology of the MT1 as an integral part of the human foot. Moreover, this chapter also discussed the history of investigating bone health, specifically osteoporosis, in order to better understand the necessity for adding the MT1 to the elements that could be used for research in this area.

An additional research area that has made use of the MT1 in bioarchaeology, and that has had some limited success, is in paleopathology, specifically dealing with osteoarthritis and gout (Auferderheide and Martin-Rodriguez 1998). Moreover, the MT1 has been applied successfully in documenting Measures of Occupational Stress (MOS), or in this case Measures of Repeated Stress, with respect to the faceting of the anterior dorsal surface – a trait that is correlated with chronic dorsiflexion (Ubelaker 1979; Molto et al. 2017). Still, the use of the MT1 in paleopathology, and paleoepidemiology, overall has been limited.

Potential areas in bioarchaeology that lacked focused research using the MT1 were human variation and measuring age-related bone loss. As I had access to the large sample of MT1s from the Dakhleh Oasis, and bone health/bone mineral density (BMD) investigation is a major emerging research interest in paleopathology (e.g., Agarwal 2012; Agarwal and Grynpas 2009; Agarwal and Stout 2009; Atwood 2008; Bowles et al. 1985; Brickley 2002; Brickley and Agarwal 2003; Brickley and Howell 2009; Dequeker et al. 1997; Ekenman et al. 1995; Farquharson et al. 1997; Holck 2007; Holroyd et al. 2008; Mays 1996; Mays 2000; Mays 2001; Molto and Sheldrick 2010; Plato et al 1994; Roberts and Wakely 1992; Turner-Walker et al. 2001), the decision to pursue both of these avenues was logical. I believe this increased focus on bone health, and density and trabecular architecture specifically, has in part been fostered by both major improvements in imaging technology (e.g., DXA, CT, μCT. etc.), and the realization that the study of bone density in antiquity has potential applications in modern diagnostics (Rothschild, 1996), particularly with regards to the antiquity of osteoporosis.

At first, a major question arose as to why the MT1 had not been a 'bone of interest' in either human variation or skeletal health research? To address the former, I believe it is because, for the most part, the MT1 shows little macroscopic variation between individuals. There are many other elements that show much more variation (e.g., skull and pelvis). The concern with this is that, in bioarchaeology, we do not get to choose those elements that survive the archaeological record, and therefore we must augment our methodological toolkit whenever possible. To address the latter, concerning skeletal health research, in my opinion, it was because clinical studies of osteoporosis, which is a major contemporary health and economic concern, had focused on the areas of

the skeleton that were predilected to osteoporosis-related fractures. These high-risk sites that are prone to fragility fractures involve the hip (including the femoral neck and sacrum), the distal radius, and the lower vertebrae. The focus on these areas is logical, and as biological anthropologists like to compare and contrast their study populations with living contemporary populations, it was reasonable for them to continue using the same methods and skeletal sites developed in clinical research.

Problems arise when only methods concerning these skeletal sites are available, even when studying contemporary living populations. In the living, measuring bone density at the weight-bearing sites (the hip and proximal femur, and vertebrae) is not only time consuming, but is invasive, as these regions are surrounded by deep soft-tissues and important structures, particularly the reproductive organs. This may be a major reason that clinical applications are, like bioarchaeological research, cross-sectional in nature. Imaging the fragility of the fracture sites is usually only conducted when individuals, particularly females, are older (peri-and menopausal years) and they are compared to a standard of females in their peak bone density years (i.e., in their early 30s). The latter standard, first recommended by a WHO study group in 1994, is typically based on Caucasian women, even though it is well known that peak innate bone density varies greatly between populations of different geographical ancestry (Trotter et al 1960; Crews 1993). Females of African geographical ancestry generally have considerably higher bone densities than Caucasians or those individuals of Asian descent. Females from these populations are still compared to the Caucasian standard. This concept is not a new one, and authors, such as Robling and Ubelaker (1997), noted this issue quite some time ago. More to the point, this cross-sectional approach means that older females today are not

compared to their own personal young adult bone density values, but to standards based on Caucasian females in their peak bone density years. While this approach reduces imaging exposure, it is not scientifically valid as it incorporates the well-known weaknesses of the cross-sectional model.

In a departure from this approach, the Baltimore Longitudinal Study of Aging (BLSA) measured bone-loss at the traditional sites (proximal femur and vertebra), as well as adding the 2nd metacarpal. This longitudinal study of males and females was important, not only for showing how bone loss in females accelerated in perimenopausal and menopausal years, but also showed that bone loss with age is systemic, and the rates of loss differed predictably between various skeletal sites. The bone showing the least changes with age in both sexes was the 2nd metacarpal (MC2), a result that is not surprising as the MC2 is not weight-bearing. The MC2 was still advocated for interpopulation comparisons when variability of bone loss between different parts of the skeleton were taken into account (Plato et al. 1994). The accessibility of the MC2 and its safety, compared to those sites covered in deep soft tissues, are reasons for its proposed use in comparative studies, but in clinical practice today, these MC2 data are rarely used. Moreover, the MC2 is not weight-bearing, unlike the vertebrae, hips and proximal femur, which could make its use in predicting bone loss and determining the risk of fracture at those sites less reliable.

The MT1, as argued, is a better candidate than the MC2 for studying bone loss, and ultimately osteoporosis, because of its weight-bearing properties. It also has the key advantages of the MC2 over bones traditionally used in bone density research in

123

antiquity. It is portable, compact, preserves well (particularly in environments like Dakhleh), has considerable compact and trabecular bone and can be readily imaged. Vertebrae, on the other hand, which have limited compact bone and are dominated by trabecular bone, are often poorly preserved, particularly in older individuals. Even in Dakhleh Oasis, the vertebrae from older individuals are prone to diagenesis (personal communication Dr. Cerroni who conducted unpublished DEXA research on a small sample of K2 vertebrae). The MT1s sampled herein are exceptionally well preserved in all age-cohorts, and showed no diagenic changes. Furthermore, the vertebrae are the foci of many diseases, in both the past and the present (Jevtic, 2004); diseases, such as tuberculosis, blastomycosis and metastatic carcinomas, cause bony changes and destruction. This can complicate, or negate, the important standardization (same vertebrae for all samples) requirement used in comparative research. Additionally, vertebral compression deformities (VCD) – the most common osteoporosis-related fracture (Bartl and Frisch, 2004; Camacho and Miller, 2007) – can lead to erroneously high BMD results due to the same bone mineral content present within a reduced volume (Gregson et al., 2013).

Like the femur, the MT1 is a thick weight-bearing 'long' bone, but on a miniature scale, with both trabecular and compact bone. The latter structures should reflect the lifelong stressors the first metatarsal has endured as the major component of the first ray of the foot in the evolution of our bipedal gait. In this regard, it is similar to the stressors the intertrochanteric femoral neck region has adapted to, especially considering the absolute lack of those forces on the MC2. Unlike the femur however, the small size of the MT1 facilitates its easy use in bioarchaeological imaging research, as the whole bone can

be visualized without cutting. Depending on the imaging machine (e.g., CT scanner with limited gantry/sample stage size), the femur, though it can be standardized for comparative purposes, may need to be sectioned in order to be analyzed. Getting permission for this destructive procedure can be difficult in most jurisdictions, not only because it is a valuable resource for a number of osteobiographical characteristics (e.g., stature estimates, metric and nonmetric variation), but skeletal remains may also hold cultural significance for members of a group or population. Additionally, an advantage not emphasized is that several MT1s can be imaged in a single radiograph or possibly a single µCT scan, depending on the size of the gantry/sample chamber and stage.

At this point it is worth repeating that the Kellis MT1s were originally selected for *a*DNA and isotopic research. The MT1 research involved both a blind design, in terms of not knowing the osteobiographies or pathologies of the individual burials, and intra- and inter-observer testing of the main data (i.e., OVD) used in the results. The blind design ensured that each specimen was treated the same, while the error testing reinforced that measurement error would not significantly contribute to the variability found. Thus, these procedures provide confidence in the results (chapter 4) generated testing the null hypotheses presented.

5.3   Human Variation using the MT1

The following section discusses the human variation results, specifically the intermetatarsal facet (IMF) and sexual dimorphism, from the Kellis 2 cemetery. To review, it was found that, of the 214 individuals examined for the IMF, 60 individuals presented with this trait. This is a prevalence of ~28%. Furthermore, of those 60

individuals, 41 (~68%) showed bilateral expression, while 10 individuals were unobservable for bilaterality because they only had 1 MT1 sampled. These findings are in agreement with Le Minor and Winter (2003), who found this trait in approximately 30% of the 412 individuals that they studied. Interestingly, these authors also found that the facet was absent in 306 non-human primates studied. This indicates that the IMF is unique to humans amongst the primates, and is most likely a derived trait related to the loss of abductibility of the first-ray of the human foot during bipedal evolution.

No correlation occurred between IMF and age or sex. This suggests that the presence of this trait is not related to structural changes that occur as an individual, whether male or female, ages. This is interesting, and allows for the interpretation that the IMF is not developmental in nature. An interesting avenue to pursue with the IMF data in the future would be to look at how the IMF is spatially distributed in the K2 cemetery. Using the male data, because the K2 burial practices follow a patriarchal system of family burials, would allow one to see if they cluster, indicating a genetic component to this trait, or if they are randomly distributed throughout the cemetery, indicating no, or little, genetic input.

The second human variation aspect in this dissertation researched using MT1 data to test sexual dimorphism in the K2 cemetery. Using the various measurements (chapter 3), and analyzed using logistic regression, resulted in K2 individuals being correctly classified as female or male between ~81-89% of the time. These results suggest the presence of MT1 sexual dimorphism in this population, and that it is generally predictable. The results were improved when using the mass of the MT1 and the "kitchen

sink" approach in selecting dependent variables. It should be noted that only the mass of the MT1 and the head height were significant predictors, even though better results were seen when all independent variables were used.

The result of mass being a significant predictor of sex is not all that surprising. On average, male metatarsals are slightly larger and bulkier than their female counterparts in this population. This obviously results in an increase in mass. Moreover, there were many more females that fell well below their sub-population bone density mean, relative to the males. This affected the results. This does not require correction because it is normal. As we see in contemporary populations, females in general, are more slight, and have less bone mass than their male counterparts from their population.

Interestingly, the only other significant predictor was head height, although in the "Kitchen Sink" method seen in **Table 5**, maximum physiological length was just above the 0.05 cut-off. This result, may be a concomitant effect of the way that the MT1 develops. Since the MT1 fuses early, (chapter 2), there is no linear growth after that point, even though much of the skeleton is still maturing. So, with length fixed at an early age, concentric growth is limited, but might occur in the MT1 head. Sexual growth differences and stress activity levels could affect this. Only the MT1 head has direct contact with the ground, with concomitant stresses, activities and body mass differences, influencing the results.

These data resulted in rejecting the Null hypothesis. The MT1 does have value in studying human variation in antiquity. As the Kellis 2 cemetery population had a nearly identical prevalence of the IMF as contemporary populations, and there was significant

sexual dimorphism with regards to the MT1, it may be useful in sexing when no other data are available. Additionally, it may be applicable to modern forensic samples when other data are not available.

5.4   Discussion of the MT1 in Bone Health Research

5.4.1   Osteo-Volumetric Density

The osteometric measurements used in the initial phase of this thesis were detailed by White et al. (2010). As is required by the scientific method, it is necessary for all data to be precise and accurate in order to properly test hypotheses (Molto 1979). My research design involved the determination of the intra- and inter-error reporting of the osteo-volumetric density (OVD), the outcome variable upon which all subsequent data and interpretations are advanced. The measurements used in the OVD calculation proved to be highly precise, thus the null hypothesis is accepted. Again, the statistical testing used the Wilcoxon Signed-rank test for observer error and the Concordance Correlation Coefficient (CCC) and the Intraclass Correlation Coefficient (ICC) for both intra- and inter-observer reliability ($p = < 5\%$ error). If these volumetric data had unacceptable error rates, it would have necessitated estimating the error for each of the five measurements used, a very arduous and time-consuming task. The result that there was slightly less concordance with the inter- versus the intra-error tests was not unexpected, but overall the results show that the osteo-volumetric density (OVD) calculations are highly reproducible and interpretable.

As noted, the osteo-volumetric density data were first tested for symmetry, as some burials were only represented by one metatarsal. The null hypothesis was accepted

indicating that in cases where only one bone (left or right) was available, it could still be used and increase the sample data. Since there were slight, but non-directional differences in symmetry, the OVD data for each burial with both MT1s available was averaged. This procedure should minimize any potential sources of error based on asymmetry, however minor they may be. Moreover, it was also done because, although the K2 cemetery may not show MT1 asymmetry, other populations may. One possible application of MT1 symmetry in bioarchaeology would be to use one side (e.g., right or left) and preserve the other for future bioarchaeological or chemical research.

As noted above, the whole mitochondrial genome (i.e., 16,569 base pairs) was successfully amplified and sequenced from a MT1 from burial 124 at Kellis (Molto et al. 2017). Interestingly, the genotype obtained, U1a1a is connected to the Jewish diaspora that is well documented in the Middle East and Europe in the Roman period. Moreover, the Next Generation Sequencing (NGS) technology that was used in that pilot research, is now being tested on subadult MT1s. If successful, not only will this prove to be important for paleo-population genetics, but it also may be ground-breaking for sexing subadults. Of course, nuclear DNA (nDNA) is less common in cells and more difficult to amplify than mtDNA, but NGS is a major breakthrough in ancient DNA (*a*DNA) research (Molto et al. 2017). As a perspective of the impact of this pilot research, B124 had previously yielded a small portion (~280 base pairs of the HV1 region) from a rib sample. The results from the MT1 are exponentially better. The use of the MT1 for both bone density and *a*DNA research has great potential for all bioarchaeological studies. Unfortunately, at present, the costs of conducting NGS research are prohibitive ($1500/sample), so major population research will be delayed, though the MT1 would be

an excellent choice in terms of the skeletal element sampled. This is one example of when one side could be used for current chemical analyses, while the other is preserved for metric analysis and future research.

In bone health/density research, it is well known that in all populations females generally have less bone density than males, even in the peak years, and that females are more prone to fragility fractures in the peri- and post-menopausal years (Camacho and Miller 2007). This study supports this pattern. This is best shown through visualized regression lines in the scatter plot in **Figure 18**, with females showing considerably greater bone loss over the whole cross-sectional life span. Furthermore, all of the female skeletons with hip fractures clustered with the lowest estimated bone densities.

Additionally, when originally analyzing the data, some young adult males with extremely low bone densities stood out and were eliminated from the healthy young adult male population, as they suffered from lepromatous leprosy. For example, burial 116, a 23-year-old male, had extreme foot changes from lepromatous leprosy. It is noteworthy that his MT1 looked normal (See Figure 2.3), but the osteo-volumetric bone density told a different story (Left MT1 had a T-Score of -1.42). This shows that osteo-volumetric density data, beyond studying age-related bone loss, may provide insights into other diseases and disorders that affect the MT1. Perhaps using the MT1 when foot changes associated with leprosy are not apparent, despite pathognomonic changes elsewhere (e.g., the facial region), bone density application could provide clues to the early effects of the disease on the endocrinological axis for bone mineralization.

Testing the overall male-female mean for the OVD data using a two sample T-test, also resulted in the null hypothesis being rejected. When the sex data were computed using the defined age-cohorts, the null hypotheses were again rejected. Plotting the individual male/female data in a regression analysis relative to age provided a very visual picture of the male/female differences: the OVD age-regression in females was graphically more dramatic in females (**Figure 18**). That is, the inverse relationship of decreasing density with increasing age is much more pronounced in females as indicated by their slope values. The disparate patterns were most evident in the curves of the older female versus male cohorts.

As the contribution of the older adult OVDs on the overall data was significant, it obviously confounded our interpretation of bone loss in the younger adult males and females. This necessitated eliminating the older-cohort male and female data, and testing the younger males and females. A major difference in osteo-volumetric density between sexes during the healthy peak years also occurred. Though both sexes are at their bone density peaks in the third decade, the baseline maximum densities are higher in males (Plato 1994; Sinclair and Dangerfield 2005).

Finding that age-related regression in bone density was accelerated in females, relative to males, was also expected given our knowledge of the impact of hormone involution in the peri- and menopausal years. Had these hypotheses been accepted then the osteo-volumetric density method for the MT1 would have failed. What is noteworthy is that MT1 bone density loss was observable in these peri- and menopausal females. Current understanding of Type I osteoporosis indicates that most of the bone loss that

occurs in these sub-groups is trabecular. The amount of loss determined in some of these females suggests that cortical bone mass may also be decreasing in the MT1 during this time frame, a finding consistent with the BLSA data (Plato et al 1994). Still, bone loss in the Kellis females is minimal prior to the 4th decade, which is consistent with other data collected on modern populations (Plato et al. 1994).

This finding is at variance to data published on Nubian females using femoral mid-shaft data (Dewey et al. 1969). This study found that Nubian females, aged 20-41, had twice the bone loss compared to Nubian males. The differences found in this study seem less marked when compared to the Nubian data. Dewey et al. (1969) hypothesized that the early onset of bone loss in Nubian females is due to nutritional factors, long lactation (2-4 years) and more pregnancies. A study by Dupras and Tocheri (2007) indicated that the average weaning age in Dakhleh was 3 years, which fits into the estimates by Dewey et al. (1969) for their Nubian population. Weaning seems to have had less influence in the Kellan females' bone density, though Nubian data were based on femoral midsections. The latter, and the cross-sectional nature of skeletal research, makes it is difficult to compare the exact bone density values of males and females in the pre-40 age-cohort between the two populations, but the data presented did not seem to show the degree of difference found by Dewy et al. (1969). It may be that the Kellis females enjoyed better nutrition than the Nubians despite having similar weaning times, and therefore pregnancy outcomes.

Noteworthy with regard to the Kellis bone density is the major outcome – hip fractures. Molto and Sheldrick (2011) found that the prevalence of hip fractures in the

older female-cohorts at Kellis is virtually identical to that reported by the WHO (2003). Recall also that eight of these K2 females clustered in the lower regression component shown in Figure 4.3 and that this result occurred in the blind design. The question follows as to whether hip fracture data can be used as a proxy for bone mineral health?

Modern data suggest that between one-third to one-half of females over the age of 50, will experience an osteoporosis-related fracture at some point in their lives (Osteoporosis Canada 2015, National Osteoporosis Foundation 2015). In Kellis 2, 49% (18/37) of the 50+ age-cohort females had ORFs, which falls in the upper range of our modern data. However, as shown, when we include subclinical K2 females (i.e., those with extremely low bone densities without evidence of fragility fractures) this number quickly exceeds modern relative frequency data for the prevalence of osteoporosis. This is possibly a statistical artifact, because unless fractures or other osteoporosis-related changes occur, many older contemporary females may not have their BMD measured or assessed for osteoporosis. The prevalence of osteoporosis in contemporary populations likely is underestimated. Problematic with this statement is that our definitions of osteoporosis are changing, in part due the impact the pharmaceutical industry has on redefining this disorder (Moynihan and Cassels 2005). Empirically, one observation is clear; age-related bone loss and osteoporosis-related fractures are part of our 'hominin' legacy, and we must have improved diagnostics to define and reduce their impact.

Although the criteria set out by the World Health Organization uses different measurement data, their approach is applicable for this research. A deficit of -2.5 standard deviations below healthy adult population average means that we would expect

only ~0.6% (6 in 1000) of the population to be below -2.5 standard deviations. As noted by Camacho and Miller (2007), the WHO standard provided a different etiological basis for diagnosing osteoporosis, but in our opinion, it is statistically relevant and is used herein as a guideline for establishing significant departures from the population mean. Notwithstanding the osteological paradox (Wood et al., 1992) and our problem with cross-sectional data, to be below -2.5 standard deviations from the healthy adult mean would, for our purposes, indicate a significant departure from what could be considered *normal* bone density during life. At the very least, individuals who fall close to or below ~-2+ standard deviations with this method should be investigated further using multiple lines of evidence (fragility fractures and BMD from imaging) for a diagnosis of osteoporosis.

Additionally, the eight older post-menopausal females in K2 with hip fractures all had extremely low and statistically significant values (< -2.0 SD) relative to the '*healthy*' females in the <40 age-cohort. No females below 40 years of age experienced observable low bone density related fractures, and the prevalence of osteoporosis-related fractures was significantly (statistically) higher in all older cohorts (40-50, 50-60, 60-70). However, two females in the <40 cohort did have very low osteo-volumetric density levels. As fractures are the litmus test for defining osteoporosis (WHO 2003), the lack of fractures, as well as the age-cohort data for these two individuals, would indicate that they were, in all likelihood, not osteoporotic, even though their values would indicate that. These younger individuals may have naturally had lower innate bone density, as is the case for some individuals in a normally distributed population. This is one of the issues with cross-sectional data, as we are unable to see if the bone density values have

remained the same since peak, or if they have seen change over-time. If they remain the same, should these individuals be considered to have a disorder, or should those values constitute their normal density? In my opinion, the latter diagnosis applies.

5.4.2   Cortical Density and Trabecular Architecture of the MT1 using μCT Analysis

This dissertation also examined the usefulness of μCT analysis to study surrogates associated to bone strength for addressing bone health in antiquity. The measures used in this study include cortical bone mineral density (BMD), cortical bone volume fraction (BVF), cortical index (CI), Trabecular Bone Volume Fraction (BVF), Trabecular Bone Mineral Density (BMD), Trabecular Thickness (TbTh), and Trabecular Spacing (TbSp) of the MT1. As previously mentioned, the traditional skeletal elements used for this type of research are the vertebrae, femur, and distal upper limb. The problems with using these skeletal elements were addressed previously and will not be discussed further here. To my knowledge, this is the first μCT bone quantity and quality research to use the MT1 in a bioarchaeological context.

Bone mineral density (BMD) estimations from imaging analyses, such as μCT, are a non-destructive means of approximating the amount of bone mineral (hydroxy-appetite) within a given region/volume of interest. This measurement can estimate both cortical and trabecular bone density. It is based on the radiodensity properties of the sample, and is commonly reported as mg/cm3. In my opinion, BMD does seem to be a relatively good proxy for bone strength. It has been estimated that between 75-90% of bone strength is associated to BMD (Jordan and Cooper 2002). Moreover, the risk of fracture has been estimated to be 1.5-3 fold more for every standard deviation below that

of the "healthy" adult population (Holroyd et al. 2008). This would mean that a post-menopausal female whose BMD is 1 standard deviation below the normal "healthy" adult population has a roughly 30% greater risk of fracture over the course of her life (Jordan and Cooper 2002). This suggests that BMD is useful for predicting osteoporotic-related fracture risk.

Like BMD, bone volume fraction (BVF), as obtained through imaging, is a non-destructive analysis of bone quantity. It is an estimate of the amount of a given region/volume of interest that is occupied by bone. This measure is dimensionless and is comparable to BMD in terms of its efficacy as a proxy for bone strength (Mow and Huiskes, 2005; WHO 2003).

The Cortical index measures bone quantity based on the thickness of the cortical bone compared to the overall thickness of the bone and medullary cavity combined. The result is expressed as a ratio that has a positive relationship with cortical thickness. This estimate can indicate the occurrence of endosteal resorption/medullary expansion, or concentric remodelling, and thus, a lower index would suggest a smaller quantity of bone and reduced bone strength. Along with cortical index, the state of the cortex itself can be viewed in cross-section and qualitative assessments can be made (See **Figure 22**). This measurement has conventionally been done using the femur (e.g., Ericksen, 1979, 1982; Thompson, 1980), and the second metacarpal (e.g., Fox et al., 1986; Fox et al., 1995; Plato et al., 1994). Standard radiographs and modern imaging have facilitated our ability to view the medullary cavity and sections of a skeletal element non-destructively, and therefore measurements of this type are easily obtained while preserving

bioarchaeological and culturally important skeletal materials. Standard radiographs have the additional caveat of superimposition, which is eliminated in 3D imaging reconstructions. The superimposition of overlying structures can obscure the view of underlining arrangements, making measurements difficult in some instances.
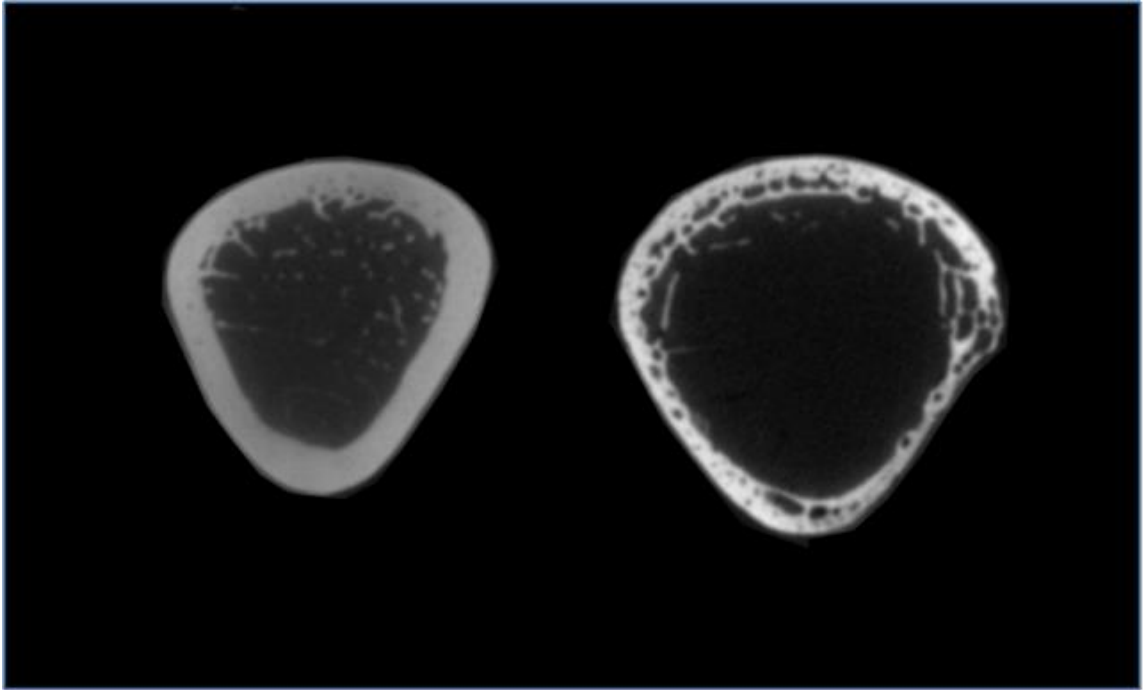
Figure 22 Mid-Shaft μCT cross-section. Left – Burial 131 (Female ~23 years old). **Right** – Burial 72 (Female ~65 years old). Note, beyond cortical thinning there is also cortical porosity which would not be accounted for in an estimation of cortical index.

Undoubtedly there is an inverse relationship with the measures of bone quantity associated to bone strength (e.g., BMD, BVF, and CI) in the human first metatarsal and increasing biological age in this sample population. For diagnosing osteoporosis, this study has shown that all individuals with osteoporosis-related fractures were below the "*healthy*" adult population in all categories observed using the MT1. As noted, this

analysis was done in-blind. The results were expected, as osteoporosis is a systemic disease that involves the entire skeletal system. Invariably, turnover rates differ between skeletal elements, and even within skeletal elements, and therefore, the extent to which a disorder, such as osteoporosis, affects the skeletal system is not homogeneous. Although weight-bearing areas of the skeleton tend to have greater bone density, they too are inversely correlated with biological age. The degree to which the associated measures of bone strength in the MT1 correlate with those obtained in the other areas of the skeleton that are traditionally used could not be determined in this study, as I had no access to the whole skeletons.

Moreover, many of the individuals with osteoporosis-related fractures did not meet the criteria used by the World Health Organization when assessing BMD in the hip region (-2.5 standard deviations) with respect to these cortical measures. When the average T-score for all measurements taken was calculated, all individuals fell at least -1.19 standard deviations below the "healthy" adult populations mean (mean= -2.15), and 6 of the 9 individuals were below ~-2.2 standard deviations. Although well below the "healthy" adult population mean, not all individuals met the WHOs diagnostic criteria. This could occur for a number of reasons. Camacho and Miller (2007), note that the WHO standard has a very different etiology based on the number of expected cases of osteoporosis in contemporary females. In this study, there was no expected value or prior odds available. Additionally, as stated previously, the turnover and bone loss rates throughout the skeleton are not homogeneous, and the MT1 is clearly a weight-bearing element.

Furthermore, the large age-range of the "healthy" adult-cohort used in this study likely contributed to these individuals not falling below -2.5 SD of the mean. Because this is a pilot study, relatively few MT1s were able to be imaged. This meant a greater than optimum age-range was used herein to represent the "healthy" adult population (<50 years of age). Given that peak bone density is reached during the early to mid-thirties (Bartl and Frisch 2004; Camacho and Miller 2007; Plato et al 1994; WHO 2003), it would be prudent for future studies to include a much larger sample of MT1s scanned from that age-cohort to create a more representative "*healthy*" adult population. Notwithstanding the osteological paradox, this would likely result in a greater "*healthy*" adult population mean (with a reduced variance and standard deviation), which would decrease the T-scores generated for those individuals in older age-cohorts, especially those individuals with osteoporosis.

A parallel result was observed using Quantitative Ultrasound (QUS) of the calcaneus (Diez-Perez et al., 2003; Frost et al., 2000; Nayak et al., 2006). These studies indicated that similar measures in the calcaneus typically underestimated the prevalence of osteoporosis when compared to DXA of the femoral neck. Researchers, such as Diez-Perez et al. (2003) and Frost et al. (2000), suggest that various T-score thresholds are required for different skeletal elements, and that those may differ from the established WHO standard for the femoral neck. A future direction of this research will be to scan the femora of the same individuals used in this study for cross-comparison and the establishment of an MT1 element specific T-score threshold standard for aiding in the diagnosing of osteoporosis in this population.

Although all of the measured dependant variables (BMD, BVF and CI) have an inverse relationship with biological age, as indicated by their respective regression functions, it appears that the adjusted coefficient of determination relating to CI is much higher than the other two variables (CI R^2= 0.58; BMD R^2= 0.37-0.43; BVF R^2= 0.39-0.48). One reason for this may be that CI does not account for some of the ways in which bone is reduced with disorders that impact bone demineralization and resorption (e.g., osteoporosis, disuse atrophy, etc.). Cortical thinning is just one way in which bone loss can be observed. Another is cortical porosity. Cortical porosity results in reduced bone mass, but may not affect the overall thickness of the cortical bone (as seen in **Figure 22**). This porosity would, however, affect the observations made pertaining to BMD and BVF, thus contributing to the variation observed in these regression lines. It is unequivocal that, in this population, bone mass decreases with biological age as observed through the measured proxies of bone strength. Due to the fact that bone maintenance and loss are multifactorial, of which some of the variables are clearly dependent of age, some measures of bone quantity may be less sensitive to these other bone loss mechanisms. I posit that using multiple observations of bone quantity is germane for understanding the ways in which bone is being demineralised and resorbed, and in the future, may help to better answer questions pertaining to bone loss and fragility in antiquity. Additionally, bone quality also contributes to overall skeletal health.

The rejection of the of the null hypotheses for the VOIs of the head and base show that there are significant differences with regards to both the amount of trabecular bone and the quality in these regions. Statistically there is more trabecular bone, denser trabecular bone, thicker trabeculae and less space between trabeculae within the head of

the MT1. These results are most likely due to the nature and difference between the joints at the base and head of the MT1, and the resulting biomechanical stress imparted on each region during the transfer of force from the lower limb to the ground during both movement and at rest.

The joint created between the proximal end (base) of the MT1 and the distal end of the medial cuneiform is known as a tarsometatarsal joint (TMT), while the joint created by the articulation of the distal end (head) of the MT1 and the base of the first proximal phalange is known as a metatarsophalangeal joint (MTP). The TMT is a gliding diarthrosis joint that is quite rigid due to being encased within a ligamentous joint capsule. The MTP joint is an ellipsoidal diarthrosis joint that is capable of flexion/extension, and adduction/abduction (Martini 2001). During periods of rest and motion, it has been estimated that 30% of the force is under the head of the MT1 (Pan et al. 2006). Additionally, Muehleman et al. (1999) found that the pressures exerted on the heads of the MT1 caused increased cortical bone density when compared to the density found in the base. The trabecular results in our investigation substantiate that study in suggesting that the force difference during rest and motion between the head and base of the MT1 results in not only denser cortical bone, but thicker, more numerous, and denser trabeculae within the head of the MT1.

The multiple regression results of the MT1 base measurements support a relationship between biological age and BVF, BMD, TbTh, and TbSp. At first glance, it may seem that although the predictor variables (BVF, BMD, TbTh, and TbSp) are significant (p = 5.7E-4, 0.001, 0.022, and 0.047, respectively), the Multiple R is quite low

(0.686), and perhaps the regression model is underwhelming. In fact, small r2 values were also found when each variable was run separately. The truth is that a regression model can perform poorly as a predictor of a response variable, in this case biological age, while still being able to statistically demonstrate a relationship between the predictor variables and the response with statistically significant p values. This analysis illustrates that although there is much variability throughout the population, there is a relationship between age and these proxy measures of bone strength – decreasing BVF, BMD, TbTh and increasing TbSp with increasing age in the base of the MT1.

Similar results were found for the head of the MT1. There was a statistically significant relationship between biological age and BVF and BMD found from the analysis. This relationship was not found in the multiple regression model for the predictor variables TbTh and TbSp. Interestingly, when these variables were run separately they were found to be significant (pTbTh = 0.0026, pTbSp = 0.0015). Similar results were found in the multiple regression models of the head, as were seen in base (low Multiple R, and low p-values for the predictor variables). I conclude that a real relationship exists between biological age and BVF and BMD in the head of the MT1, but the predictability is weak.

The differences between the multiple regression models of the base and head of the MT1 reflect the varying forces/stresses in those regions during normal use (i.e., standing, and locomotion). Generally, while BVF and BMD decrease in both, the loss is greater in the base. A significant decrease in TbTh and increase in TbSp is only observed in the base of the MT1. The increased amount of force and stress in the head may account

for a better maintenance of both trabecular thickness and spacing, while natural declines in BVF and BMD are still occurring. The trabecular structures may be changing little in thickness and number due to adaptation to biomechanical stress, while still losing density due to systemic bone maintenance breakdown.

From these results, it is difficult to determine which region should be the focus of future investigations. The head of the MT1 has higher innate bone properties in all areas (higher BVF, BMD, TbTh, and lower TbSp) when compared to the base. Additionally, due to it being a smaller region, much more of the trabecular structures are considered when using VOIs of the same size when compared to the base. The head is also under more force/stress, and is therefore able to give a better indication of the breakdown of the body's bone maintenance system with age, if that indeed is occurring. Conversely, the base demonstrates a better relationship between biological age and trabecular thickness and spacing, probably in part due to this lack of force/stress as opposed to the head of the MT1. It would appear that considering both regions may be the best course for future research. This would allow for the comparison of a stressed and non-stressed (relatively speaking) region of the same skeletal element to be compared and contrasted in order to differentiate between normal age-related bone loss and increased bone loss due to a systemic disorder like osteoporosis. In fact, in this study it was seen that while BVF and BMD were lost at similar rates in both regions (even though the head was innately higher to begin with), TbTh and TbSp behaved differently over the life-course in the two regions. Trabecular thickness decreased more rapidly and trabecular spacing increased more rapidly in the base of the MT1 when compared to the head. This is probably due to less stress adaptation occurring in that region of the element.

The results in **Table 16** showed that individuals with osteoporosis-related fractures were below the healthy adult-population mean with regards to the proxy measures of trabecular bone strength. For a number of reasons, this type of analysis is difficult to interpret when using a bioarchaeological sample, and should be used more to identify trends rather than establishing absolute values. First, because bioarchaeological samples are cross-sectional, an individual's innate bone properties cannot be known. For example, if an individual had a high innate bone density as a young adult (1+ standard deviations or more), even if he/she underwent abnormal bone density loss during the latter years of life, they would appear normal, or close to normal, in a cross-sectional bioarchaeological study. Second, the biological age assigned to each individual is not absolute. In this study, we used the midrange value from an age-at-death estimation range. Knowing this property, and also to simplify the analysis, we chose to seriate the subsample into only two age-cohorts. The '*healthy*' adult population were those individuals that had midrange age-at-death estimations below 50 years of age, and the older age-cohort consisted of individuals that had midrange age-at-death estimations of 50 years of age or older. Of course, because age-at-death estimations are a range, there may have been some blurring of this categorization (i.e., individuals assigned to the wrong category). Given the nature and reality of bioarchaeological samples, and the low number of samples that could be used in this study, these problems were unavoidable, but this does not diminish the value of the trends that were seen.

Individuals with osteoporosis-related fractures had below normal average T-Scores, collectively or individually, for the base and head regions of the MT1. Additionally, all proxy measures of bone strength (BVF, BMD, TbTh, and TbSp),

regardless of the region, were on average below the healthy adult mean for all females with osteoporosis-related fractures (n=9). Does this mean that all individuals met the criteria of osteoporosis of < -2.5 standard deviations, as set out by WHO (2003) for BMD of the hip? As noted by Camacho and Miller (2007), the WHO standard (< -2.5 SD) has a very different etiology based on the number of expected cases of osteoporosis in contemporary females, as well as the values seen in the hip region. This cut-off may not be applicable to other elements of the skeleton as the turnover and bone loss rates throughout the skeleton are not homogeneous. A future direction of this research will be to compare the values obtained from the MT1 with those from the hip, vertebra, and distal radius from the same individuals.

To review, μCT analysis of the MT1 as a proxy for bone health appears promising. Both cortical and trabecular bone showed age-related reduction, and all females with osteoporosis-related fractures were below the mean of the healthy adult female populations. So, what does this mean for the MT1 in bioarchaeological and clinical research? A case that initiated my interest in the Kellis 2 population was the hip fracture seen in Burial 191 (See **Figure 23**). This 48-55 years old female had a complete intertrochanteric fracture resulting in a pseudo-arthrosis, or a false joint. This picture alone illustrated several things to me about the Kellis population. First, a person in this condition must have had considerable care from their family or community. When this injury first occurred, there is no way this individual could have cared for themselves. Her compromised mobility would mean she would require assistance just to have the basic essentials (eat, drink, use the toilet etc.). This individual lived with this injury for so long that they eventually made a "new" joint at the distal end of the femur. This indicated to

me the second of my observations – the perseverance of the people of the Dakhleh Oasis. An injury like this in today's society with modern intervention still results in a very high mortality rate unless treated immediately (WHO 2003; WHO 2007), yet this female survived. In the Kellis sample, 5 of 8 individuals survived for some time (Molto and Sheldrick 2010), which shows the importance of community care. The four who died immediately probably had their nutrient arteries severed from the fracture.
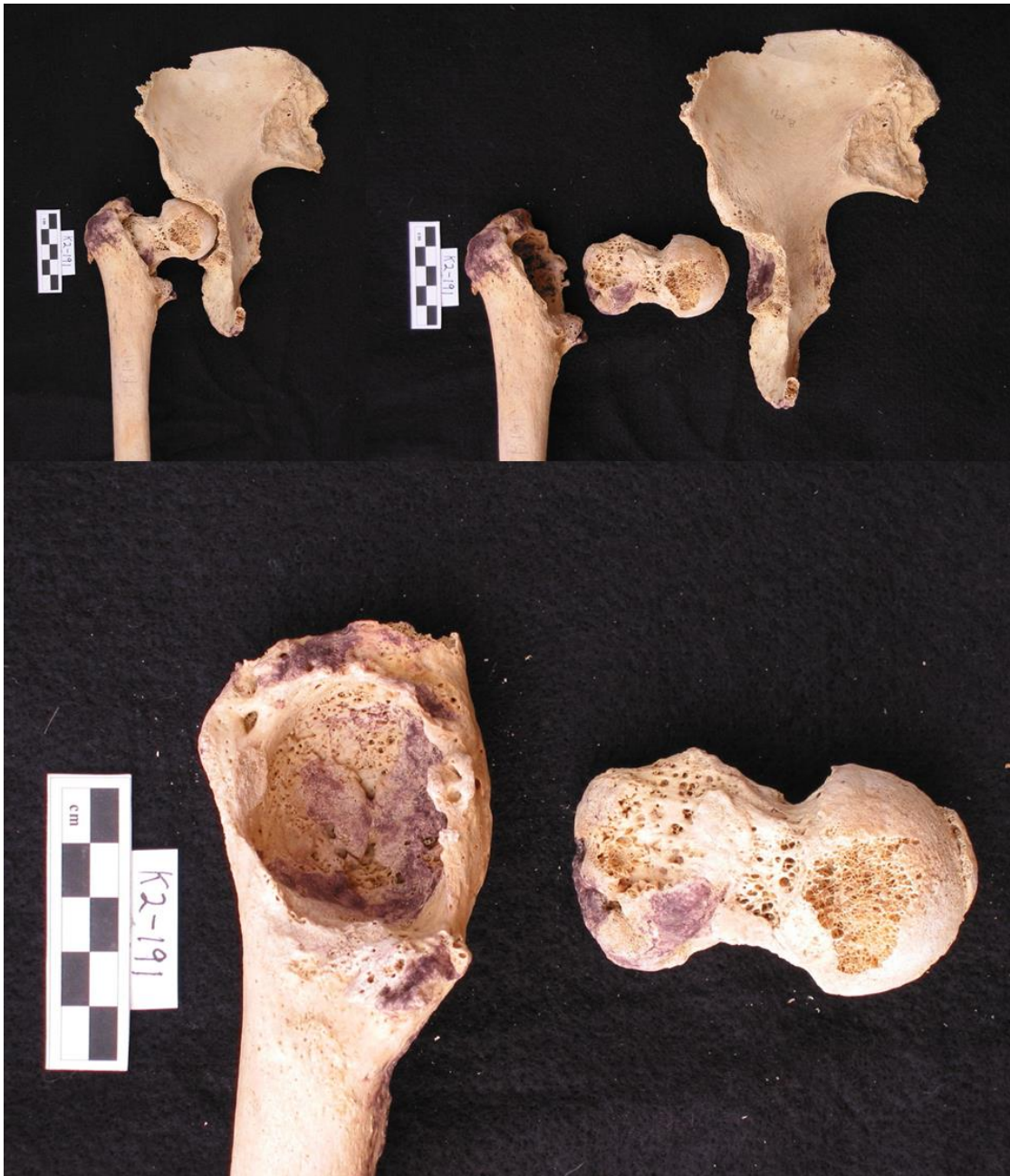
Figure 23 Intertrochanteric Fracture. Burial 191 with an intertrochanteric fracture and resulting pseudo-arthrosis (false joint).

5.5 General Summary of the MT1 in Research

The recent emergence of bone density research in bioarchaeology may, in part, be concomitant to the importance of osteoporosis in our aging Western populations (WHO 2003). There is little doubt that osteoporosis research in bioarchaeology offers a real potential to contribute to clinical medicine. However, paleo studies have a number of significant problems to overcome in order to achieve this goal, a major one being, which skeletal elements can best be used and standardized for this type of comparative research. I have shown the potential of MT1 bone density research and its ideal properties for the logistics of conducting bioarcheological research (portable, easily scanned etc). The MT1 osteo-volumetric density method developed herein, is non-destructive, and its calculation is straightforward, reliable and reproducible, which is a prerequisite for all objective scientific research (Molto, 1979). Furthermore, μCT analysis of the MT1 shows real promise in studying bone health in antiquity.

Since this research involved an 'age-cohort cross-sectional design' it is worthwhile to note that in modern clinical practice females rarely know their optimal or peak bone densities. Their values are traditionally assessed when they are older, and therefore, already have had declining bone health and are at a greater risk for osteoporosis. These individuals are then compared to cross-sectional data, based on normal bone density for ~30-year-old healthy, often Caucasian, females. This problem is partly ameliorated herein, but it does speak to an important issue concerning bone density and health research. When there is a family history of bone health issues, or prolonged disease, I suggest that those individuals consult with their health care providers for information concerning bone loss, including the risks involved in early bone health

assessment through imaging. There may very well be many individuals in the lower age-cohorts with low bone density who do not contribute to the prevalence data because they have never been assessed. This may be a reason that we see an increased prevalence in the K2 females when compared to modern clinical statistics. Moreover, if tests were to indicate that an individual had low innate bone density, but was not showing a decline with age in a longitudinal assessment, would it be correct to conclude that they have a bone density disorder? Probably not. The real danger is in a change in bone density, not just low bone density.

To expand this hypothesis, one of the major objectives of studying disease in antiquity at the individual (paleopathology) and population (paleoepidemiology) levels is to try and benefit clinical medicine (Rothschild, 1996). This objective has rarely been fulfilled. However, this is changing with the development of evolutionary medicine juxtaposed against evidence-based medicine. Both fields had a similar genesis when they emerged in the early 1990s and both share key research design elements (meta-analysis, blind studies, epidemiological statistics, use of modern technologies etc.).

More importantly it is now recognized that our understanding of chronic diseases that plague Western societies today has benefited greatly from evolutionary medicine. The role of microbes in chronic diseases is a case in point (Ewald, 2010). For example, Ewald (2010) notes that in the mid-1970s only one cancer, Burkitt's lymphoma, had an accepted microbial cause. Now at least 20% of all cancers are accepted as being caused by microbes, and this is probably an underestimate, as the study the molecular phylogenies of the various pathogenic microbes is providing a temporal perspective of

the human host-pathogen co-evolution. For example, in Dakhleh samples there are three cases, two females and a male in their early thirties, with carcinomas (Molto and Sheldrick 2014). Some paleopathologists rejected the cancer diagnosis when these cases were presented because of their young ages. Yet today, cancer of the uterine cervix and testes are most common in the young adult-cohort, and they share a common association with the human papillomavirus (HPV). Molecular Phylogenetic analyses indicate the HPV has potentially been associated with humans throughout our evolution (Ewald 2010), and it has an African origin (Ong et al. 1993). Hence a high probability that HPV was endemic to ancient Kellis, and given its associations to cancer development, gives weight to the cancer diagnosis in those three young individuals.

The methods outlined herein are potentially valuable in this role for documenting our legacy with bone demineralization with age. Again, it is worth repeating that in modern society few younger females with a family history of osteoporosis have their own bone density estimated. In clinical medicine, measuring bone density is expensive and invasive, the latter because they often focus on bones that are surrounded by important soft tissues (i.e., in the spine and pelvis). I posit that my research on the MT1 opens up future research avenues that could ultimately lead to a less invasive and inexpensive radiological technique, which may assist in developing patient-specific longitudinal standards. I doubt that any young adults, both male and female, would object to having their MT1s x-rayed to develop their own bone mass values.

It is germane to reemphasize that some medical researchers have expressed concern with our changing definitions of osteoporosis based on bone density values,

leading to overuse of drugs and their side effects (Moynihan and Cassels 2005). Undoubtedly our understanding and treatment of osteoporosis today is at some cross-roads (Moynihan and Cassels 2005). The latter authors note that the pharmaceutical industry is having an enormous influence on how we define and grade these skeletal changes, which has encouraged the use of drugs to treat this 'disease'. One drug, in particular (Fosamax), has shown the problems of over diagnosing and treating osteoporosis. This drug was launched by Merck in 1995. Before the drug was launched, Merck was subsidizing bone density testing machines to ensure that individuals would get the diagnosis for which Fosamax would be prescribed (Moynihan and Cassels 2005).

Noteworthy, a year before the Foxamax launch, the WHO-based standard for the diagnosis of osteoporosis, which is based on bone density of 30-year-old individuals, was published. Translated, this meant that the bones of many older women would be automatically defined as abnormal and they would be prescribed drug treatments. It is worthwhile to note that Fosamax has many extreme side effects, and key among these is that it increases cortical bone, not trabecular bone density (Moynihan and Cassels 2005)! Since Type 1 osteoporosis mainly involves trabecular bone loss, this alone should have resulted in the FDA ruling not approving Fosamax as a prescription for type 1 osteoporosis treatment.

In my opinion, paleoepidemiology does have a role in assisting our understanding and treating modern chronic diseases like osteoporosis. With regards to the study of bone health in antiquity, bioarchaeologists have long realized the importance of developing new research methods for analyzing and interpreting normal, variational, and

pathological patterns in the human skeleton given the oft compromised nature of archaeologically-derived human remains. The concerns listed previously regarding the use of the femur, vertebrae and MC2 in bone density research, in addition to differential skeletal preservation and recovery, suggest an expansion of the skeletal elements used in this area of research is needed.

I have presented a new method based on the MT1 that, though requiring more testing, has shown its ability in detecting bone loss in ancient skeletons from Roman Period Egypt. While I am not advocating for the abandonment of the established skeletal research used in BMD research, the MT1 seems at least an equally valid approach that has many advantages to the established methods, especially given that we researcher do not get to choose those elements that preserve in the archaeological record for study.

5.6 Conclusions and Future Research

From this research, I have a couple of succinct conclusions and future research directions:

1. The MT1 proved useful when looking at human variation in the K2 sample. The IMF showed similarities in prevalence to modern research numbers. For future research, a spatial analysis of the distribution of the IMF in the Kellis 2 cemetery could illuminate the genetic heritability, or lack thereof, of this trait. Moreover, it would be interesting to see if other skeletal populations have similar prevalence and distribution data when compared to the Kellis sample. There was sexual dimorphism of this skeletal element in K2. This dimorphism allowed me to create a logistic regression model to help sex any further skeletons excavated, or otherwise not yet analyzed, from the site. Moreover, if standards were created for contemporary populations, this element could

be useful in forensic identification. A dorsal-plantar and and medial-lateral shaft measurement may help increase the performance of this sexing methodology.

2. Age-related, as well as osteoporosis-related, bone loss can be observed in the human first metatarsal. The extent to which this loss can be compared to the loss observed in osteoporosis-related high-risk (both in terms of frequency and morbidity/mortality) fracture sites, such as the femur, vertebra, and distal upper-limb could not be determined in this study.

3. The osteo-volumetric density methodology of the MT1 provides a simple and cost-effective means of evaluating bone density and diagnosing osteoporosis in antiquity. The method is reliable and reproducible. At the very least, this method can serve to cull the sample size that will be used in more expensive and time-consuming imaging methods.

4. A proof concept for the method was demonstrated first by finding significant sex differences, particularly with age, and then testing the method against hip fracture (femoral neck) and other fragility fracture data for post-menopausal females in the Kellis 2 cemetery. Had the data not shown reduced bone density for these individuals, and for the sex and age patterns, the method would not be valid.

5. Given its proof of concept, the osteo-volumetric density method should now be tested against standard radiograph comparisons (using the same metatarsals), and be cross-compared to data from the K2 femora. This will determine if the MT1 can be used in addition to, or as an alternative to, the more traditional skeletal elements that have been applied in bioarchaeological research. The expansion of the available skeletal

elements for use in bioarchaeological bone health research is important due to the reality of differential preservation and excavation of human remains.

6. There are caveats with this approach. First, we recommend that a population-specific standard be created, which presumes a large number of MT1 samples. This method would not be suitable for individual samples. Second, it should be noted that because fractures accumulate with age, only individuals in the upper age-cohorts with fractures that were in osteoporotic high-risk areas of the skeleton (i.e., hip, vertebra, and distal upper limb), and were either peri-mortem (fresh or in a state of healing at the time of death), or a result of compression (e.g., vertebral or sacral compression deformities) should be considered.

7. In general, individuals diagnosed with osteoporosis-related fractures in the Kellis 2 population had negative T-Scores for most, if not all, measures of cortical strength and trabecular bone architecture (BVF, BMD, CI, TbTh, and TbSp). All of these did not meet the standard used by the WHO (2003), which was established using the BMD of the hip region. Future research should focus on defining the relationship between the measures taken from the hip region, vertebra, distal radius, and the human first metatarsal in the Kellis population.

8. Each region (head and base) has some advantages for studying trabecular bone health in antiquity. Age-related bone loss in the base is observed using all trabecular properties (BVF, BMD, TbTh, TbSp) that were examined in this study. Although when grouped in a multiple regression, age-related bone loss could not be observed using TbTh and TbSp in the head of the MT1, the head has much higher innate bone properties when compared to the base. This makes this region much easier to

investigate in comparison. It is suggested that both regions be used in future trabecular studies congruently, as this may allow for the observation of bone loss in areas of high and low stress (relatively) within the same skeletal element.

9. The use of the MT1 in this research is not meant to replace other proven methods, but to augment the ways in which we can study bone loss in antiquity. Taphonomic processes and recovery methods influence the data that biological anthropologists have to investigate the lives of individuals and populations in the past – this method looks to increase the tools we have to answer those questions.

References

Adelaar R. (1986). The practical biomechanics of running. *The American Journal of Sports Medicine*. 14 (6): 497-500.

Agarwal SC. (2012). The Past of Sex, Gender, and Health: Bioarchaeology of the Aging Skeleton. *American Anthropologist* 114(2):322-335.

Agarwal S, Grynpas M. (2009). Measuring and interpreting age-related loss of vertebral bone mineral density in a medieval population. *Am J Phys Anthropol* 139:244-252.

Agarwal S, Stout S. (2003). *Bone loss and osteoporosis: An anthropological perspective*. Kluwer Academic/Plenum Publishers, New York, New York.

Andersen JG., Manchester K., and Shahzady Ali R. (1992). Diaphyseal remodeling in leprosy: a radiological and palaeopathological study. *International Journal of Osteoarchaeology*. 2(3): 211-219

Atwood ML. (2008). *Osteoporosis in a Prehistoric Bay Area Population*. Doctoral Dissertation, San Jose State University.

Aufderheide A. and Rodriguez-Martin C. (1998). *The Cambridge Encylopedia of Human Paleopathology*. Cambridge University Press.

Aufderheide C., Zlonis M., and Cartmell LL., Zimmerman MR., Sheldrick P., Cook M., and Molto JE. (1999). Human mummification practices at Ismant El-Kharab. *The Journal of Egyptian Archaeology*. 85(1): 197-210

Bartl R., and Frisch B. (2004). *Osteoporosis: Diagnosis, Prevention, Therapy*. Springer-Verlag Berlin Heidelberg. Germany.

Bartonicek J., and Vicek, E. (2001). Femoral neck fracture – the cause of death of Emperor Charles IV. *Archives of Orthopaedic and Trauma Surgery*. 121: 353-354.

Bass W. (1995). Human Osteology: *A laboratory and field manual*. 4th addition, Special Publication No. 2, Missouri Archaeological Society.

Birrell M. (1999). Excavations in the cemeteries of Ismant el-Kharab. In *Dakhleh Oasis Project: Preliminary Reports on the 1992-1993 and 1993-1994 Field Seasons*, ed. C.A. Hope and A.J. Mills, 29-41. Oxford: Oxbow Books.

Bowen GE. (1998). *The spread of Christianity in Egypt in light of recent discoveries from ancient Kellis*. Doctoral Dissertation, Monash University, Melbourne, Australia.

Bowles EA., Weaver DS., Telewski FW., Wakefield AH., Jaffe MJ., and Miller LC. (1985). Bone measurements by enhanced contrast image analysis: Ovariectomized and intact Macaca Fascicularis as a model for human Postmenopausal Osteoporosis. *Am J Phys Anthropol* 67:99-103.

Brickley M. (1997). *Age-Related Bone Loss and Osteoporosis in Archaeological Bone: A Study of Two London Collections, Redcross Way and Farringdon Street*. Doctoral Dissertation, Institute of Archaeology, University College London.

Brickley, M. (2002). An investigation of historical and archaeological evidence for age-related bone loss and osteoporosis. *International Journal of Osteoarchaeology*. 12: 364-371.

Brickley M., and Agarwal SC. (2003). Techniques for the investigation of Age-Related Bone Loss and Osteopososis in Archaeological Bone. 157-168 IN: Agarwal, S. and S. Stout (2003). *Bone Loss and Osteoporosis: An Anthropological Perspective*. Kluwer Academic/Plenum Publishers, New York, New York.

Brickley M., and Howell PGT. (1999). Measurement of changes in trabecular bone structure with age in an archaeological population. *Journal of Archaeological science*. 26: 151-157.

Brooks S., and Suchey JM. (1990). Skeletal age determination based on the os pubis: a comparison of the Acsádi-Nemeskéri and Suchey-Brooks methods. *Human Evolution* 5(3):227-238.

Buikstra JE., and Ubelaker DH. (1994). *Standards for data collection from human skeletal remains: Proceedings of a seminar at the Field Museum of Natural History (Arkansas Archaeology Research Series 44)*. Fayetteville Arkansas Archaeological Survey.

Byers K., Akoshima B., and Curran B. (1989). Determination of adult stature from metatarsal length. *American Journal of Physical Anthroplogy*. 79: 275-279.

Camacho P., and Miller P. (2007). *Osteoporosis: A guide for clinicians*. Lippincott, Williams and Wilkins. Philadelphia, PA, USA.

Chen WM., Vee-Sin Lee P., Park S., Lee S., Shim V., and Lee T. (2010). A novel gait platform to measure isolated plantar metatarsal forces during walking. *Journal of Biomechanics*. 43: 2017-2021.

Cook MA. (1994). The Mummies of Dakhleh. In Herring, A., and Chan, L. (eds*): Strength in Diversity: a reader in physical anthropology*. Canadian Scholar's Press Inc., Toronto.

Cook M., Molto JE., and Anderson C. (1989). Flourochrome labelling in Roman Period skeletons from Dakhleh Oasis, Egypt. *American Journal of Physical Anthropology*. 80: 137-143.

Cooper C. (1999). Epidemiology of Osteoporosis. *Osteoporosis International*. 2: 2-8.

Cooper DML., Thomas CDL., Clement JG., Hallgrimsson B. (2006). Three-dimensional microcomputed tomography imaging of basic multicellular unit-related resorption spaces in human cortical bone. *The Anatomical Record*. 288(7): 806-816.

Cornwall M., and McPoil (2002). Motion of the calcaneus, navicular, and first metatarsal during the stance phase of walking. *Journal of the American Podiatric Medical Association*. 92(2): 67-76.

Crews DE. (1993). Biological anthropology and human aging: Some current directions in aging research. *Annual Review of Anthropology* (22):395-423.

Dahab KA., Ebraheem AM., and El Sayed EA. (2001). *A study of hydrogeological conditions of the Nubian Sandstone Aguifer in the Area between Abu Simbel and Toschka, Western Desert, Egypt*. American Geophysical Union, Spring Meeting 2001.

Dawe E., and Davis J. (2011). Anatomy and biomechanics of the foot and ankle. *Orthopaedics and Trauma* 25(4): 279-286.

Dequeker J., Ortner D., Stix A., Cheng X., Brys P., and Boonen S. (1997). Hip fracture and osteoporosis in a XIIth Dynasty female skeleton from Lisht, Upper Egypt. *Journal of bone and mineral research*. 12 (6): 881-888.

De Groote I., and Humphrey L. (2011). Body Mass and Stature Estimation Based on the First Metatarsal in Humans. *American Journal of Physical Anthropology*. 144: 625-632.

Dewey JR., Armelagos GJ., and Bartley MH. (1969). Femoral cortical involution in three Nubian archaeological populations. *Human Biology*. 41(1): 13-28.

Diez-Perez A., Marin F., Vila J., Abizanda M., Cervera A., Carbonell C., Alcolea RM., Cama A., Rama T., Galindo E., and Olmos C. (2003). Evaluation of calcaneal quantitative ultrasound in a primary care setting as a screening tool for osteoporosis in postmenopausal women. *Journal of Clinical Densitometry*. 6(3): 237-245.

Donoghue H., Marcsik A., Matheson C., Vernon K., Nuorala E., Molto JE., Greenblatt C., and Spigelman M. (2005). Co-infection of Mycobacterium tuberculosis and Mycobacterium leprae in human archaeological samples: a possible explanation for the historical decline of leprosy. *Proceeding of the Biological Sciences, Royal Society*. 272(1561): 389-394.

Dupras TL. (1999). *Dining in the Dakhleh Oasis, Egypt: Determination of diet using documents and stable isotopic analysis*. PhD Dissertation, McMaster University, Hamilton Ontario, Canada.

Dupras TL., Schwarcz HP., and Fairgrieve SI. (2001). Infant feeding and weaning practices in Roman Egypt. *American Journal of Physical Anthropology*. 115(3): 204-212.

Dupras, TL. and Tocheri MW. (2007). Reconstructing infant weaning histories at Roman period Kellis, Egypt using stable isotope analysis of dentition. *American Journal of Physical Anthropology*. 134(1): 63-74.

Edwards J. (2005). *An investigation of non-metric discontinuous trait variation of the atlas in ancient Egyptian Population samples from the Dakhleh Oasis, Egypt*. Unpublished Thesis, Lakehead University.

Ekenman I., Eriksson A., and Lindergren J. (1995). Bone density in Medieval skeletons. *Calcified Tissue International*. 56: 355-358.

Ericksen MF., (1979). Aging changes in the medullary cavity of the proximal femur in American Blacks and Whites. *American Journal of Physical Anthropology*. 51(4): 563-569.

Ericksen MF., (1982). Aging changes in thickness of the proximal femoral cortex. *American Journal of Physical Anthropology*. 59(2): 121-30.

Ewald PW. (2010). *Evolutionary Medicine and the Causes of Chronic Disease*. In: Michael Muehlenbein, M.P. Editor. Human Evolutionary Biology. Cambridge University Press, USA, New York, New York, p 502-517.

Fairgrieve SI., (1993). *Amino acid residue analysis of type I collagen in human hard tissue: An assessment of cribra orbitalia in an ancient skeletal sample from tomb 31, site 31/435-d5-2, Dakhleh Oasis, Egypt*. PhD ed. Canada: University of Toronto, Canada.

Fairgrieve S, Molto JE. (2000). Cribra orbitalia in two temporally disjunct population samples from the Dakhleh Oasis, Egypt. *Am J Phys Anthropol* 111:319-331.

Farquharson, MJ, Speller RD, Brickley M. (1997). Measuring bone mineral density in archaeological bone using energy dispersive low angle X-ray scattering techniques. *Journal of Archaeological science* 24(8):765-772.

Fox KM., Kimura S., Powell-Threets K., Plato CC. (1995). Radial and Ulnar Cortical Thickness of the Second Metacarpal. *Journal of Bone and Mineral Research*. 10(12): 1930-1934.

Fox KM., Tobin JD., Plato CC. (1986). Longitudinal Study of Bone Loss in the Second Metacarpal. *Calcif Tissue Int*. 39: 218-225.

Frost HM. (2003). On Changing Views about Age-Related Bone Loss. 19-30 IN: Agarwal, S. and S. Stout (2003). *Bone Loss and Osteoporosis: An*

Anthropological Perspective. Kluwer Academic/Plenum Publishers, New York, New York.

Frost ML., Blake GM., Fogelman I. (2000). Can the WHO criteria for diagnosing osteoporosis be applied to calcaneal quantitative ultrasound? *Osteoporosis International*. 11(4): 321-330.

Garcia-Aznar J., Bayod J., Rosas A., Larrainzar R., Garcia-Bogalo R., Doblare M., and Llanos L. (2009). Load Transfer Mechanisms for Different Metatarsal Geometries: A finite Element Study. *Journal of Biomechanical Engineering*. 131(2).

Garrahan N., Mellish R., and Compston J. (1986). A new method for the two-dimensional analysis of bone structure in human iliac crest biopsies. *Journal of Microscopy*. 142: 341-349.

Genant H., Engelke K., Fuerst T., Gluer C., Grampp S., Harris S., Jerhas M., Lang T. (1996). Noninvasive assessment of bone mineral and structure: State of the art. *J. Bone Miner. Res.* 11:707-730.

Glasoe W., Yack H., and Saltzman C. (1999). Anatomy and Biomechanics of the First Ray. *Journal of the American Physical Therapy Association*. 79(9): 854-859.

Grave A., Molto JE., Parr RL., Walters S., Praymak R. and Maki J. (2000). Mitochondrial DNA research in the Dakhleh Oasis, Egypt: A preliminary report. *Ancient Biomolecules vol.* 3:239-253.

Gregson CL., Hardcastle SA., Cooper C., Tobias JH. (2013). "Friend or Foe": high bone mineral density on routine bone density scanning (DXA), a review of causes and management. *Rheumatology (Oxford, England)* 52(6): 968–985.

Gross T., and Bunch R. (1989). A mechanical model of metatarsal stress fracture during distance running. *The American Journal of Sports Medicine*. 17(5): 669-674.

Gruber HE., Ivey JL., Thompson ER., Chesnut CH 3rd, and Baylink DJ. (1985). Osteoblast and osteoclast cell number and cell activity in postmenopausal osteoporosis. *Mineral and Electrolyte Metabolism*. 12(4): 246-254.

Grynpas, M. D. (2003). The Role of Bone Quality on Bone Loss and Fragility. 33-46 IN: Agarwal, S. and S. Stout (2003). *Bone Loss and Osteoporosis: An Anthropological Perspective*. Kluwer Academic/Plenum Publishers, New York, New York.

Haddow SD. (2012). *Dental morphological analysis of Roman era burials from the Dakhleh Oasis, Egypt*. Unpublished PhD thesis, Institute of Archaeology, University College, London, England.

Holck, P. (2007). Bone Mineral Densities in the Prehistoric, Viking-Age and Medieval Populations of Norway. *International Journal of Osteoarchaeology*. 17: 199-206.

Holroyd, C., C. Cooper, and E. Dennison (2008). Epidemiology of Osteoporosis. *Best Practice and Research Clinical Endocrinology and Metabolism*. 22(5): 671-685.

Hope CA., (1995). The excavations at Ismant el-Kharab in 1995/6 and 1996/7: A brief report. *Bulletin of the Australian Centre for Egyptology*. 8: 49-64.

Hope CA., and McKenzie J. (1999). Interim Report on the West Tombs. In Hope CA., Mills AJ. Eds, *Dakhleh Oasis Project: Preliminary Reports on the 1992-1993 and 1993-1994 Field Seasons*, Oxbow Books, Oxford. 53-68.

Hyer CF., Philbin TM., Berlet GC., and Lee TH. (2005). The incidence of the intermetatarsal facet of the first metatarsal and its relationship to metatarsus primus varus: a cadaveric study. *J Foot Ankle Surg*. 44(3): 200-202.

Iscan MY., Loth SR., and Wright RK. (1984). Metamorphosis at the sternal rib end: A new method to estimate age at death in white males. *Am. J. Phys. Anthropol*. 65(2): 147-156.

Işcan MY*., and* Loth SR. (1985). Determination of age from the sternal rib in white males*: a test of the phase method. J Forensic Sci*. **31***:122–32.*

Jayasinghe J., Jones S., and Boyde A. (1994). Three dimensional photographic study of cancellous bone in human fourth lumbar vertebral bodies. *Anatomy and Embryology*. 189: 259-274.

Jevtic V. (2004). Vertebral Infection. *European Radiology* 14(E):43-52.

Jordan, KM., and Cooper C. (2002). Epidemiology of Osteoporosis. *Best Practice and Research Clinical Rheumatology*. 16(5): 795-806.

Jurmain R., Kilgore L., Trevathan W., and Bartelink E. (2017). *Essentials of Physical Anthropology*. Wadsworth Publishing; 15 Edition, Boston, USA.

Keron J. (2015). Spatial analysis in bioarchaeology. PhD Dissertation, Department of Anthropology, The University of Western Ontario, London, Canada.

Kilmartin TE., Barrington RL., and Wallace WA. (1991). Metatarsus primus carus. A statistical study. The Bone and Joint Journal. 73(6): 937-940.

Kirby K. (2000). Biomechanics of the normal and abnormal foot. *Journal of the American Podiatric Medical Association*. 90(1): 1-5.

Knudstad JE., and Frey RA. (1999). The architectural survey of the Romano-Byzantine town at Ismant el-Kharab. In Churcher CS., Mills AJ., eds. *Reports from the survey of the Dakhleh Oasis 1977-1987*. Oxbow Books, Oxford. 189-214.

Lai and Lovell N. (1992). Skeletal markers of occupational stress in the fur trade: a case study from a Hudson's Bay Company fur trade post. *International Journal of Osteoarchaeology* 2:221-234.

Leakey MD. (1981). Tracks and tools. *Philosophical transactions of the Royal Society of London. Series B, Biological Sciences*. 95-102.

Leakey M, and Walker MA. (2003). Early hominid fossils from Africa. *Scientific American*. 13: 14-19.

Le Minor JM, and Winter M. (2003). The intermetatarsal articular facet of the first metatarsal bone in humans: a derived trait unique with primates. *Ann Anat*. 185(4): 359-365.

Lovell NC. and Dublenko AA. (1999). Further aspects of fur trade life depicted in the skeleton. International Journal of Osteoarchaeology. 9(4): 248-256.

Maggiano C., Dupras TL., and Biggerstaff J. (2003). Ancient antibiotics: Evidence of Tetracycline in human and animal bone from Kellis. In Bowen GE., and Hope CA. eds. *The Oasis Papers 3: Proceeding of the third International Conference of the Dakhleh Oasis Project*, Oxbow Books, Oxford. 331-344.

Martini F. (2001). *Fundamentals of Anatomy and Physiology, 5th edition*. Prentice Hall International. New Jersey, USA.

Mays S. (1996). Age-dependent cortical bone loss in a Medieval population. *International Journal of Osteoarchaeology*. 6: 144-154.

Mays S. (2000). Age dependent cortical bone loss in women from 18th century and early 19th century London. *American Journal of Physical Anthropology*. 112(3): 349-362.

Mays S. (2001). Effects of age and occupation on cortical bone in a group of 18th-19th century British Men. *American Journal of Physical Anthropology*. 116: 34-44.

Mays S., Lees B., and Stevenson J. (1998). Age-dependent bone loss in the femur in a medieval population. *International Journal of Osteoarchaeology*. 8(2): 97-106.

Meema H., and Meema S. (1987). Postmenopausal osteoporosis: Simple screening method for diagnosis before structural failure. *Radiology*. 164: 405-410.

Mills A. (2010). Dakhleh: A study of environmental change and cultural evolution. The Dakhleh Oasis Project: The Dakhleh Trust, London, England.

Molleson T. (1989). Seed preparation in the Mesolithic: the osteological evidence. *Antiquity*. 63:356-362.

Molto JE. (1979). The assessment and meaning of interobserver error in population studies based on discontinuous cranial traits. *Am J Phys Anthropol* 51:333-334.

Molto JE. (2000). Humeral varus deformity in Roman Period burials from Kellis 2, Dakhleh, Egypt. *Am J Phys Anthropol* 113:103-109.

Molto JE. (2001). *The comparative skeletal biology and paleoepidemiology of the people from Ein Tirghi and Kellis, Dakhleh oasis, Egypt. In: Dakhleh Oasis Project: Monograph 6*, CA Marlow, Mills AJ, editors. Oxbow Books, Great Britain. p 81-100.

Molto JE. (2002). *Bio-archaeological research of Kellis2: an overview. In Dakhleh Oasis Project: Monograph 11*, Hope CA, Bowen GE, editors. Oxbow Books Great Britain. p 239-256.

Molto JE (2003). Leprosy in Roman Period skeletons from Kellis 2, Dakhleh, Egypt. In *the "Past and Present of leprosy*. CA Roberts, ME Lewis and K Manchester (editors). BAR Int Series 1054:179-191.

Molto JE, Stewart JD, Reimer PJ. (2005). *Radio carbon dating the Kellis 2 cemetery: A conundrum*. Paper presented at the Dakhleh Oasis Conference Cairo, Egypt.

Molto JE. and Chemm R. (2006). *The bioarchaeology of Hei Heru, A late Shang Dynasty site in Anyang, China: An overview of molecular and morphogenetic research.* Invitational paper presented at a special symposium entitle: Science and technology in Asian Bioarchaeological Research. Leiden, The Netherlands.

Molto JE. (2017). Complete mitochondrial genome sequencing of a burial from a Romano-Byzantine cemetery in the Dakhleh Oasis, Egypt. Preliminary indications. paper accepted for publication in *Genes* pending minor changes, July 6.

Molto JE., Brown L., and Teeter MA. (2017). Metatarsal faceting. Submitted to the *International Journal of Osteoarchaeology.*

Molto JE., and Sheldrick P. (2010). *The Paleoepidemiology of osteoporotic related hip fractures in a Roman Period Population Sample from the village of Kellis, The Dakhleh Oasis Egypt*. Paper presented at the 37th Annual Meeting of the Paleopathology Asociation, Alburquerque, New Mexico. April 13-14, 2010.

Molto JE. and Sheldrick P. (2014). *Paleo-oncology in Egypt: Case studies from the Dakhleh Oasis*. Paper presented at the 42 Annual meeting of the Paleopathology Association, Calgary, Alberta.

Mountrakis C., Eliopoulos C., Koilias C., Manolis S. (2010). Sex Determination Using Metatarsal Osteometrics from the Athens Collection. *Forensic Science International*. 200: 178e.1-178e.7.

Mow VC., and Huiskes R. (2005). *Basic orthopaedic biomechanics & mechano-biology*. Lippincott Williams & Wilkins. 133-134.

Moynihan R. and Cassels A. (2005). *Selling Sickness: How the World's Biggest Pharmaceutical Companies are Turning us All into Patients*. National Books, United States.

Muehleman C., Bareither D., and Manion B. (1999). A Densitometric analysis of the human first metatarsal bone. *Journal of Anatomy*. 195: 191-197.

National Osteoporosis Foundation. 2015. 1150 17th Street, NW Suite 850 Washington, DC 20036. www.nof.org.

Nayak S., Olkin I., Liu H., Grabe M., Gould MK., Allen E., Owens DK., and Bravata DM. (2006). Meta-analysis: Accuracy of quantitative ultrasound for identifying patients with osteoporosis. *Annals of Internal Medicine*. 114(11): 832-841.

Ong CK., Chan SY., Campo MS., Fujinaga K., Mavromara-Nazos P., Labropoulou V., Pfister H., Tay SK., Meulen J., and Villa LL. (1993). Evolution of human papillomavirus type 18: an ancient phylogenetic root in Africa and intratype diversity reflect co-evolution with human ethnic groups. *J of Virology* (11)6424-6431.

Osteoporosis Canada. 2015. 1090 Don Mills Road, Suite 301, Toronto, Ontario, M3C 3R6. www.osteoporosis.ca

Pan Z., Jaing P., Wang J., Wang Q., Zeng Y. (2006). Finite Element Analysis of Metatarsal Deficit and Reconstruction Using Ilium, Fibula and Scapula. *Communications in Numerical Methods in Engineering*. 22: 799-808.

Parfitt M. (2003). New Concepts of Bone Remodeling: A Unified Spatial and Temporal Model with Physiologic and Pathophysiologic Implications. 3-15 In: Agarwal, S. and S. Stout (2003). *Bone Loss and Osteoporosis: An Anthropological Perspective*. Kluwer Academic/Plenum Publishers, New York, New York.

Parfitt M., Drezner MK., Glorieux F., Kanis J., Malluche H., Meunier P., Ott S., and Recker R. (1987). Bone histomorphometry: Standardization of nomenclature, symbols and units. Report of the ASBMR Histomorphometry Nomenclature Committee. *Journal of Bone Mineral Res*. 2: 595-610.

Phenice TW. (1969). A newly developed visual method of sexing the *0s* pubis. *Am. J. Phys. Anthropol*. 30297-301.

Plato C., Fox K., and Tobin J. (1994). Skeletal changes in human aging. In: Crews D, Garruto R, editors. *Biological Anthropology and Aging: Perspectives on Human Variation over the Life Span*. Oxford University Press: New York:272-300.New York.

Plato C., Roy T., Sherman S., and Tobin JD. (1990). Bone mineral density in normal men and women: the effect of age at different bone sites. *Journal of Bone Mineral Research* 5 (suppl 2). 248.

Rath B., Notermans H., Franzen J., Knifka J., Walpert J., Frank D., Koebke J. (2009). The microvascular anatomy of the metatarsal bones: a plastination study. *Surg Radiol Anat*. 31: 271-277.

Roberts C., and Wakely J. (1992). Microscopical findings associated with the diagnosis of osteoporosis in palaeopathology. *International Journal of Osteoarchaeology* 2(1):23-30.

Robling A., and Ubelaker D. (1997). Sex Estimation from Metatarsals. *Journal of Forensic Science*. 42(6): 1062-1069.

Rothschild BM. (1996). The Dunlop-Dottridge Memorial Lecture. *Paleopathology as a Clinical Science with Implications for Patient Care, Education, and Research*. Annual Meeting of the Canadian Rheumatology Association. Lake Louise, Canada, February 24, 1996.

Rothschild BM., and Heathcote GM. (1995). Characterization of gout in a skeletal population sample: Presumptive diagnosis in a micronesian population. *American Journal of Physical Anthropology*, *98*(4), 519-525.

Rothschild B., and Martin L. (1993). *Paleopathology: Disease in the fossil record*. CRC Press, Boca Raton.

Saul F. and Saul J. (1989). "Osteobiography: A Maya example", pp. 287-302 in: Reconstruction of Life from the Skeleton (M. Iscan and K. Kennedy, eds.). Wiley-Liss, New York.

Schild R., and Wendorf F. (1997). *The prehistory of the Dakhleh Oasis and adjacent desert*. Wroclaw: zaklad narodowy imiena Ossolinskich Wydnawnictwo Polskiej Akademii.

Scheuer L. and Black S. (2004). *The Juvenile Skeleton*. Elsevier Academic Press. London, UK.

Schultz M. (2003). Differential Diagnoses of Intravitam and Postmortem Bone Loss at the Micro-Level. 173-188 IN: Agarwal, S. and S. Stout (2003). *Bone Loss and Osteoporosis: An Anthropological Perspective*. Kluwer Academic/Plenum Publishers, New York, New York.

Sinclair D., and Dangerfield P. (2005). *Human growth after birth*. 6th edition. Oxford University Press.

Singh M., Nagrath A., and Maini P. (1970). Changes in the trabecular pattern of the upper end of the femur as an index of osteoporosis. *J. Bone Joint Surg. Br*. 52(a): 457-467.

Stewart JD, Molto JE, Reimer PJ. (2006). The chronology of Kellis 2: The interpretive significance of radiocarbon dating of human remains. In: *Dakhleh Oasis Project: Monograph14*, GE Bowen, CA Hope, editors. Oxbow Books, Great Britain. p 373-378.

Swartz JH. (2007). *Skeleton keys: An introduction to human skeletal morphology, development and analysis*. Oxford Press, New York.

Thanheiser U., Walter J., and Hope C. (2002). Roman agriculture and gardening in Egypt as seen from Kellis: In Hope C. and Bowen (eds), *Dakhleh Oasis Project: Preliminary Reports on the 1994-1995 to 1998-1999 field seasons*. Oxford: Oxbow Books.

Thompson DD. (1980). Age changes in bone mineralization, cortical thickness, and haversian canal area. *Calcified Tissue International*. 31(1): 5-11.

Thomsen JE., Ebbesen, and Mosekilde L. (2000). A new method of comprehensive static histomorphometry applied on human lumbar vertebral cancellous bone. *Bone*. 27: 129-138.

Thurston H. (2012). *Secrets of the Sands: The revelations of Egypt's Everlasting Oasis*. Arcade Publishing: New York.

Trotter M., Broman GE., and Peterson RR. (1960). Density of bones of white and negro skeletons. *JBJS*. 42(1): 50-58.

Turner-Walker G., Syversen U., Mays S. (2001). The archaeology of osteoporosis. *European Journal of Archaeology* 4(2):263-269.

Ubelaker DH. (1979). Skeletal evidence for kneeling in prehistoric Ecuador. *American Journal of Physical Anthropology*.

Virtama, P., and Helela T. (1969). Radiographic measures of cortical bone. Variations in a normal population between 1 and 90 years of age. *Acta Tadiol. Suppl*. 293.

Waldron T. (2009). *Paleopathology*. Cambridge University Press.

Weinstein R., Simmons D., and Lovejoy C. (1981). Ancient bone disease in Peruvian mummy revealed by quantitative skeletal histomorphometry. *American Journal of Physical Anthropology*. 54: 321-326.

Weiss E., DeSilva J., and Zipfel B. (2012). Brief Communication: Radiographic study of the metatarsal one basal epiphyseal fusion: A note of caution on age determination. *American Journal of Physical Anthropology*. 147: 489-892.

Wheeler S., Williams L., Beauchesne P., and Dupras TL. (2013). Shattered lives and broken childhoods: Evidence of physical child abuse in ancient Egypt. *International Journal of Paleopathology*. 3(2): 71-82.

White T., Black M., and Folkens P. (2011). *Human Osteology, 3ʳᵈ edition*. Elsevier Academic Press. Oxford, UK.

Williams L. (2009*). Investigating seasonality of death at Kellis 2 cemetery using solar alignment and isotopic analysis of mummified tissues.* PhD Dissertation. London: The University of Western Ontario, Canada.

World Health Organization (WHO) (2003). Scientific Group Meeting on Prevention and Management of Osteoporosis. *WHO technical report series 921*, Geneva.

World Health Organization (WHO). (2007). WHO scientific group on the assessment of Osteoporosis at primary health care level. *Summary Meeting Report*, Brussels, Belgium. 5-7 May, 2004.

Wolpoff, M., D. Frauer (1985). Sexual Dimorphism. *Anuual Review of Anthropology*. 14: 429473.

Wood J., Milner G., Harpending H., and Weiss K. (1992). The Osteological Paradox: Problems of Inferring Prehistoric Health from Skeletal Samples. *Current Anthropology*. 33(4): 343-370.

Appendices

APPENDIX A

Key Terms and Definitions for MT1 Growth and Development

Abduction – to draw away from the midline of the body or from an adjacent part or limb.

Adduction – to draw inward toward the median axis of the body or toward an adjacent part of limb.

Articulation – a location where two or more bones contact one another.

Biomechanics – the study of the mechanics of a living body, especially of the forces exerted by muscles and gravity on the skeletal structure.

Bipedal – the act of using two limbs for locomotion.

Caudal – of or towards the posterior part of the body.

Centre of ossification – a site of bone formation through accumulation of osteoblasts within connective tissue (membranous ossification), or of destruction of cartilage before onset of ossification (endochondral ossification).

Chondrification – conversion into cartilage.

Distal – anatomically located far from a point of reference, such as an origin or a point of attachment.

Diaphysis – the shaft or central part of a long bone.

Dorsal – pertaining to the back of the body or the top of the foot.

Dorsiflexion – flexion or bending toward the extensor aspect of a limb, as of the hand or foot.

Ectoderm – the outermost of the three primitive germ layers of the embryo; from it are derived the epidermis and epidermic tissues, such as the nails, hair, and glands of the skin, the nervous system, external sense organs and mucous membrane of the mouth and anus. Also called *ectoblast*.

Endoderm – the innermost of the three primary germ layers of an embryo, developing into the gastrointestinal tract, the lungs, and associated structures. Also called *hypoblast*.

Embryo – in humans, the developing organism from fertilization to the end of the eighth week.

Epiphysis - the expanded articular end of a long bone, developed from a secondary ossification center, which during the period of growth is either entirely cartilaginous or is separated from the shaft by a cartilaginous disk.

Evert – to turn inside out or outward.

Extension – a movement of a joint that results in an increased angle between tow bones or body surfaces.

Facet – a small, smooth-surfaced process for articulation.

Fetus – the unborn offspring in the postembryonic period, in humans from nine weeks after fertilization until birth.

Flexion - movement of a limb to decrease the angle of a joint.

Hallux – the '*big*' toe.

Inferior – located beneath or directed downward.

Insertion – the site of attachment, as of a muscle to the bone that it moves.

Intrauterine – within the uterus.

Lateral – denoting a position farther from the median plane or midline of the body or a structure.

Medial – relating to, situated in, or extending toward the middle; median.

Mesoderm – the middle embryonic germ layer, lying between the ectoderm and the endoderm, from which connective tissue, muscle, bone, and the urogenital and circulatory systems develop. Also called *mesoblast*.

Ossification – formation of or conversion into bone or a bony substance.

Phalanx - a bone of a finger or toe. Also called a *phalange*.

Plantar – pertaining to the sole of the foot.

Prismoid – a solid having sides that are trapezoids and bases or ends that are parallel and similar but not congruent polygons.

Proximal – Nearer to a point of reference such as an origin, a point of attachment, or the midline of the body.

Proximodistal – from the centre outwards.

Reniform – shaped like a kidney.

Sesamoid – designating any of certain small modular bones or cartilages that develop in a tendon or in the capsule of a joint.

Superior – located above or higher.

Supernumerary – exceeding a fixed, prescribed, or standard number.

Tuberosity – a projection or protuberance, especially one at the end of a bone for the attachment of a muscle or tendon.

APPENDIX B

Raw MT1 Data

TEETER Metatarsel 1 Dakhleh Oasis - Measurements in grams and mm

Site	Burial #	Side	Age	Sex	Weight	Max. Length	Head Width	Head Height	Base Height	Base Width	Shaft Height	Shaft Width
K2	2	R	25	F	5.58	53.75	17.47	16.95	23.13	15.58	10.47	11.31
K2	2	L	25	F	5.54	53.1	17.28	16.71	23.62	16.05	10.98	10.99
K2	4	R	55	M	5.93	54.74	21.16	19.37	29.33	18.62	11.54	12.76
K2	5	R	55	F	4.2	57.37	19.85	16.86	27.59	19.54	11.86	13.07
K2	5	L	55	F	3.95	56.51	18.68	17.69	26.85	19.21	11.84	13.01
K2	6	R	29	M	5.03	58.81	20.6	20.44	29.69	21.08	12.67	14.22
K2	6	L	29	M	5.77	60.77	21.49	21.05	29.73	22.85	12.87	14.71
K2	8	R	72	F	4.25	64.41	20.1	18.64	27.74	16.61	11.55	12.45
K2	8	L	72	F	4.03	64.24	19.16	18.56	27.01	16.78	11.46	12.13
K2	9	R	29	M	8.68	62.17	21.15	18.79	28.37	20.68	13.98	14.09
K2	9	L	29	M	8.08	61.27	20.59	19.17	28.88	18.19	13.76	14.55
K2	10	R	18mos	U	6.32	56.34	25.19	18.17	16.82	18.11	x	x
K2	16	R	29	M	7.85	63.33	21.04	19.01	27.8	21.32	11.98	12.92
K2	16	L	29	M	7.53	62.79	21.91	18.99	28.05	20.61	12.23	12.57
K2	19	R	45	F	5.9	55.43	19.51	18.47	26.79	17.15	11.08	12.06
K2	19	L	45	F	6.2	56.18	19.95	18.17	26.17	17.32	11.53	12.23
K2	20	R	55	F	3.8	53.19	19.12	18	26.6	18.38	11.23	11.4
K2	20	L	55	F	3.68	53.19	18.94	17.94	26.04	18.03	10.97	10.77
K2	21	R	45	F	5.36	55.73	18.35	16.3	26.15	17.73	12.39	12.94
K2	21	L	45	F	5.49	55.38	18.49	15.82	26.29	17.82	12.33	13.33

K2	22	R	22	F	4.75	51.04	17.36	16	23.97	14.1	10.99	9.98
K2	22	L	22	F	4.55	51.25	16.64	15.85	23.38	14.74	10.65	9.82
K2	25	R	19	F	5.26	61.26	19.05	17.7	27.13	17.88	11.73	13.45
K2	25	L	19	F	5.45	61.97	19.49	17.55	26.56	18.59	12.2	13.05
K2	26	R	19	F	5.82	58.5	19.84	18.54	24.72	16.22	11.1	12.65
K2	26	L	19	F	5.59	59.08	19.62	18.44	24.29	16.4	10.74	12.18
K2	27	L	30	F	4.56	56.7	17.57	16.85	24.43	18.56	11.3	13.12
K2	30	R	38	F	6.21	60.63	22.1	19.41	29.04	21.55	11.42	13.25
K2	30	L	38	F	6.68	58.87	21.17	19.61	28.66	21.15	11.47	12.95
K2	33	L	27	U	6.87	60.8	21.1	18.61	27.81	17.71	13	11.96
K2	41	R	60	F	3.57	61.55	22.3	19.72	28.65	19.9	11.78	13.11
K2	41	L	60	F	3.25	61.49	21.19	19.56	28.43	19.97	11.66	12.98
K2	42	R	46	M	9.25	68	23.4	21.63	29.55	18.47	12.34	12.47
K2	42	L	46	M	8.38	67.49	22.91	22.67	29.26	19	12.27	12.09
K2	44	R	63	F	4.27	62.65	23.11	19.51	25.44	16.02	11.12	12.66
K2	44	L	63	F	4.68	65	20.54	19.69	26.04	16.96	11.24	12.96
K2	52	R	30	F	5.69	60.32	19.7	17.06	25.33	17.63	9.97	11.95
K2	52	L	30	F	5.81	59.35	19.7	17.89	26.76	17.62	10.24	10.7
K2	58	R	48	F	4.52	56.55	20.19	18.4	26.27	17.63	11.25	12.21
K2	58	L	48	F	3.88	56.31	19.16	17.54	25.1	16.52	11.27	12.21
K2	59	R	45	M	9.62	63.35	20.76	22.36	29.08	20.13	12.36	13.62
K2	60	L	37	M	8.53	64.82	21.9	19.35	28.17	18.25	12.18	14.9
K2	64	R	7	U	1.81	36.17	13.26	12.82	16.58	12.92	9.15	9.34
K2	64	L	7	U	1.76	36.04	12.67	12.63	17.04	13.21	8.48	9.37
K2	67	R	10.5	U	4	46.47	16.68	14.78	19.2	14.32	10.82	12.6
K2	67	L	10.5	U	4.07	46.72	17.43	15	19.08	14.97	10.78	12.8
K2	68	R	30	F	5.07	55.68	18.62	17.5	25.15	15.35	11.16	12.08

K2	68	L	30	F	5.24	54.92	18.62	17.6	25.18	16.09	11.33	11.61
K2	69	R	29	M	9.68	61.58	22.16	20.16	28.85	20.05	12.79	14.53
K2	69	L	29	M	9.97	60.54	22.15	19.79	28.93	19.66	12.93	14.21
K2	72	R	65	F	5.69	63.53	22.9	19.39	28.76	20.63	12.61	15.4
K2	72	L	65	F	5.58	62.62	21.51	18.46	27.92	20.1	12.91	15.43
K2	73	R	38	F	7.88	65.43	21.52	19.02	28.5	18.76	12.58	14.97
K2	73	L	38	F	7.84	64.76	21.34	19.2	29.25	19.41	12.56	15.73
K2	76	R	50	F	3.5	54.75	18.49	18.25	25.68	16.35	11.42	12.42
K2	76	L	50	F	3.13	55	18.87	17.73	25.6	17.06	11.32	11.91
K2	79	R	55	M	8.05	61.87	22.02	20.86	28.42	20.14	13.37	14.79
K2	79	L	55	M	7.71	61.61	22.03	19.56	27.99	20.07	12.5	14.6
K2	81	L	40	M	5.54	62.02	20.06	19.45	27.03	18.62	11.59	13.52
K2	82	R	60	F	3.58	52.28	19.91	18.15	26.23	17.39	11.35	11.49
K2	82	L	60	F	4.03	52.46	20.27	18.45	26.27	17.43	11.28	12.02
K2	85	R	48	F	5.54	54.22	18.68	16.98	25.7	17.51	10.68	12.2
K2	85	L	48	F	5.83	55.51	18.9	16.69	25.35	18.38	10.64	12.23
K2	87	L	70	M	6.96	61.36	23.08	20.61	30.36	19.77	13.05	15.68
K2	89	R	61	M	10.85	68.3	25.24	21.71	34.05	22.05	12.55	14.01
K2	89	L	61	M	10.51	66.46	24.08	22.82	33.97	21.42	12.48	14.07
K2	90	R	15	U	3.37	47.5	18.22	17.29	20.2	14.86	10.22	10.6
K2	90	L	15	U	4.78	53.07	18.91	17.37	25.98	17.98	10.46	12.14
K2	91	R	55	F	3.81	57.85	19.94	17.31	26.21	17.64	10.32	11.98
K2	91	L	55	F	3.68	58.06	19.2	17.47	25.81	17.51	10.89	10.95
K2	105	R	58	F	4.84	58.24	20.58	18.72	26.62	18.99	11.07	12.36
K2	105	L	58	F	4.71	57.64	20.6	17.75	26.64	18.1	10.97	12.14
K2	107	R	27	M	8.62	60.4	19.6	19.75	28.04	17.02	11.79	12.68
K2	107	L	27	M	8.86	60.58	19.79	20.19	28.47	17.21	11.8	12.67

K2	111	R	37	M	12.24	69	22.9	23.56	31.94	20.66	12.22	14.43
K2	116	R	23	M	7.33	62.58	20.24	18.73	27.72	18.21	10.98	12.89
K2	116	L	23	M	6.63	63.7	20.97	18.05	30.03	18.8	11.49	13.48
K2	119	L	37	M	7.89	60.19	21.05	20.2	27.38	20.8	10.34	11.76
K2	131	R	23	F	7.41	61.57	20.34	17.73	26.16	18.57	11.12	11.52
K2	131	L	23	F	6.15	59.76	18.82	17.63	25.44	17.44	10.62	11.09
K2	132	R	19	M	5.81	55.56	19.2	18.89	26.25	18.96	12	13.26
K2	132	L	19	M	5.55	55.98	18.2	18.75	26.08	18.61	12.11	12.9
K2	135	R	40	F	5.33	53.78	19.81	17.7	26.62	19.61	10.88	12.6
K2	135	L	40	F	5.23	55.2	19.4	17.5	26	17.91	11.07	12.54
K2	136	R	30	M	10.34	63.79	22.15	21.01	31.38	23.03	14.7	15.4
K2	136	L	30	M	10.03	62.41	21.72	20.79	30.81	22.73	14.83	15.28
K2	138	R	46	M	5.92	60.4	21.51	18.99	28.98	20.16	11.17	12.66
K2	138	L	46	M	5.28	58.52	20.32	18.96	28.26	19.67	11.2	12.87
K2	139	R	29	M	9.2	64.19	22.03	20.33	29.81	21.33	12.68	13.54
K2	140	R	Adult	U	11.53	64.8	22.74	21.79	28.41	20.91	14.2	15.33
K2	140	L	Adult	U	11.64	64.14	23.16	21.95	28.82	21.19	13.85	15.16
K2	141 a	R	42	F	4.9	58.85	20.6	17.88	28.17	18.94	11.22	11.91
K2	141 a	L	42	F	4.51	57.83	19.94	17.33	27.63	19.33	10.98	12.13
K2	141 b	R	U	U	9.36	63.78	23.03	19.51	28.77	19.63	11.97	13.69
K2	143	L	19	M	5.96	58.02	18.69	16.45	24.67	17.28	10.61	11.09
K2	159	R	20	M	5.13	52.75	17.99	16.11	23.53	17.69	10.13	11.85
K2	159	L	20	M	5.29	52.45	17.65	16	23.96	17.78	10.1	11.9
K2	165	R	55	F	3.3	59.11	19.45	16.74	26.12	16.61	11.3	12.4
K2	165	L	55	F	3.22	58.68	19.07	16.34	25.9	17.46	11.38	12.34
K2	166	R	31	F	4.7	56.41	19.72	18.55	26.93	18.44	11.08	11.14
K2	169	R	23	F	6.21	56.54	19.29	15.69	26.02	19.86	11.3	13.48

K2	170	R	26	F	7.11	54.31	21.54	18.21	26.57	17.72	12.35	13.14
K2	177	R	55	F	4.47	55.63	20.12	17.99	26.33	17.95	11.75	12.83
K2	177	L	55	F	4.8	55.39	19.14	18.36	26.89	17.87	11.85	12.46
K2	184	R	22	F	4.24	60.05	18.37	16.78	24.39	17.51	9.78	9.92
K2	184	L	22	F	4.35	61.31	18.57	17.31	24.18	17.8	9.86	9.98
K2	187	R	14	U	4.43	52.74	18.21	16.83	20.34	15.78	9.47	11.52
K2	187	L	14	U	4.34	52.79	17.96	16.62	20.12	15.91	9.84	10.7
K2	190	R	19	F	3.84	52.59	17.5	16.36	24.11	17.45	10.96	12.3
K2	190	L	19	F	4.56	54.47	17.9	16.78	24.84	18.25	10.82	12.19
K2	194	R	23	M	4.1	56.28	18.32	16.44	25.08	16.89	11.93	13.86
K2	194	L	23	M	3.98	56.52	17.72	15.87	24.54	16.94	12.28	14.09
K2	198	R	38	F	5.98	58.44	18.47	17.84	25.9	17.62	11.03	11.13
K2	198	L	38	F	5.78	57.47	18.64	18.17	25.33	17.48	10.85	11.55
K2	199	R	35	M	6.1	63.59	22.17	19.53	28.7	20.27	11.51	14.56
K2	199	L	35	M	6.12	63.15	21.36	19.06	28.4	19.95	12.1	15.29
K2	202	R	66	F	4.77	57.29	19.12	17.93	27.69	18.78	11.79	13.24
K2	202	L	66	F	5.18	58.05	19.77	18.02	27.26	18.8	12.2	13
K2	204	R	25	F	6.57	54.51	18.96	16.87	24.56	18.41	10.57	12.73
K2	204	L	25	F	6.49	54.14	19.4	16.99	24.76	17.94	10.93	12.62
K2	207	R	60	F	NA	NA	NA	NA	NA	NA	13.56	13.43
K2	210	R	54	F	3.08	58.29	18.46	18.86	27.47	19.03	12.99	13.99
K2	210	L	54	F	3.67	58.89	20.7	19.62	26.75	18.41	13.11	13.85
K2	211	R	55	M	6.6	68.56	21.13	21.23	30.95	22.38	12.83	13.66
K2	211	L	55	M	6.5	67.86	22.69	19.38	30.75	22.31	13.12	13.44
K2	213	R	55	M	11.99	70.87	27.89	24.89	33.3	20.5	14.76	13.85
K2	213	L	55	M	11.1	71.94	27.52	24.06	32.45	21.08	14.43	13.66
K2	214	R	23	F	7.08	59.32	18.69	17.83	26.43	19.19	11.28	11.95

K2	214	L	23	F	6.54	59.4	18.83	17.6	26.24	18.78	11.01	11.84
K2	215	L	40	M	11.13	68.02	21.43	18.74	28.72	18.44	12.77	12.54
K2	218	R	29	M	7.01	58.65	20.32	19.76	27.42	18.07	10.9	11.3
K2	218	L	29	M	7.48	58.82	20.46	19.85	28.03	18.73	11.24	11.93
K2	219	L	5.5	U	1.33	36.24	13.51	12.48	17.29	13.12	8.92	9.87
K2	220	R	35	M	7.89	61.15	21.57	20.02	28.35	18.66	11.52	12.13
K2	220	L	35	M	7.84	61.23	20.33	19.37	28.4	19.61	11.07	12.49
K2	222	R	29	M	8.04	62.42	21.99	19.9	29.98	16.6	13.13	14.34
K2	222	L	29	M	7.98	62.83	21.12	19.54	30.11	19.76	13.5	14.8
K2	225	R	36	M	7.48	56.07	19.84	18.79	27.02	17.28	12.33	11.96
K2	225	L	36	M	7.69	56.34	20.13	18.81	27.81	18.09	11.67	11.96
K2	227	L	23	M	8.6	62.25	21.87	19.14	28.28	18.75	12.61	12.2
K2	228	R	35	M	5.96	59.22	19.82	19.33	27.52	16.56	12.01	12.15
K2	228	L	35	M	5.84	58.2	19.73	19.69	28.19	16.25	11.86	11.9
K2	231	R	25	M	8.01	57.69	19	20.3	25.64	16.9	11.2	11.66
K2	231	L	25	M	7.94	56.91	19.43	19.4	25.95	17.18	11.16	12.22
K2	239	R	14	U	6.1	51.37	19.8	19.12	22.34	17.51	11.11	11.8
K2	239	L	14	U	7.16	53.99	20.2	18.49	27.14	18.35	11.23	11.31
K2	240	R	46	M	8.45	56.06	22.34	20.3	28.9	18.91	12.87	12.31
K2	240	L	46	M	8.51	56.19	22.03	20.2	28.87	19.09	12.53	13.19
K2	242	L	25	M	8.17	62.44	21.29	19.29	27.72	19.58	12.59	13.77
K2	243	R	15	U	4.67	50.73	18.82	17.19	22.47	18.56	12.08	13.88
K2	243	L	15	U	4.43	50.42	18.62	17.26	22.38	18.56	12.3	13.94
K2	245	R	36	M	9.21	59.35	22.01	19.1	27.76	19.46	11.84	11.94
K2	245	L	36	M	9.03	59.74	22.77	19.64	28	19.11	11.9	11.83
K2	249	R	29	M	8.41	64.45	21.67	19	29.5	18.22	12.27	12.5
K2	249	L	29	M	8.16	63.32	22.02	18.66	30.59	18.56	12.26	12.66

K2	250	R	45	M	10.61	66.88	23.14	20.65	31.29	21.76	12.63	14.49
K2	251	R	61	M	7.39	64.8	22.4	18.48	29.44	20.56	12.61	12.34
K2	251	L	61	M	7.51	65.19	22.63	20.99	28.25	21.71	12.42	12.37
K2	252	R	61	M	7.02	55.72	24.25	20.29	28.06	20.6	12.18	14.64
K2	252	L	61	M	6.67	56.32	24.67	20.48	28.44	20.47	11.75	14.43
K2	253	R	22	M	9.73	59.05	21.3	19.42	29.62	19.21	13	13.6
K2	253	L	22	M	9.3	58.41	20.77	19.25	30.33	18.66	12.96	13.02
K2	254	R	31	F	6.7	58.1	20.17	18.32	26.29	17.24	10.42	10.95
K2	254	L	31	F	6.55	57.59	20.01	17.85	26.44	16.66	10.4	10.21
K2	259	R	44	M	8.54	70	22.23	20.74	30.48	21.6	12.82	15.19
K2	259	L	44	M	7.79	69.55	21.71	19.98	30.13	20.28	12.98	16.07
K2	261	R	70	F	3.58	58.16	19.88	18.04	27.43	18.8	10.93	12.21
K2	261	L	70	F	3.87	58.47	20.58	18.69	27.91	18.84	10.6	13.52
K2	262	L	23	M	6.03	55.84	18.52	18.44	26.44	16.48	10.8	12.12
K2	264	R	23	M	6.23	54.8	18.76	17.01	24.69	17.78	9.67	10.34
K2	264	L	23	M	6.07	54.83	17.85	16.98	24.64	16.85	9.93	10.2
K2	265	R	51	M	9.19	62.1	21.53	20.28	28.46	18.31	13.26	14.22
K2	265	L	51	M	8.59	62.31	20.34	20.29	27.8	18.7	13.08	14
K2	266	R	55	F	3.37	59.05	19.49	18.34	27.74	18.03	12.5	12.66
K2	267	R	55	F	6.39	58.91	19.13	17.72	28.27	17.24	10.92	11.14
K2	268	R	23	M	7.88	61.87	21.95	19.51	29.29	20.58	12.64	13
K2	268	L	23	M	7.91	60.99	22.03	20.77	28.23	19.95	12.98	12.45
K2	270	R	27	F	5.92	56.97	18.28	16.65	25.86	14.9	11.44	11.67
K2	270	L	27	F	5.99	57.17	18.41	17.08	25.79	15.6	12.16	11.25
K2	271	R	31	F	4.22	51.28	17.94	17.26	25.07	14.85	9.1	10.44
K2	274	R	20	M	7.77	60.96	19.82	19.44	27.08	18.28	12.56	13.44
K2	274	L	20	M	7.87	59.89	20.25	19.6	28.6	17.78	12.61	13.77

K2	275	L	55	F	4.72	63.95	22.49	21.05	28.34	19.63	12.46	12.68
K2	279	L	23	F	6.54	58.3	19	17.14	26.33	18.25	10.16	12.07
K2	280	L	60	F	6.18	56.36	20	16.41	29.68	17.8	12.47	13.3
K2	281	R	60	M	6.5	58.44	19.73	18.08	27.09	17.78	11.05	11.4
K2	281	L	60	M	6.57	57.84	20.03	18.93	27.6	18.77	11.47	11.73
K2	282	R	27	F	5.34	57.9	18.89	17.49	24.6	17.39	11.61	12.06
K2	282	L	27	F	5.59	59.07	19.7	16.93	25.08	17.14	11.59	12.39
K2	283	R	55	F	4.88	55.53	19.72	17.94	26.37	18.41	11.4	12.39
K2	283	L	55	F	4.84	55.59	19.27	17.92	26.05	18.31	11.19	12.59
K2	284	R	33	F	6.68	53.64	19.02	18.05	25.97	17.54	11.44	12.07
K2	284	L	33	F	7.08	53.42	20.05	18.39	25.84	17.59	11.55	12.4
K2	285	R	19	F	5.53	56.91	18.24	17.16	24.63	16.27	11.74	11.65
K2	285	L	19	F	5.56	58.53	17.5	16.61	24.2	16.58	12.03	11.89
K2	287	R	15	U	4.37	51.98	18.79	17.03	21.02	15.69	11.11	11.99
K2	287	L	15	U	4.65	52.86	18.68	16.59	20.91	15.79	11.27	12.2
K2	288	R	15	U	4.77	53.35	19.36	17.03	21.08	15.86	10.21	11.38
K2	288	L	15	U	6.71	59.63	18.88	17.01	24.61	16.9	10.57	11.84
K2	289	L	34	F	5.73	55.52	19.26	18.26	28.21	18.21	11.51	11.13
K2	290	R	10	U	3.72	45.73	19.49	15.64	21.46	16.47	10.54	12.38
K2	290	L	10	U	4.11	46.77	20.45	16.88	22.25	17.8	10.93	12.6
K2	291	R	50	F	4.96	54.71	20.4	16.35	27.59	18.49	10.01	12.59
K2	291	L	50	F	4.82	54.86	20.21	16.45	28.02	17.78	10.23	12.01
K2	293	R	45	M	8.25	58.02	22	19.91	28.6	19.56	12.39	12.81
K2	293	L	45	M	7.88	58.55	21.53	19.69	28.27	18.94	12.34	12.4
K2	294	R	45	F	5.11	57.22	19.47	18.4	27.39	16.47	12.17	11.17
K2	294	L	45	F	5.26	58.4	18.95	17.84	26.79	17.5	11.97	11.66
K2	300	R	60	F	5.73	59.73	21.77	19.61	28.99	20.12	13.05	14.51

K2	300	L	60	F	5.22	58.69	21.3	19.5	29.1	19.53	13	13.55
K2	301	L	19	M	10.45	66.02	21.86	19.4	28.25	19.87	11.2	13.62
K2	303	R	23	M	8.76	60.49	20.58	18.86	26.45	18.6	11.43	13.42
K2	303	L	23	M	9.15	61	20.73	19.25	27.03	19.37	11.78	13.49
K2	305	R	29	M	9.56	59.44	21.4	22.51	29.9	19.88	13.33	13.88
K2	305	L	29	M	9.6	61.18	21.14	22.82	30.09	21.1	13.3	13.9
K2	306	R	65	F	3.77	55.34	19.31	18.8	26.18	16.73	11	10.32
K2	306	L	65	F	3.89	55.81	19.03	19.46	26.34	16.85	10.86	10.18
K2	307	R	23	F	6.21	53.97	19.1	18.07	25.71	17.64	11.46	11.12
K2	307	L	23	F	6.17	55.02	18.82	17.55	25.91	17.5	11.34	11.46
K2	308	R	36	M	9.38	58.34	21.31	18.58	28.15	19.67	12.88	13.88
K2	308	L	36	M	8.87	58.99	21.23	18.84	27.78	20.19	12.8	13.44
K2	310	R	21	M	6.32	56.11	19.2	18.25	25.89	17.92	11.9	12.42
K2	310	L	21	M	6.61	56.3	19.14	17.83	25.82	18.24	11.95	12.55
K2	312	R	37	F	6.64	59.4	19.96	17.74	26.79	17.8	11.66	11.68
K2	312	L	37	F	7.27	61.47	21.01	18.44	26.45	19.34	11.9	12.61
K2	314	R	53	F	5.24	57.92	18.91	16.74	25.24	17.16	11.32	11.78
K2	314	L	53	F	5.3	58.27	19.15	16.68	25.61	17.91	11.51	12.11
K2	318 a	R	30	F	6.31	53.57	19.89	18.82	25.22	17.9	11.81	13.82
K2	320	R	21	F	5.61	55.59	18.08	15.93	22.95	16.12	9.84	11.1
K2	320	L	21	F	5.61	56.36	17.67	15.66	22.71	16.33	9.68	11.28
K2	321	R	40	M	8.45	59.4	20.74	19.6	26.21	20.49	12.13	13.81
K2	321	L	40	M	8.31	59.56	20.19	19.68	26.8	19.79	12.31	13.71
K2	324	L	55	M	8.3	61.37	24.3	22.73	30.49	20.72	14.07	15.35
K2	327	R	21	F	6.09	57.89	18.57	17.31	24.02	16.76	10.06	10.89
K2	327	L	21	F	5.74	57.41	18.07	17.11	24.35	16.49	10.12	10.33
K2	377	R	55	F	4.59	61.06	21.47	20.12	26.93	18.67	11.94	12.76

K2	377	L	55	F	4.42	60.61	20.49	19.7	26.48	18.78	11.4	13
K2	393	L	45	M	6.4	54.36	18.85	16.55	25.91	17.17	9.8	10.8
K2	401	R	23	F	4.98	56.95	18.08	17.44	25.31	17.33	11.51	13.09
K2	401	L	23	F	5.11	55.65	19.08	18.99	26.65	18.71	12.59	13.4
K2	402	R	29	M	8.12	60.48	21.86	20.98	28.02	18.07	11.69	12.37
K2	402	L	29	M	8.26	60.49	22.71	21.07	28.7	18.54	11.88	12.44
K2	403	L	20	F	7.26	60.63	19.27	16.76	26.47	16.9	12.15	12.63
K2	409	R	33	F	5.89	56.17	19.53	18.08	28.57	18.34	12.14	12.66
K2	409	L	33	F	6	56.41	18.9	16.62	28.09	18.7	12.16	12.67
K2	411	R	30	F	4.78	59.92	20.87	17.71	26.81	17.54	12.63	12.56
K2	411	L	30	F	5.2	61.03	20.83	18.13	27.46	18.83	12.72	12.63
K2	412	R	50	M	5.91	65.72	23.42	20.33	29.94	21.41	13.41	15.03
K2	412	L	50	M	6.19	64.88	23.33	20.81	30.83	21.62	13.46	15.72
K2	413	R	27	F	4.34	58.94	19.01	18.68	26.06	17.67	11.95	12.17
K2	413	L	27	F	3.58	57.74	18.03	17.98	26.96	17.78	11.43	12.22
K2	414	R	55	M	8.64	62.46	23.89	20.32	32.08	22.21	13.09	14.62
K2	414	L	55	M	8.67	63.06	24.2	19.88	32.01	21.6	13.68	13.84
K2	415	R	40	F	5.22	59.31	19.82	18.6	26.97	17.58	12.73	13.71
K2	415	L	40	F	5.28	59.83	20.47	17.7	26.05	18.61	12.46	14.38
K2	417	R	27	F	5.63	54.09	18.23	16.76	26.61	16.38	11.69	11.39
K2	417	L	27	F	5.22	54.01	18.17	17.3	25.36	16.92	11.67	11.86
K2	418	R	20	M	5.93	62.71	23.14	20.17	31.08	20.79	13.18	13.6
K2	418	L	20	M	6.19	61.4	22.89	20.95	31.59	21.1	13.05	13.3
K2	422	R	31	F	4.37	56.63	17.95	16.73	26.16	16.89	11.34	11.68
K2	422	L	31	F	4.71	58.17	18.11	17.44	26.7	16.98	11.02	11.97
K2	423	L	23	F	5.09	57.66	19.76	17.91	25.85	18.25	11	10.46
K2	424	R	22	F	7.2	60.53	20.38	17.97	26.48	19.36	12.92	13.36

K2	424	L	22	F	6.96	58.92	20.18	17.84	26.73	18.6	12.79	13.42
K2	425	R	40	F	5.32	61.86	21.01	18.12	27.93	18.69	12.7	12.13
K2	425	L	40	F	5.42	60.51	20.46	18.56	27.67	19.75	12.74	12.17
K2	426	L	27	M	5.73	55.52	18.6	16.49	25.22	17.41	10.34	11.1
K2	427	R	40	M	7.76	62.47	21.99	21.55	30.68	19.96	12.7	12.88
K2	427	L	40	M	7.69	62.38	22.01	21.3	31.57	20.58	12.32	13.53
K2	430	L	45	F	5.8	58.74	19.72	19.94	26.27	18.6	13.53	13.66
K2	431	R	22	F	6.58	59.74	19.74	15.77	26.54	18.53	10.26	11.15
K2	431	L	22	F	6.3	59.07	18.92	16.67	26.74	16.93	10.09	10.77
K2	434	R	33	F	5.93	55.39	19.03	17.83	25.97	17.49	10.38	12.23
K2	434	L	33	F	5.96	54.4	19.05	17.92	25.59	17.8	10.38	12.33
K2	437	R	40	M	7.92	59.3	23.61	16.17	31.42	22.33	10.52	10.84
K2	437	L	40	M	7.37	58.21	21.19	18.7	30.01	20.34	11.7	12.58
K2	438	R	65	F	4.64	64.3	19.42	20.58	28.57	20.36	13.77	12.4
K2	438	L	65	F	3.84	63.67	19.06	21.38	28.96	18.87	13.54	13.3
K2	440	R	20	F	7.17	58.57	19.07	16.6	25.17	16.34	11.03	12.09
K2	440	L	20	F	7.06	58.65	18.57	16.36	25.51	16.94	11.21	11.81
K2	441	R	25	F	7.08	61.27	20.93	19.76	26.39	19.32	12.24	13.88
K2	441	L	25	F	7.6	62.53	21.83	20.75	26.23	19.35	13.05	13.67
K2	442	R	U	U	3.49	49.46	18.02	16.06	20.35	15.68	10.91	10.91
K2	443	R	60	F	4.9	62.79	20.26	18.8	26.94	17.57	12.97	11.46
K2	443	L	60	F	4.39	62.35	19.78	18.62	26.52	18.82	12.08	12.63
K2	451	R	27	F	7	63.58	19.69	18.06	26.63	18.26	10.65	11.525
K2	451	L	27	F	6.29	61.87	19.34	18.43	26.09	16.48	10.68	10.86
K2	452	R	60	F	3.52	59.93	18.73	18.13	26.79	17.76	10.73	11.38
K2	452	L	60	F	3.35	60.1	19.16	18.05	27.29	17.71	10.99	11.92
K2	453	L	38	M	8.51	61.34	21.42	20.08	29.87	20.8	13.63	15.02

K2	455	R	40	M	10.55	61.69	22.07	19.61	30.95	22.02	12.99	14.55
K2	455	L	40	M	9.76	60.51	21.92	20.52	30.08	21.4	13	14.09
K2	456	R	30	F	6.95	59.98	20.82	18.83	28.79	18.35	11.85	12.05
K2	456	L	30	F	6.57	59.29	20.39	18.89	27.63	18.5	11.82	12.24
K2	457	R	35	M	8.44	58.79	20.3	17.62	27.73	20.49	11.7	12.99
K2	457	L	35	M	7.77	58.89	20.34	17.73	27.97	20.3	11.01	13.46
K2	458	R	50	F	4.81	59.82	18.76	17.29	27.11	18.01	11.08	11.74
K2	458	L	50	F	4.44	59.49	19.14	17.61	27.15	16.45	11.05	10.94
K2	459	R	55	F	3.52	63.89	19.78	18.85	29.66	18.68	13.48	13.96
K2	459	L	55	F	3.9	65.15	21.6	20.91	29.81	18.75	13.39	13.55
K2	460	R	25	F	7.22	61.26	19.93	17.06	26.38	16.69	11.85	13.24
K2	460	L	25	F	7.3	61.23	19.13	16.83	26.21	17.05	11.66	12.6
K2	461	R	40	M	8.42	66.09	24.3	20.21	30.1	19.96	13.28	14.89
K2	463	R	35	F	5.49	55.56	19.15	17.54	26.03	17.12	10.97	11.27
K2	463	L	35	F	5.36	55.66	18.51	17.6	25.86	17	10.39	10.77
K2	466	R	35	M	9.93	60.59	21.35	21.93	29.65	21.23	12.45	13.18
K2	466	L	35	M	9.34	59.8	21.2	22.11	29.66	20.68	12.59	13.15
K2	468	R	15	U	3.26	47.29	16.6	15.09	19.31	16.29	10.33	12.7
K2	468	L	15	U	3.21	47.16	16.49	14.73	19.27	17.81	10.04	12
K2	469	R	38	M	10.53	65.2	22.5	23.25	32.17	20.5	13.52	13.53
K2	469	L	38	M	9.77	63.56	22.35	21.49	30.37	20.02	13.01	13.92
K2	470	R	50	F	3.98	55.24	17.64	17.33	26.87	16.43	11.93	11.68
K2	470	L	50	F	4.17	55.86	18.18	17.96	27.19	16.15	11.98	11.83
K2	474	R	33	F	5.81	59.51	19.11	17.71	25.55	18.78	10.59	11.61
K2	474	L	33	F	5.8	58.95	18.86	18.06	25.89	18.14	10.7	11.44
K2	475	R	35	F	6.49	58.26	19.74	16.08	26.28	17.07	10.32	11.43
K2	475	L	35	F	6.61	59.66	19.79	16.24	26.99	16.9	10.76	11.44

K2	479	R	9	U	2.7	39.41	18.39	14.51	18.55	14.23	10.13	11.11
K2	482	R	45	M	10.86	64.11	22.86	21.42	29.75	21.89	13.07	15.17
K2	482	L	45	M	9.96	63.29	22.3	21.09	30.61	21.28	13.32	14.44
K2	485	R	17	F?	4.48	51.92	16.17	14.88	22.78	13.91	9.36	10.53
K2	485	L	17	F?	4.36	52	16.08	15.53	22.84	13.82	10	10.66
K2	486	R	33	F	5.84	56.75	20.06	19.19	26.48	18.77	10.57	12.06
K2	486	L	33	F	5.93	56.82	19.9	18.71	27.23	18.85	10.08	12.16
K2	488	R	51	M	11.1	65.81	24.55	22.1	29.06	21.3	12.33	14.21
K2	488	L	51	M	10.39	64.62	24.19	23.26	29.11	21.36	12.25	14.09
K2	491	R	40	F	8.05	61.97	20.25	18.35	27.87	18.77	13.2	11.87
K2	491	L	40	F	7.55	62.92	20.57	18.24	28.53	19.22	12.73	12.37
K2	494	L	50	F	3.8	47.26	15.62	18.2	27.96	18.56	11.38	10.87
K2	496	R	22	F	5.11	52.85	17.83	16.52	22.74	16.31	9.35	10.8
K2	496	L	22	F	5.38	54.12	17.88	16.22	22.9	16.09	9.44	10.81
K2	500	R	45	F	4.64	55.05	19.9	18.83	26.28	19.01	12.57	13.58
K2	500	L	45	F	4.33	54.13	18.87	17.49	25.42	19.73	12.39	13.28
K2	506	R	25	F	6.09	56.29	17.89	17.08	24.83	17.02	10.06	10.87
K2	506	L	25	F	5.73	55.04	17.94	17.02	24.56	16.7	10.45	10.52
K2	507	R	45	F	6.52	61.22	19.77	19.17	25.82	17	11.71	11.01
K2	507	L	45	F	6.55	61.17	20.53	19.77	25.98	17.26	11.57	10.88
K2	511	R	25	F	4.87	51.79	17.98	15.75	22.55	16.52	9.9	12.04
K2	511	L	25	F	4.64	51.59	17.97	16.61	22.14	16.25	10.29	11.66
K2	512	R	22	M	6.93	58.63	21.72	20.26	27.37	19.51	11.87	12.13
K2	512	L	22	M	7.14	58.04	20.21	19.45	27.12	19.19	11.43	11.8
K2	513	R	22	F	7.06	56.5	20.39	17.94	26.01	19.08	10.95	12.65
K2	513	L	22	F	6.84	57.16	19.85	18.05	25.9	18.97	10.89	12.2
K2	517	R	60	M	6.11	63.76	24.12	18.45	32.42	18.77	14.56	15.89

K2	517	L	60	M	6.26	65.91	24.67	20.34	32.29	26.24	15.04	18.37
K2	522	R	27	M	12.02	69.97	22.53	21.45	31.52	22.45	14.54	15.56
K2	522	L	27	M	12.53	69.7	23	20.16	30.7	22.93	14.76	16.65
K2	523	R	20	F	4.83	60.37	18.73	16.82	25.25	17.44	11.63	11.86
K2	523	L	20	F	4.93	61.2	18.74	16.57	24.47	17.63	11.23	11.67
K2	526	R	40	F	6.66	58.2	19.9	17.1	27.11	16.67	11.42	11.87
K2	526	L	40	F	6.1	58.79	20.08	17.4	25.81	17.57	10.82	11.64
K2	528	R	55	F	3.82	61.32	20.69	17.01	27.44	19.67	12.5	13.76
K2	528	L	55	F	3.6	62.46	20.9	17.74	27.94	19.7	12.75	14.78
K2	530	R	40	F	6.21	68.65	24.39	20.97	29.94	22.12	14.2	15.83
K2	530	L	40	F	5.76	68.45	24.23	20.7	29.93	20.31	14.21	15.52
K2	531	R	37	M	9.23	64.74	19.74	18.82	26.93	17.36	12.96	12.72
K2	531	L	37	M	9.11	64.68	19.45	19.46	27.95	17.12	13.03	12.1
K2	535	R	35	M	9.38	61.77	23.52	20.78	29.98	19.61	12.84	14.71
K2	535	L	35	M	9.12	60.99	23.15	20.03	28.87	19.64	12.69	14.38
K2	536	R	25	F	8.41	62.01	20.25	18.67	25.99	17.43	11.53	12.2
K2	539	R	40	M	8.97	66.01	22.66	18.15	30.82	21.58	13.4	15.28
K2	539	L	40	M	9.47	66.84	21.76	18.46	30.51	21.92	13.53	15.91
K2	540	R	30	F	4.33	57.67	21.34	16.32	25.82	19.66	11.02	11.84
K2	540	L	30	F	4.1	56.65	20.24	17.16	25.34	18	11.07	11.09
K2	541	R	65	F	3.97	57.74	21.91	19.1	27.47	19.23	12.11	13.37
K2	541	L	65	F	3.97	56.45	20.75	19.68	27.55	18.05	12.36	13.27
K2	543	R	25	M	9.07	64.91	22.76	21.65	30.64	20.55	13.75	15.09
K2	543	L	25	M	8.43	65.81	22.94	22.42	29.88	19.66	13.76	14.38
K2	546	R	50	F	4.17	53.06	18.79	17.72	23.49	17.25	10.82	10.23
K2	546	L	50	F	4	53.25	17.2	16.29	24.15	17.28	10.45	10.4
K2	547	R	35	F	5.11	59.96	20.66	16.35	26.33	19	10.35	12.2

K2	548	R	50	F	4.79	57.36	19.31	17.84	25.97	18.62	10.09	11.29
K2	548	L	50	F	4.92	58.93	18.91	18.03	25.2	18.93	10.8	11.31
K2	583 a	R	18mos	U	1.95	36.01	13.38	13.5	16.94	12.66	8.9	9.79
D	D7-3	R	60	F	2.82	54.84	21.53	18.44	27.96	15	11.92	11.41
NT	NT 10	R	45	M	5.47	65.52	25.89	22.05	33.45	25.15	13.87	16.92
NT	NT 10	L	45	M	4.54	64.85	25.55	19.77	31.89	22.18	13.86	16.15

Burial	Element	Date Scanned	Shaft Location	Mean	SD	Total V (mm^3)	Bone V (mm^3)	Voxel	BMC (mg)	BMD (mg/cm^3)	Tissue MC (mg)	Tissue MD (mg/cm^3)	BVF
4	MT1	Aug-13	Proximal	-138.1081	1039.609	1175.2362	251.1146	1188450	177.5506	151.0765	171.747	683.9389	0.2137
			Mid-Shaft	-195.3183	999.6232	1175.2362	242.9158	1188450	161.779	137.6566	157.0818	646.6515	0.2067
			Distal	-179.2802	934.1402	1175.2362	263.2699	1188450	152.1014	129.422	147.583	560.5769	0.224
5	MT1	Aug-13	Proximal	-475.0846	802.3015	1175.2362	146.9003	1188450	88.8388	75.5923	87.0032	592.2599	0.125
			Mid-Shaft	-454.6565	805.0232	1175.2362	159.3711	1188450	92.0022	78.284	90.2906	566.5432	0.1356
			Distal	-445.5326	737.514	1175.2362	180.6172	1188450	80.1216	68.1749	79.1979	438.485	0.1537
6	MT1	Aug-13	Proximal	34.6653	1232.336	1175.2362	275.6863	1188450	245.2262	208.6612	238.2711	864.2832	0.2346
			Mid-Shaft	60.9309	1311.461	1175.2362	276.0027	1188450	265.3346	225.7713	256.6157	929.7578	0.2348
			Distal	34.6929	1266.002	1175.2362	259.0207	1188450	247.9359	210.9669	236.2948	912.2624	0.2204
8	MT1	Aug-13	Proximal	-410.8483	870.28	1175.2362	161.8591	1188450	106.4488	90.5765	103.4265	638.9908	0.1377
			Mid-Shaft	-458.2991	828.6042	1175.2362	149.3557	1188450	93.8079	79.8205	91.219	610.7497	0.1271
			Distal	-450.3558	813.0227	1175.2362	154.9053	1188450	91.6087	77.9492	89.1704	575.6442	0.1318
16	MT1	Aug-13	Proximal	-25.1824	1144.726	1175.2362	259.7119	1188450	214.8631	182.8254	208.4844	802.7526	0.221
			Mid-Shaft	-34.5368	1188.118	1175.2362	270.7607	1188450	224.1471	190.7251	218.1384	805.6503	0.2304
			Distal	-15.3089	1115.82	1175.2362	291.4649	1188450	216.2787	184.03	209.6212	719.1986	0.248
19	MT1	Aug-13	Proximal	-101.6977	1143.086	1175.2362	228.7708	1188450	198.2998	168.7319	191.4278	836.7669	0.1947
			Mid-Shaft	-107.1298	1241.917	1175.2362	236.0618	1188450	218.5211	185.938	213.7319	905.4064	0.2009
			Distal	-93.459	1150.198	1175.2362	253.0558	1188450	206.2467	175.4938	199.5505	788.5632	0.2153
20	MT1	Aug-13	Proximal	-432.0986	830.1184	1175.2362	155.4265	1188450	97.139	82.6548	94.692	609.2402	0.1323
			Mid-Shaft	-410.0606	917.5625	1175.2362	159.6223	1188450	114.454	97.3881	111.3664	697.6872	0.1358
			Distal	-392.8481	856.5875	1175.2362	183.2526	1188450	105.8489	90.0661	103.2173	563.2517	0.1559
21	MT1	Aug-13	Proximal	-222.2995	1001.262	1175.2362	200.115	1188450	151.9402	129.2848	145.9783	729.4719	0.1703
			Mid-Shaft	-202.8174	1038.507	1175.2362	211.7284	1188450	163.865	139.4316	158.4344	748.2906	0.1802
			Distal	-171.27	956.0012	1175.2362	258.5094	1188450	156.0883	132.8144	151.2309	585.0112	0.22
25	MT1	Aug-13	Proximal	-140.0921	1049.904	1175.2362	222.791	1188450	175.4651	149.302	170.0234	763.1518	0.1896

Burial	Element	Date Scanned	Shaft Location	Mean	SD	Total V (mm^3)	Bone V (mm^3)	Voxel	BMC (mg)	BMD (mg/cm^3)	Tissue MC (mg)	Tissue MD (mg/cm^3)	BVF
			Mid-Shaft	-75.1942	1176.009	1175.2362	246.7734	1188450	212.2059	180.5645	206.6743	837.5065	0.21
			Distal	-84.2184	1154.029	1175.2362	249.7994	1188450	207.4035	176.4781	199.9738	800.5377	0.2126
26	MT1	Aug-13	Proximal	-98.3821	1107.014	1175.2362	225.7082	1188450	191.7026	163.1184	183.3062	812.1379	0.1921
			Mid-Shaft	-124.5557	1201.433	1175.2362	231.6959	1188450	207.4203	176.4924	201.5651	869.9553	0.1971
			Distal	-154.9161	1106.091	1175.2362	236.9924	1188450	186.0611	158.318	179.3853	756.9242	0.2017
27	MT1	Aug-13	Proximal	-208.8091	1039.347	1175.2362	215.3289	1188450	163.9052	139.4658	158.1155	734.2974	0.1832
			Mid-Shaft	-293.1766	1097.868	1175.2362	186.6623	1188450	161.1193	137.0952	157.2218	842.2796	0.1588
			Distal	-325.1434	985.3764	1175.2362	191.8667	1188450	138.3946	117.759	134.454	700.7675	0.1633
30	MT1	Aug-13	Proximal	-183.1744	945.3016	1175.2362	230.7555	1188450	150.6399	128.1784	146.4744	634.7603	0.1963
			Mid-Shaft	-200.1127	985.0498	1175.2362	239.5991	1188450	157.084	133.6616	153.5617	640.9111	0.2039
			Distal	-162.8028	941.0998	1175.2362	268.4408	1188450	155.4669	132.2856	151.0363	562.6427	0.2284
41	MT1	Aug-13	Proximal	-532.3233	750.483	1175.2362	131.3462	1188450	75.8366	64.5288	74.4415	566.7579	0.1118
			Mid-Shaft	-553.213	737.5791	1175.2362	121.5563	1188450	70.2486	59.774	68.6814	565.0176	0.1034
			Distal	-503.2397	664.2489	1175.2362	160.4549	1188450	63.1263	53.7137	62.7589	391.1308	0.1365
44	MT1	Aug-13	Proximal	-392.8848	866.961	1175.2362	182.7166	1188450	110.1349	93.713	107.7945	589.9544	0.1555
			Mid-Shaft	-459.9561	868.4023	1175.2362	152.0306	1188450	101.1475	86.0657	98.5696	648.3536	0.1294
			Distal	-384.4597	866.4317	1175.2362	193.4193	1188450	110.2729	93.8304	107.9712	558.2238	0.1646
72	MT1	Aug-13	Proximal	-362.5266	914.3507	1175.2362	178.2943	1188450	121.5412	103.4186	118.7209	665.8705	0.1517
			Mid-Shaft	-344.1105	944.835	1175.2362	188.2405	1188450	129.0225	109.7843	125.7008	667.7672	0.1602
			Distal	-353.218	815.6633	1175.2362	200.2683	1188450	103.6139	88.1643	101.3507	506.0746	0.1704
85	MT1	Aug-13	Proximal	-122.7483	1164.07	1175.2362	224.7144	1188450	200.049	170.2202	193.5587	861.3541	0.1912
			Mid-Shaft	-116.3056	1259.105	1175.2362	230.2294	1188450	220.3404	187.4861	215.1206	934.375	0.1959
			Distal	-15.0785	1287.72	1175.2362	260.9233	1188450	246.2166	209.5039	239.195	916.7254	0.222
90	MT1	Aug-13	Proximal	-352.8813	839.3148	1175.2362	169.1235	1188450	105.0269	89.3667	100.8893	596.5423	0.1439
			Mid-Shaft	-371.5827	1018.114	1175.2362	168.3422	1188450	137.3943	116.9079	134.0641	796.3784	0.1432

Burial	Element	Date Scanned	Shaft Location	Mean	SD	Total V (mm^3)	Bone V (mm^3)	Voxel	BMC (mg)	BMD (mg/cm^3)	Tissue MC (mg)	Tissue MD (mg/cm^3)	BVF
			Distal	-305.6792	940.4042	1175.2362	213.0812	1188450	134.0978	114.1029	130.7125	613.4398	0.1813
116	MT1	Aug-13	Proximal	25.4159	1234.484	1175.2362	273.492	1188450	243.1113	206.8617	234.054	855.7985	0.2327
			Mid-Shaft	35.6116	1327.423	1175.2362	277.7096	1188450	265.1742	225.6348	257.0829	925.7258	0.2363
			Distal	96.1299	1278.877	1175.2362	293.0273	1188450	267.5159	227.6274	257.0114	877.0901	0.2493
131	MT1	Aug-13	Proximal	-110.414	1052.774	1175.2362	227.1599	1188450	179.6153	152.8334	170.4963	750.5561	0.1933
			Mid-Shaft	-84.3282	1235.734	1175.2362	248.3012	1188450	223.4019	190.091	217.811	877.2046	0.2113
			Distal	43.2836	1247.468	1175.2362	294.837	1188450	252.839	215.1389	244.9142	830.6766	0.2509
135	MT1	Aug-13	Proximal	-230.196	1015.392	1175.2362	194.2282	1188450	152.924	130.1219	147.8952	761.4507	0.1653
			Mid-Shaft	-158.7098	1165.337	1175.2362	222.2966	1188450	193.9996	165.0728	188.8761	849.6582	0.1892
			Distal	-141.1261	1109.595	1175.2362	240.5167	1188450	188.3118	160.2332	181.2381	753.5363	0.2047
166	MT1	Aug-13	Proximal	-308.3753	933.964	1175.2362	193.98	1188450	130.3585	110.9211	126.5477	652.3749	0.1651
			Mid-Shaft	-402.6367	909.2761	1175.2362	174.4169	1188450	115.1576	97.9868	112.5421	645.2477	0.1484
			Distal	-281.4829	873.4653	1175.2362	258.1989	1188450	126.8101	107.9018	125.0507	484.3191	0.2197
169	MT1	Aug-13	Proximal	-110.6796	1065.87	1175.2362	227.5199	1188450	182.2986	155.1165	174.7095	767.8869	0.1936
			Mid-Shaft	-56.091	1207.791	1175.2362	242.4223	1188450	219.7603	186.9925	213.5532	880.914	0.2063
			Distal	-25.2952	1130.199	1175.2362	266.4848	1188450	212.4415	180.7649	203.7584	764.6156	0.2267
177	MT1	Aug-13	Proximal	-300.9496	952.3644	1175.2362	191.666	1188450	134.441	114.3949	130.53	681.0285	0.1631
			Mid-Shaft	-318.1653	980.1603	1175.2362	194.953	1188450	139.1782	118.4258	135.9905	697.5552	0.1659
			Distal	-277.883	895.4561	1175.2362	231.7849	1188450	128.9841	109.7517	125.8933	543.1469	0.1972
184	MT1	Aug-13	Proximal	-257.9003	1013.654	1175.2362	189.8672	1188450	149.8375	127.4956	145.2594	765.0576	0.1616
			Mid-Shaft	-295.0928	1090.131	1175.2362	186.0422	1188450	159.5663	135.7738	155.9145	838.0599	0.1583
			Distal	-282.0739	1063.101	1175.2362	200.2337	1188450	158.1901	134.6028	153.8627	768.4158	0.1704
190	MT1	Aug-13	Proximal	-215.0879	989.6284	1175.2362	183.0439	1188450	147.5945	125.5871	140.7304	768.8339	0.1558
			Mid-Shaft	-175.8412	1157.486	1175.2362	208.0043	1188450	188.2673	160.1953	182.5438	877.5962	0.177
			Distal	-111.7571	1163.279	1175.2362	244.0718	1188450	204.6325	174.1203	196.4002	804.6821	0.2077

Burial	Element	Date Scanned	Shaft Location	Mean	SD	Total V (mm^3)	Bone V (mm^3)	Voxel	BMC (mg)	BMD (mg/cm^3)	Tissue MC (mg)	Tissue MD (mg/cm^3)	BVF
194	MT1	Aug-13	Proximal	-366.1351	888.8581	1175.2362	164.9711	1188450	114.1356	97.1172	110.8089	671.6867	0.1404
			Mid-Shaft	-331.9032	967.7646	1175.2362	164.5736	1188450	130.5358	111.072	125.8517	764.7139	0.14
			Distal	-398.8241	765.9548	1175.2362	185.7663	1188450	87.1811	74.1817	85.5139	460.3302	0.1581
261	MT1	Aug-13	Proximal	-450.877	868.4255	1175.2362	144.5408	1188450	102.0969	86.8736	99.6299	689.2857	0.123
			Mid-Shaft	-509.3378	837.9719	1175.2362	126.5818	1188450	90.3256	76.8574	87.9445	694.764	0.1077
			Distal	-518.485	783.3283	1175.2362	123.5518	1188450	80.4586	68.4616	78.3633	634.2544	0.1051
437	MT1	Aug-13	Proximal	167.9703	1273.359	1175.2362	323.2258	1188450	283.6341	241.3422	276.4938	855.4198	0.275
			Mid-Shaft	-77.9879	1130.902	1175.2362	267.5893	1188450	206.5034	175.7122	201.7347	753.8967	0.2277
			Distal	-91.7779	1032.352	1175.2362	292.7534	1188450	188.2118	160.1481	183.7898	627.7972	0.2491
459	MT1	Aug-13	Proximal	-429.2356	826.1479	1175.2362	161.9214	1188450	98.7021	83.9849	96.5956	596.5586	0.1378
			Mid-Shaft	-425.0034	848.0223	1175.2362	161.5427	1188450	102.6551	87.3485	100.3435	621.1579	0.1375
			Distal	-418.3091	776.683	1175.2362	179.9606	1188450	90.4633	76.9746	88.8621	493.7863	0.1531
D7-3	MT1	Aug-13	Proximal	-487.1853	756.2792	1175.2362	132.4004	1188450	77.9323	66.312	75.9492	573.6331	0.1127
			Mid-Shaft	-522.9274	767.0561	1175.2362	126.0676	1188450	76.5702	65.153	74.5332	591.2162	0.1073
			Distal	-516.5757	686.565	1175.2362	155.2504	1188450	64.9532	55.2682	64.4346	415.0365	0.1321
68	MT1	Jul-14	Proximal	-324.8173	932.7813	1175.2433	207.6802	1188450	131.7842	112.1336	129.3494	622.8298	0.1767
			Mid-Shaft	-268.1332	1004.831	1175.2433	226.3791	1188450	155.1608	132.0244	152.4643	673.4911	0.1926
			Distal	-302.6606	938.2249	1175.2433	234.2664	1188450	137.7975	117.2502	135.266	577.4024	0.1993
76	MT1	Jul-14	Proximal	-587.9773	650.2542	1175.2433	138.6015	1188450	56.8524	48.375	56.65	408.7257	0.1179
			Mid-Shaft	-576.664	716.8483	1175.2433	143.5756	1188450	69.3831	59.0372	68.9056	479.9256	0.1222
			Distal	-581.7944	626.4144	1175.2433	176.3048	1188450	52.1377	44.3633	52.1377	295.7247	0.15
141	MT1	Jul-14	Proximal	149.214	1415.75	1175.2362	293.5158	1188450	304.5296	259.122	294.0166	1001.706	0.2498
			Mid-Shaft	167.4109	1493.936	1175.2362	306.5938	1188450	327.1014	278.3282	316.5837	1032.5834	0.2609
			Distal	293.1954	1513.403	1175.2362	341.8	1188450	362.3985	308.3623	347.7225	1017.3274	0.2908
165	MT1	Jul-14	Proximal	-607.6855	655.6218	1175.2433	139.2789	1188450	56.7089	48.2529	56.5717	406.1756	0.1185

Burial	Element	Date Scanned	Shaft Location	Mean	SD	Total V (mm^3)	Bone V (mm^3)	Voxel	BMC (mg)	BMD (mg/cm^3)	Tissue MC (mg)	Tissue MD (mg/cm^3)	BVF
			Mid-Shaft	-594.1076	687.2673	1175.2433	146.9091	1188450	62.6397	53.2993	62.4282	424.9441	0.125
			Distal	-570.8487	640.6928	1175.2433	176.1723	1188450	55.8611	47.5316	55.8611	317.0825	0.1499
170	MT1	Jul-14	Proximal	-100.2044	984.152	1175.2433	256.906	1188450	173.5843	147.7007	167.5623	652.2319	0.2186
			Mid-Shaft	-127.4286	1059.935	1175.2433	267.8421	1188450	189.1325	160.9305	185.0524	690.9011	0.2279
			Distal	-77.3689	1014.941	1175.2433	326.9143	1188450	190.2923	161.9173	185.9436	568.7839	0.2782
198	MT1	Jul-14	Proximal	-303.8577	889.0801	1175.2433	219.2087	1188450	125.9066	107.1324	123.3405	562.6624	0.1865
			Mid-Shaft	-341.7048	926.6249	1175.2433	212.0115	1188450	130.3957	110.9521	128.4664	605.9407	0.1804
			Distal	-335.5541	957.5134	1175.2433	216.0126	1188450	137.3127	116.8377	134.8658	624.3425	0.1838
210	MT1	Jul-14	Proximal	-544.2225	661.0543	1175.2433	185.4461	1188450	60.94	51.8531	60.94	328.6133	0.1578
			Mid-Shaft	-562.8719	624.0661	1175.2433	202.8129	1188450	54.4408	46.323	54.4408	268.4289	0.1726
			Distal	-513.2034	601.1278	1175.2433	254.7404	1188450	52.2916	44.4943	52.2916	205.274	0.2168
213	MT1	Jul-14	Proximal	211.1948	1321.561	1175.2362	335.8953	1188450	305.1007	259.608	289.6489	862.319	0.2858
			Mid-Shaft	355.1617	1456.327	1175.2362	374.1482	1188450	369.9711	314.8058	353.6789	945.2908	0.3184
			Distal	640.7136	1259.008	1175.2362	494.0867	1188450	418.9016	356.4403	391.7862	792.9503	0.4204
219	MT1	Jul-14	Proximal	-583.676	789.386	1175.1444	130.9119	1188350	77.8881	66.2796	76.6132	585.2275	0.1114
			Mid-Shaft	-620.5336	833.4821	1175.1444	116.8914	1188350	82.0564	69.8267	80.4423	688.1792	0.0995
			Distal	-636.2334	713.5529	1175.1444	129.8498	1188350	62.3394	53.0483	61.915	476.8199	0.1105
275	MT1	Jul-14	Proximal	-381.9659	919.0951	1175.2362	218.6536	1188450	123.8229	105.36	122.0584	558.2271	0.1861
			Mid-Shaft	-423.1986	929.7508	1175.2362	192.6658	1188450	119.7082	101.8589	117.3829	609.2567	0.1639
			Distal	-390.3608	833.0243	1175.2362	236.4089	1188450	104.3797	88.816	103.5398	437.9689	0.2012
279	MT1	Jul-14	Proximal	-220.3171	974.896	1175.2433	239.4571	1188450	154.2255	131.2286	150.7152	629.4037	0.2038
			Mid-Shaft	-249.4079	1024.671	1175.2433	242.0915	1188450	163.4657	139.091	161.0038	665.0535	0.206
			Distal	-245.6621	1041	1175.2433	247.6936	1188450	167.8548	142.8256	165.142	666.7189	0.2108
284	MT1	Jul-14	Proximal	-72.3064	1065.605	1175.2433	280.7372	1188450	198.1113	168.5705	192.864	686.9912	0.2389
			Mid-Shaft	-75.2638	1126.13	1175.2433	289.3752	1188450	213.345	181.5326	209.6801	724.596	0.2462

Burial	Element	Date Scanned	Shaft Location	Mean	SD	Total V (mm^3)	Bone V (mm^3)	Voxel	BMC (mg)	BMD (mg/cm^3)	Tissue MC (mg)	Tissue MD (mg/cm^3)	BVF
			Distal	-53.252	1107.579	1175.2433	324.8307	1188450	215.0505	182.9838	210.1921	647.082	0.2764
289	MT1	Jul-14	Proximal	-316.8674	954.8855	1175.2433	213.1201	1188450	137.3394	116.8604	134.8483	632.7341	0.1813
			Mid-Shaft	-266.6235	1015.243	1175.2433	228.1729	1188450	156.8884	133.4944	153.8879	674.4356	0.1941
			Distal	-232.9059	977.251	1175.2433	263.0856	1188450	154.84	131.7515	151.6491	576.425	0.2239
294	MT1	Jul-14	Proximal	-438.681	812.6369	1175.2433	199.1807	1188450	98.264	83.6117	97.3459	488.7315	0.1695
			Mid-Shaft	-476.6669	787.7869	1175.2433	182.8047	1188450	90.5945	77.0858	89.8364	491.4338	0.1555
			Distal	-368.6134	789.7057	1175.2433	252.8536	1188450	100.5076	85.5206	100.0057	395.5083	0.2151
312	MT1	Jul-14	Proximal	-194.3441	1027.971	1175.2433	239.5422	1188450	166.8689	141.9867	162.457	678.198	0.2038
			Mid-Shaft	-195.9385	1077.665	1175.2433	253.887	1188450	179.9886	153.1501	176.5418	695.356	0.216
			Distal	-106.1389	1049.817	1175.2433	298.9417	1188450	190.9281	162.4584	186.3721	623.4396	0.2544
417	MT1	Jul-14	Proximal	-347.0905	856.0433	1175.2433	195.6009	1188450	113.2904	96.3974	110.7722	566.3172	0.1664
			Mid-Shaft	-301.4697	955.7346	1175.2433	225.855	1188450	141.8126	120.6666	139.4331	617.3569	0.1922
			Distal	-263.1836	928.4591	1175.2433	249.0276	1188450	140.6884	119.71	137.7704	553.2336	0.2119
434	MT1	Jul-14	Proximal	-245.6818	1036.484	1175.2433	225.493	1188450	161.7933	137.6679	158.4567	702.7121	0.1919
			Mid-Shaft	-293.1271	1026.936	1175.2433	221.3179	1188450	155.5423	132.349	153.2183	692.2993	0.1883
			Distal	-258.4393	1011.504	1175.2433	239.2574	1188450	157.0333	133.6177	153.3564	640.9686	0.2036
438	MT1	Jul-14	Proximal	-436.7569	960.3533	1175.2362	179.4276	1188450	122.126	103.9162	119.3259	665.0367	0.1527
			Mid-Shaft	-360.0888	1012.428	1175.2362	197.7288	1188450	140.3357	119.4107	136.4285	689.9776	0.1682
			Distal	-333.9749	883.3529	1175.2362	223.0383	1188450	117.4395	99.9284	114.6111	513.8629	0.1898
452	MT1	Jul-14	Proximal	-620.0077	688.658	1175.2433	135.9255	1188450	60.199	51.2226	59.9199	440.8286	0.1157
			Mid-Shaft	-576.9213	763.3214	1175.2433	148.4617	1188450	75.8629	64.5508	75.1671	506.3062	0.1263
			Distal	-604.9382	628.3517	1175.2433	162.0925	1188450	49.7091	42.2968	49.7091	306.671	0.1379
460	MT1	Jul-14	Proximal	-129.1287	1164.234	1175.2433	242.9864	1188450	203.5194	173.1721	196.7549	809.7362	0.2068
			Mid-Shaft	-87.9813	1307.952	1175.2433	261.7199	1188450	242.293	206.1642	237.2177	906.3801	0.2227
			Distal	-27.5387	1284.164	1175.2433	281.2079	1188450	249.6418	212.4171	242.6647	862.9368	0.2393

Burial	Element	Date Scanned	Shaft Location	Mean	SD	Total V (mm^3)	Bone V (mm^3)	Voxel	BMC (mg)	BMD (mg/cm^3)	Tissue MC (mg)	Tissue MD (mg/cm^3)	BVF
463	MT1	Jul-14	Proximal	-282.545	988.3777	1175.2433	220.7721	1188450	149.0098	126.7906	146.2882	662.6208	0.1879
			Mid-Shaft	-281.7122	1027.415	1175.2433	224.6505	1188450	158.2547	134.6569	155.7771	693.4197	0.1912
			Distal	-285.1668	949.9677	1175.2433	232.4795	1188450	139.0816	118.3428	135.5325	582.987	0.1978
475	MT1	Jul-14	Proximal	-213.5881	985.2057	1175.2433	251.2001	1188450	158.7536	135.0815	155.5158	619.0913	0.2137
			Mid-Shaft	-292.0368	955.2069	1175.2433	237.7612	1188450	144.0343	122.557	141.7585	596.2221	0.2023
			Distal	-339.9621	820.5275	1175.2433	249.8325	1188450	109.2282	92.941	108.1778	433.0012	0.2126
491	MT1	Jul-14	Proximal	-113.9405	1183.783	1175.2433	254.7176	1188450	212.7226	181.003	207.6974	815.4027	0.2167
			Mid-Shaft	-142.9477	1214.616	1175.2433	254.057	1188450	215.2163	183.1249	210.8515	829.9377	0.2162
			Distal	-21.4325	1188.052	1175.2433	294.9851	1188450	232.2159	197.5896	224.2592	760.2391	0.251
496	MT1	Jul-14	Proximal	-261.5294	947.0442	1175.2433	215.5844	1188450	141.32	120.2475	137.5285	637.9337	0.1834
			Mid-Shaft	-283.8877	1026.71	1175.2433	226.3296	1188450	157.6775	134.1659	155.1915	685.6881	0.1926
			Distal	-302.227	988.0033	1175.2433	232.7347	1188450	147.1445	125.2034	144.3503	620.2355	0.198
583a	MT1	Jul-14	Proximal	-477.4035	980.6312	1175.1444	140.5249	1188350	117.3054	99.8221	113.7377	809.378	0.1196
			Mid-Shaft	-450.6255	1081	1175.1444	154.7688	1188350	139.3944	118.619	136.3232	880.8182	0.1317
			Distal	-463.1711	957.3815	1175.1444	170.1312	1188350	117.5	99.9877	114.7934	674.7346	0.1448

Burial	Volume (mm^3)	Volume of Bone (mm^3)	BMC (mg)	BMD (mg/cc)	TMC (mg)	TMD (mg/cc)	BVF	Calib. Tb.Th. 3D (mm)	Calib. Tb.Sp. 3D (mm)
4B	123.6102	47.4129	10.5184	85.0935	10.5184	221.8472	0.3836	0.227839	0.478616
4H	123.6102	73.8032	14.5539	117.7401	14.5539	197.1985	0.5971	0.210626	0.193105
5B	123.6102	33.8405	7.1283	57.6674	7.1283	210.6434	0.2738	0.18341	0.628029
5H	123.6102	58.252	10.4648	84.6598	10.4648	179.6472	0.4713	0.18282	0.279598
6B	123.6102	14.8451	2.6811	21.6897	2.6811	180.6031	0.1201	0.151372	1.99534
6H	123.6102	34.2796	5.2921	42.8132	5.2921	154.3818	0.2773	0.138803	0.404249
8B	123.6102	17.0562	2.8406	22.9802	2.8406	166.5426	0.138	0.132995	0.832409
8H	123.6102	36.8339	7.3205	59.2223	7.3205	198.7432	0.298	0.156498	0.537808
16B	123.6102	31.4197	6.0146	48.6579	6.0146	191.428	0.2542	0.176821	0.63779
16H	123.6102	84.4663	21.2143	171.6228	21.2143	251.1573	0.6833	0.317435	0.238808
19B	123.6102	62.7346	18.6941	151.234	18.6941	297.9864	0.5075	0.349575	0.476894
19H	123.6102	82.5311	25.1718	203.6382	25.1718	304.9974	0.6677	0.357972	0.274258
20B	123.6102	17.2204	2.5942	20.987	2.5942	150.6474	0.1393	0.124826	0.813101
20H	123.6102	60.2842	11.5199	93.1953	11.5199	191.0931	0.4877	0.178316	0.255807
21B	123.6102	53.6656	12.7701	103.3095	12.7701	237.957	0.4342	0.222179	0.403983
21H	123.6102	91.0483	27.5299	222.7153	27.5299	302.3656	0.7366	0.39237	0.211986
25B	123.6102	33.9345	6.4416	52.1121	6.4416	189.8242	0.2745	0.160001	0.578747
25H	123.6102	60.126	12.7131	102.8484	12.7131	211.4412	0.4864	0.194615	0.286481
26B	123.6102	42.0522	9.0965	73.59	9.0965	216.3139	0.3402	0.209169	0.443684
26H	123.6102	63.8145	13.701	110.8406	13.701	214.7008	0.5163	0.203635	0.25377
27B	123.6102	29.6575	5.7667	46.6522	5.7667	194.4424	0.2399	0.159154	0.597429
27H	123.6102	77.7468	21.568	174.4842	21.568	277.4135	0.629	0.349741	0.309084
30B	123.6102	45.1672	10.1998	82.5157	10.1998	225.8229	0.3654	0.206219	0.486857
30H	123.6102	70.7564	16.0448	129.8014	16.0448	226.7606	0.5724	0.242415	0.25997
41B	123.6102	6.0609	0.8135	6.5814	0.8135	134.227	0.049	0.112789	1.37395
41H	123.6102	33.4133	5.1729	41.8486	5.1729	154.816	0.2703	0.130724	0.421679
44B	123.6102	33.8405	6.5583	53.0565	6.5583	193.8009	0.2738	0.172206	0.657859
44H	123.6102	75.3557	19.3962	156.9145	19.3962	257.3955	0.6096	0.30079	0.276344
68B	123.6109	12.1495	2.0223	16.36	2.0223	166.4491	0.0983	0.156045	2.249186
68H	123.6109	72.5695	16.8752	136.5183	16.8752	232.5378	0.5871	0.294688	0.275056
72B	123.6102	35.5364	8.3354	67.4328	8.3354	234.5587	0.2875	0.19787	0.649435
72H	123.6102	70.7001	16.1788	130.886	16.1788	228.8377	0.572	0.225987	0.237652
76B	123.6109	1.3142	0.0975	0.7885	0.0975	74.1621	0.0106	0.104606	3.686114
76H	123.6109	24.0527	3.1579	25.5472	3.1579	131.2913	0.1946	0.136958	0.760358
85B	123.6102	45.1612	11.3332	91.685	11.3332	250.9497	0.3654	0.231969	0.552581
85H	123.6102	61.7477	14.7717	119.502	14.7717	239.2259	0.4995	0.202835	0.323297
90B	123.6102	69.7567	20.1195	162.7661	20.1195	288.4247	0.5643	0.497527	0.392714
90H	123.6102	59.6741	11.5148	93.1543	11.5148	192.9619	0.4828	0.174593	0.242413

Burial	Volume (mm^3)	Volume of Bone (mm^3)	BMC (mg)	BMD (mg/cc)	TMC (mg)	TMD (mg/cc)	BVF	Calib. Tb.Th. 3D (mm)	Calib. Tb.Sp. 3D (mm)
116B	123.6102	15.6837	2.4324	19.6776	2.4324	155.0884	0.1269	0.125588	0.827929
116H	123.6102	32.3493	6.1776	49.9762	6.1776	190.9644	0.2617	0.154464	0.507251
131B	123.6102	61.2266	16.3296	132.1056	16.3296	266.7076	0.4953	0.412214	0.386368
131H	123.6102	82.9316	19.9831	161.6621	19.9831	240.9588	0.6709	0.326154	0.228779
135B	123.6102	33.8484	6.9918	56.5633	6.9918	206.5621	0.2738	0.190848	0.638505
135H	123.6102	89.3405	24.2936	196.5342	24.2936	271.9218	0.7228	0.328813	0.182572
141B	123.6102	38.1609	7.0312	56.8823	7.0312	184.2522	0.3087	0.19902	0.718941
141H	123.6102	79.9303	16.438	132.9829	16.438	205.6546	0.6466	0.25226	0.186139
165B	123.6109	7.5264	1.0374	8.3928	1.0374	137.8392	0.0609	0.13776	1.745556
165H	123.6109	49.8043	8.5712	69.3398	8.5712	172.0966	0.4029	0.184087	0.348263
166B	123.6102	42.513	10.2114	82.6096	10.2114	240.1945	0.3439	0.19649	0.487996
166H	123.6102	63.9974	14.5826	117.9724	14.5826	227.8621	0.5177	0.237054	0.30676
169B	123.6102	55.7976	13.4605	108.8944	13.4605	241.237	0.4514	0.248145	0.321802
169H	123.6102	74.3837	16.9875	137.4279	16.9875	228.3766	0.6018	0.254652	0.265897
170B	123.6109	53.0736	12.8866	104.2516	12.8866	242.8069	0.4294	0.383176	0.442289
170H	123.6109	76.6655	18.058	146.0872	18.058	235.5425	0.6202	0.299021	0.270032
177B	123.6102	46.425	9.9543	80.5301	9.9543	214.4175	0.3756	0.172848	0.400147
177H	123.6102	72.9359	17.082	138.1922	17.082	234.205	0.59	0.259764	0.262584
184B	123.6102	34.2222	7.9099	63.9909	7.9099	231.1342	0.2769	0.25367	0.76544
184H	123.6102	45.1118	7.3656	59.5874	7.3656	163.2746	0.365	0.167811	0.342472
190B	123.6102	27.4078	3.386	27.3926	3.386	123.5415	0.2217	0.169857	0.520631
190H	123.6102	46.6633	4.9351	39.925	4.9351	105.7606	0.3775	0.132867	0.27676
194B	123.6102	28.8823	5.9127	47.8333	5.9127	204.7167	0.2337	0.189573	0.813571
194H	123.6102	53.5974	10.2549	82.9613	10.2549	191.3313	0.4336	0.171148	0.330413
198B	123.6109	46.1899	12.4646	100.8372	12.4646	269.8548	0.3737	0.398513	0.740025
198H	123.6109	80.18	19.8829	160.8507	19.8829	247.9784	0.6486	0.368269	0.279136
210B	123.6109	5.9353	0.5591	4.5233	0.5591	94.205	0.048	0.112306	1.721017
210H	123.6109	31.6731	3.4951	28.2751	3.4951	110.3496	0.2562	0.131761	0.392764
213B	123.6102	43.8243	11.7513	95.0674	11.7513	268.146	0.3545	0.317473	1.285361
213H	123.6102	62.7366	14.6115	118.2065	14.6115	232.9027	0.5075	0.259181	0.316647
219B	123.6109	24.4601	5.5848	45.1807	5.5848	228.3239	0.1979	0.186367	0.71832
219H	123.6109	24.3395	3.7377	30.2379	3.7377	153.5665	0.1969	0.135202	0.643403
261B	123.6102	6.4554	1.1412	9.2327	1.1412	176.7895	0.0522	0.155965	2.208215
261H	123.6102	70.2086	18.0814	146.2779	18.0814	257.5387	0.568	0.331431	0.380218
275B	123.6102	9.3133	1.5638	12.6509	1.5638	167.9084	0.0753	0.168864	2.77737
275B2	123.6102	14.0421	2.1979	17.7808	2.1979	156.5207	0.1136	0.159107	1.388954
275H	123.6102	48.3415	7.9879	64.6218	7.9879	165.2394	0.3911	0.184981	0.32532
279B	123.6109	33.6113	7.9799	64.5565	7.9799	237.4168	0.2719	0.32983	1.534842

Burial	Volume (mm^3)	Volume of Bone (mm^3)	BMC (mg)	BMD (mg/cc)	TMC (mg)	TMD (mg/cc)	BVF	Calib. Tb.Th. 3D (mm)	Calib. Tb.Sp. 3D (mm)
279H	123.6109	82.2774	21.6091	174.8151	21.6091	262.6365	0.6656	0.36538	0.287183
284B	123.6109	33.5965	6.4973	52.5629	6.4973	193.3939	0.2718	0.206812	0.673541
284H	123.6109	82.0094	20.4632	165.5454	20.4632	249.5227	0.6634	0.331761	0.24783
289B	123.6109	16.0012	2.6812	21.6907	2.6812	167.5627	0.1294	0.190853	1.658461
289H	123.6109	66.7202	16.1319	130.5052	16.1319	241.7838	0.5398	0.281472	0.331193
294B	123.6109	26.4923	6.3967	51.7487	6.3967	241.4553	0.2143	0.258868	1.33441
294H	123.6109	54.7507	9.555	77.2987	9.555	174.5176	0.4429	0.219081	0.474355
312B	123.6109	48.8184	10.8772	87.9957	10.8772	222.8099	0.3949	0.278695	0.572552
312H	123.6109	60.7652	12.9663	104.8959	12.9663	213.3835	0.4916	0.227581	0.352943
417B	123.6109	13.6644	1.9936	16.1283	1.9936	145.8994	0.1105	0.142368	1.787798
417H	123.6109	82.845	20.5027	165.8647	20.5027	247.4825	0.6702	0.33496	0.243904
434B	123.6109	43.1827	12.6294	102.1704	12.6294	292.4636	0.3493	0.459141	1.076044
434H	123.6109	85.7108	21.7608	176.0426	21.7608	253.8861	0.6934	0.400954	0.292809
437B	123.6102	53.2839	17.8408	144.3313	17.8408	334.8256	0.4311	0.371287	0.650898
437H	123.6102	51.6839	14.7443	119.2807	14.7443	285.2787	0.4181	0.242146	0.511303
438B	123.6102	4.0702	0.5106	4.1304	0.5106	125.4377	0.0329	0.13497	2.575732
438H	123.6102	33.5211	4.6811	37.87	4.6811	139.6467	0.2712	0.136526	0.482743
452B	123.6109	10.1855	1.5065	12.1872	1.5065	147.9023	0.0824	0.139086	1.664349
452H	123.6109	24.2119	3.1181	25.2249	3.1181	128.7824	0.1959	0.130371	0.606693
459B	123.6102	3.381	0.4159	3.3649	0.4159	123.0231	0.0274	0.110233	2.69969
459H	123.6102	39.0381	5.6101	45.3855	5.6101	143.7085	0.3158	0.124686	0.31915
460B	123.6109	40.0321	8.4793	68.5966	8.4793	211.8122	0.3239	0.285661	0.675242
460H	123.6109	87.3741	20.4784	165.6681	20.4784	234.3759	0.7068	0.324868	0.194693
463B	123.6109	17.4024	2.4814	20.0741	2.4814	142.5877	0.1408	0.140595	1.482767
463H	123.6109	57.9172	10.4573	84.5983	10.4573	180.5557	0.4685	0.211368	0.402661
475B	123.6109	35.864	6.4598	52.259	6.4598	180.119	0.2901	0.213377	0.858749
475H	123.6109	76.4054	18.5505	150.0714	18.5505	242.79	0.6181	0.327844	0.319397
491B	123.6109	40.6502	9.3717	75.8162	9.3717	230.5453	0.3289	0.386088	0.764921
491H	123.6109	77.7681	19.1322	154.7776	19.1322	246.016	0.6291	0.277179	0.228443
496B	123.6109	73.237	19.5066	157.8064	19.5066	266.3489	0.5925	0.402974	0.317962
496H	123.6109	88.629	20.6015	166.6644	20.6015	232.4469	0.717	0.354935	0.222849
D7-3B	123.6102	5.4349	0.6854	5.5445	0.6854	126.1035	0.044	0.113852	1.422359
D7-3H	123.6102	26.6919	3.8295	30.9804	3.8295	143.4704	0.2159	0.120488	0.467931

Burial	Dorsal-Ecto			Dorsal Endo			Plantar Endo			Plantar Ecto		
	X	Y	Z	X	Y	Z	X	Y	Z	X	Y	Z
4	14.447	17.5925	2.4785	13.6394	17.5925	2.4077	2.7187	17.5925	2.569	1.8306	17.5925	2.4974
5	-9.4341	17.2298	1.3537	-8.5676	17.2298	1.3151	3.3454	17.2298	1.2282	4.2336	17.2298	1.3493
6	10.4602	18.9501	-1.8622	9.4171	18.9501	-1.7677	-1.7431	18.9501	-1.8559	-3.0252	18.9501	-1.7583
8	11.1426	17.7338	7.5613	10.4977	17.7338	7.5406	0.8993	17.7338	7.6102	0.2481	17.7338	7.5253
16	11.3401	18.9517	3.9785	9.961	18.9517	4.0551	0.6643	18.9517	3.9053	-0.8843	18.9517	3.8947
19	10.2729	16.9606	3.6749	8.8001	16.9606	3.6134	0.5127	16.9606	3.6625	-1.1659	16.9606	3.5926
20	10.6425	16.7634	-2.4518	9.7041	16.7634	-2.3835	0.4214	16.7634	-2.3406	-0.7823	16.7634	-2.3166
21	-9.8102	17.5594	4.2693	-9.0653	17.5594	4.2297	2.6341	17.5594	4.253	3.4951	17.5594	4.2075
25	-10.4144	16.7624	4.5706	-8.6843	16.7624	4.5002	0.8782	16.7624	4.4615	2.2536	16.7624	4.4567
26	-5.7997	17.1552	2.2	-4.3429	17.1552	2.1603	3.8423	17.1552	2.2171	5.1481	17.1552	2.1773
27	-8.917	16.8396	3.0828	-7.928	16.8396	3.137	0.6122	16.8396	3.1018	1.4356	16.8396	3.0397
30	9.9402	19.1534	0.4383	8.7919	19.1534	0.4116	-0.7539	19.1534	0.4331	-2.2672	19.1534	0.4583
41	1.2952	27.6091	1.3029	1.2952	27.0594	1.3264	1.2952	16.2598	1.169	1.2952	15.5177	1.2624
44	-0.6812	11.0921	0.2989	-0.3712	11.9358	0.2989	2.4439	21.7768	0.2989	2.5362	22.3078	0.2989
68	9.2297	20.5603	-7.2965	7.3179	20.5603	-7.2472	-1.4993	20.5603	-7.2588	-2.6966	20.5603	-7.2084
72	0.797	11.3091	0.4088	0.797	11.9571	0.4439	0.797	23.2326	0.5101	0.797	23.8464	0.5954
76	11.3943	21.1082	1.1068	10.4323	21.1082	1.2646	1.2065	21.1082	1.2342	0.3696	21.1082	1.1553
85	2.0922	10.2274	2.8131	2.0922	11.6275	2.8265	2.0922	20.1538	2.7685	2.0922	21.6192	2.7128
90	10.819	17.2625	5.1578	9.7842	17.2625	5.095	1.2195	17.2625	5.064	0.3614	17.2625	5.0731
116	1.1955	26.928	2.6899	1.1955	25.9089	2.6893	1.1955	16.8165	2.6161	1.1955	15.1224	2.5473
131	-0.0689	16.6837	-1.8128	-0.067	15.3009	-1.7631	-0.0683	6.7391	-1.7966	-0.0664	5.2227	-1.7484
135	10.8989	18.3564	4.5753	9.7093	18.3564	4.6213	1.5462	18.3564	4.5763	0.3504	18.3564	4.5765
141	-8.8441	23.1057	12.1524	-7.2458	23.1057	12.0571	1.53	23.1057	12.1987	3.0792	23.1057	12.2006
165	16.0755	20.4108	1.9736	15.0035	20.4108	1.974	4.8282	20.4108	2.0109	3.8903	20.4108	1.9232
166	11.198	17.3601	4.3682	10.329	17.3601	4.3438	0.1729	17.3601	4.4206	-0.2498	17.3601	4.3822
169	1.6937	10.3211	-0.6484	1.6937	11.7998	-0.6662	1.6937	20.3937	-0.6865	1.6937	21.7199	-0.6892
170	18.6609	22.3068	-22.0599	17.3562	22.3068	-21.9597	8.2131	22.3068	-21.998	6.5172	22.3068	-21.9215
177	13.5687	18.5562	2.7043	12.2707	18.5562	2.7074	2.2307	18.5562	2.6377	1.3135	18.5562	2.6557
184	8.6834	17.6595	6.4574	7.3922	17.6595	6.4421	0.3689	17.6595	6.5082	-0.9287	17.6595	6.4431
190	9.5517	18.3529	4.0687	8.2631	18.3529	4.0777	0.209	18.3529	4.042	-1.0338	18.3529	4.0507
194	12.5086	17.0608	3.2196	11.6648	17.0608	3.2034	0.1719	17.0608	3.1931	-0.5354	17.0608	3.1601
198	8.7052	21.0106	-3.0391	6.8784	21.0106	-3.0622	-0.7247	21.0106	-3.0963	-2.1683	21.0106	-2.9898
210	8.8075	22.9494	-9.8708	8.01	22.9494	-9.8221	-3.5942	22.9494	-9.8241	-4.5425	22.9494	-9.8447
213	-9.493	24.1508	12.9902	-8.4566	24.1508	13.0229	4.417	24.1508	12.9865	5.5313	24.1508	13.0862
219	5.8086	18.9174	1.5016	5.2231	18.9174	1.5325	-2.341	18.9174	1.5523	-3.0592	18.9174	1.516
261	2.4907	10.4602	2.5619	2.4907	10.9029	2.472	2.4907	21.0726	2.4993	2.4907	21.6901	2.5105

Burial	Dorsal-Ecto			Dorsal Endo			Plantar Endo			Plantar Ecto		
	X	Y	Z	X	Y	Z	X	Y	Z	X	Y	Z
275	7.462	21.6581	9.2726	6.3615	21.6581	9.3244	-4.2374	21.6581	9.1923	-5.4794	21.6581	9.228
279	-9.8886	21.2567	-8.293	-8.0172	21.2567	-8.2449	-0.8795	21.2567	-8.2605	0.4777	21.2567	-8.2635
284	-11.3256	20.8102	-5.1017	-9.8021	20.8102	-5.0966	-1.1136	20.8102	-5.0674	0.5332	20.8102	-5.0618
289	10.9261	20.9618	-7.9149	9.6155	20.9618	-7.7702	0.3504	20.9618	-7.7934	-1.2432	20.9618	-7.8547
294	8.2418	21.4559	-7.6687	7.1954	21.4559	-7.6238	-3.7831	21.4559	-7.6754	-4.6121	21.4559	-7.6834
312	9.3975	21.0574	-3.6334	8.2414	21.0574	-3.7062	-1.2302	21.0574	-3.7523	-2.3994	21.0574	-3.8256
417	8.3172	20.1608	-1.4826	7.008	20.1608	-1.577	-2.0916	20.1608	-1.5115	-3.2165	20.1608	-1.6021
434	4.4509	22.4044	2.3319	3.1359	22.4044	2.3913	-3.9905	22.4044	2.2856	-5.5875	22.4044	2.3328
437	11.7298	18.1611	3.238	9.9413	18.1611	3.1906	1.1876	18.1611	3.158	-0.6581	18.1611	3.1105
438	-9.9894	20.1627	7.7615	-9.1613	20.1627	7.7623	3.8824	20.1627	7.7157	4.9026	20.1627	7.6945
440	0.797	23.5987	5.1198	0.797	23.3498	3.4983	0.797	21.9194	-5.1276	0.797	21.4531	-6.7852
452	10.6665	21.1072	-5.5253	10.0364	21.1072	-5.5759	-0.6093	21.1072	-5.5889	-1.3731	21.1072	-5.6402
459	1.3948	12.1558	3.8824	1.3948	13.0849	3.8691	1.3948	24.9696	3.8616	1.3948	25.8968	3.8483
460	-0.8967	14.6906	2.9875	-0.8967	16.0096	2.9101	-0.8967	24.8449	2.9546	-0.8967	26.3257	2.9387
463	9.0064	21.3583	-0.8518	7.5728	21.3583	-0.8328	0.0793	21.3583	-0.7952	-1.3608	21.3583	-0.8555
475	10.8855	21.4569	-0.9775	9.0325	21.4569	-1.0345	1.1218	21.4569	-1.0953	-0.4148	21.4569	-1.0758
491	0.0996	15.7681	-7.3003	0.0996	17.2819	-7.2885	0.0996	28.0419	-7.2805	0.0996	29.2559	-7.3467
496	11.8419	20.91	1.8417	10.0714	20.91	1.8556	3.4068	20.91	1.9077	1.8023	20.91	1.8359
583a	6.0165	18.3423	2.724	5.0289	18.3423	2.8163	-1.8991	18.3423	2.8028	-3.1512	18.3423	2.8362
D7-3	8.5881	17.2615	1.7666	7.6948	17.2615	1.8307	-3.4476	17.2615	1.8401	-4.2377	17.2615	1.8521

Curriculum Vitae

Name: Mathew Adam Teeter

Post-secondary   Laurentian University
Education and   Sudbury, Ontario, Canada
Degrees: 2001-2005 B.Sc. (Hons.) Biology and Forensic Biology

                       The University of Western Ontario
                       London, Ontario, Canada
                       2007-2010 M.A. Bioarchaeology

                       The University of Western Ontario
                       London, Ontario, Canada
                       2011- Ph.D. Bioarchaeology

Honours and   Province of Ontario Graduate Scholarship
Awards: 2011-12

                       Social Science and Humanities Research Council (SSHRC)
                       Doctoral Fellowship
                       2014-2015

Related Work   Teaching Assistant
Experience   The University of Western Ontario
                       2007-2014

                       Teaching Assistant
                       Laurentian University
                       2004-2005